Large-Scale Brain Simulation to Characterize Neural Circuits of Schizophrenia
Nianqi Deng, Integrated Program in Neuroscience
McGill University, Montreal
Submitted April 2024
A thesis submitted to McGill University in partial fulfillment of the requirements of the
degree of Master of Science

Table of content

Abstract (EN)	iii
Abstract (FR)	. v
Acknowledgments	vii
Contribution of authorsv	iii
List of Tables	ix
List of Figures	X
List of Abbreviations	xii
Introduction	. 1
CHAPTER 1: BACKGROUND INFORMATION	3
1. 1. Complex threads of Schizophrenia	3
1.1.1. Neuroimaging of Schizophrenia	.3
1. 1. 2. Current status of Schizophrenia research	. 4
1. 2. Large-scale brain simulation's applications in brain disorders	. 7
1. 2. 1. Overview of large-scale brain simulation	7
1. 2. 2. Brain disease research based on large-scale brain models	. 9
1. 2. 3. Exploration of the genetics and transcriptomics of Schizophrenia	10
CHAPTER 2: RATIONALE & HYPOTHESIS	15
CHAPTER 3: MATERIAL & METHODS	17
3. 1. Data source and analysis	17
3. 1. 1. The source and statistical analysis of magnetic resonance imaging data	17
3. 1. 2. Genetic data and mapping methodologies	19
3. 2. Develop neural network models of brain activity obtained using MRI imaging	22
3. 2. 1. Wilson-Cowan single brain region neural field model	26

3. 2. 2. Blood oxygen level dependence model	31
3. 3. Model optimization methods	34
3. 3. 1. Optimization strategy for whole brain model	34
3. 3. 2. Parameter optimization process based on Bayesian optimization	36
3. 3. 3. Riemann distance	42
CHAPTER 4: RESULTS	47
4. 1. Single patient modeling	47
4. 2. Computing and Analyzing Global Brain Connectivity	53
4. 3. Model construction from a genetic perspective	58
4. 3. 1. Integration results of transcriptome data models	59
4. 4. Model modification	64
4. 4. 1. Network properties of schizophrenic patients and healthy controls	65
4. 5. Identification of Potentially Impaired Brain Regions	71
CHAPTER 5: SUMMARY & DISCUSSION	73
CHAPTER 6: FUTURE RESEARCH	75
References	77

Abstract (EN)

Background: Schizophrenia is a complex disorder with multifactorial etiology involving genetic, environmental, and biological factors. These intertwined factors contribute to the exceptionally complex and challenging pathogenesis of the disease. Despite some advancements in schizophrenia research, the lack of standardized therapeutic approaches undoubtedly adds to the challenges posed by the disorder. Therefore, deeper understanding of this disorder is warranted to identify more effective treatment strategies.

The brain, composed of intricate networks of neurons forming complex synaptic connections, represents the most sophisticated structure governing cognitive processes and behaviors within the nervous system. Recent technological advancements such as magnetic resonance imaging, large-scale brain models, and transcriptomic data offer the potential to reveal aberrant connectivity patterns within the brains of schizophrenia patients, providing new perspectives for research and intervention.

Objective: This research primarily focuses on differences in brain activity patterns between individuals with schizophrenia and healthy controls.

Methods: A mesoscopic-scale brain model is constructed employing a standard MRI dataset containing details of structural and functional connections. Using a field model methodology, this study attempts to simulate brain neural behaviors in different groups and individuals, approximating the empirical functional and structural connectivity data. The interconnected neural network model utilizes coupled Wilson-Cowan models with each representing a given brain region, traversing high-dimensional parameter spaces, thereby enhancing our understanding of brain operations under different conditions. Furthermore, in exploring the role of receptor expression in schizophrenia, this study integrates receptor gene expression maps from the Allen Brain Institute. This integration aims to reveal potential variations in receptor expression among schizophrenic patients, establishing a connection between the computational model and the biological impacts triggered by receptor expressions.

Results: Through whole-brain simulations using the original Wilson-Cowan model, we observed some differences between the two groups at the aggregate level. However, it is worth noting that

these differences are not captured by significant differences in the model parameters, which may imply that the differences between the groups stem from other factors not directly captured by the model. Preliminary findings highlight differences among the participant groups, particularly concerning 5-HT1A receptor expression. For a more refined exploration, specifically regarding variations in receptor expression in distinct brain regions, this study applies some adjustments to the original receptor expression data. The adjusted fitting results align with previous literature reports.

Conclusion: This study elucidates brain characteristics through large-scale simulations, revealing SC-FC correlations and optimal structure-function relationships. Focused on schizophrenia, it constructs a mesoscopic brain model, integrating receptor expression data to highlight differences in patients, particularly in 5-HT1A receptor expression.

Keywords: Whole-Brain Computational Model, Schizophrenia, Functional Networks, Genomics

Abstract (FR)

Contexte: La schizophrénie est un trouble complexe dont l'étiologie multifactorielle implique des facteurs génétiques, environnementaux et biologiques. Ces facteurs imbriqués contribuent à la pathogenèse exceptionnellement complexe et difficile de la maladie. Malgré certains progrès dans la recherche sur la schizophrénie, le manque d'approches thérapeutiques standardisées ajoute indéniablement aux défis posés par le trouble. Par conséquent, une investigation et une exploration plus approfondies sont justifiées pour identifier des stratégies de traitement plus efficaces.

Le cerveau, composé de réseaux complexes de neurones formant des connexions synaptiques complexes, représente la structure la plus sophistiquée gouvernant les processus cognitifs et les comportements au sein du système nerveux. Les récents progrès technologiques tels que l'imagerie par résonance magnétique, les modèles cérébraux à grande échelle et les données transcriptomiques offrent le potentiel de révéler des schémas de connectivité aberrants dans les cerveaux des patients schizophrènes, ouvrant de nouvelles perspectives pour la recherche et l'intervention.

Objectif: Cette recherche se concentre principalement sur les différences dans les schémas d'activité cérébrale entre les individus schizophrènes et les témoins en bonne santé.

Méthodes: Un modèle cérébral à l'échelle mésoscopique est construit en utilisant un ensemble de données d'IRM standard contenant des détails sur les connexions structurelles et fonctionnelles. En utilisant une méthodologie de modèle de champ, cette étude tente de simuler les comportements neuronaux cérébraux dans différents groupes et individus, en approximant à travers des données empiriques de connectivité fonctionnelle et structurelle. Le modèle de réseau neuronal interconnecté utilise des modèles couplés Wilson-Cowan, chacun représentant une région cérébrale donnée, traversant des espaces de paramètres de haute dimension, améliorant ainsi notre compréhension des opérations cérébrales dans différentes conditions. De plus, en explorant le rôle de l'expression des récepteurs dans la schizophrénie, cette étude intègre des cartes d'expression des gènes de récepteurs de l'Institut du Cerveau Allen. Cette intégration vise à révéler des variations potentielles dans l'expression des récepteurs chez les patients schizophrènes, établissant un lien entre le modèle computationnel et les impacts biologiques

déclenchés par les expressions de récepteurs.

Résultats: Les résultats indiquent quelques différences entre les deux groupes au niveau de la population en utilisant le modèle Wilson-Cowan original mais sans exprimer de disparités de paramètres significatives. Les résultats préliminaires mettent en évidence des différences entre les groupes de participants, notamment en ce qui concerne l'expression des récepteurs 5-HT1A. Pour une exploration plus raffinée, notamment en ce qui concerne les variations de l'expression des récepteurs dans des régions cérébrales distinctes, cette étude applique quelques ajustements aux données d'expression des récepteurs originales. Les résultats ajustés concordent avec les rapports de littérature précédents.

Conclusion: Cette étude éclaire les caractéristiques du cerveau à travers des simulations à grande échelle, révélant des corrélations SC-FC et des relations structure-fonction optimales. Axée sur la schizophrénie, elle construit un modèle cérébral mésoscopique, intégrant des données d'expression des récepteurs pour mettre en évidence les différences chez les patients, notamment dans l'expression des récepteurs 5-HT1A.

Mots clés: Modèle informatique du cerveau entier, schizophrénie, réseaux fonctionnels, génomiqu

Acknowledgments

I would first like to express my sincere gratitude towards the patients and their families who volunteered to participate in this study, as well as towards the healthy control participants for taking the time to contribute to scientific research.

I would like to thank my supervisors, Dr. Anmar and Dr. Guo, for guiding me throughout this whole process and providing ample support. I have learned so much from them both and am beyond grateful to have had them by my side.

I would also like to thank my committee members, Dr. Misic and Dr. Cook, for their guidance and expertise, as well as Dr. Boudrias for her help.

Finally, I would like to express my gratitude towards my family and friends who supported me in any way they could throughout my graduate studies. They gave me the strength to persist and persevere throughout this experience and I will continue to do so in the years to come.

Contribution of authors

The body of work presented in this thesis would not have been made possible without a close collaboration between myself and my M.Sc. supervisors, Anmar Khadra and Daqing Guo. Listed below are the specific contributions:

Nianqi Deng (author) conducted this overall thesis, which consisted of writing this manuscript, construct the model, analysis the data, interpreting results, and thesis preparation/revision.

Dr. Anmar Khadra (Supervisor): study conception and design, assistance in data analysis and results interpretation.

Dr. Daqing Guo (Co-Supervisor): study conception and design, assistance in data analysis and results interpretation.

Dr. Misic, Bratislav and Cook, Erik (Advisory Committee): guidance in data analysis and interpretation.

List of Tables

Table 3- 1 Subject Information	17
Table 3- 2 Brain region arrangement and names	23
Table 4-1 Division of brain lobes	53
Table 4-2 Brain functional sub-network partitions	57

List of Figures

Figure 3-1 Display of Original Microarray Data and Mapping Results
Figure 3-2 The schizophrenia group and the control group experienced SC and FC 24
Figure 3-3 Conceptual diagram of the model
Figure 3-4 illustration of Incorporating Transcriptomic Data into the Model
Figure 3-5 illustration of the average excitatory firing rates across various brain regions obtained through model simulations
Figure 3-6 illustration of the average inhibitory firing rates across various brain regions obtained through model simulations
Figure 3-7 Process of BOLD signal simulation for control group subjects
Figure 3-8 Process of BOLD signal simulation for schizophrenia group patients in the model
Figure 3-9 Traversing the coupling factor G to simulate the optimal functional connectivity 34
Figure 3-10 Iterative optimization process
Figure 3-11 Iterative process of the Bayesian optimization algorithm in the two-dimensional parameter space of the Wilson-Cowan model
Figure 3-12 Parameter topology space using different distance metrics during model parameter search
Figure 4-1 Results of the model parameter search using the Bayesian optimization method48
Figure 4-2 Envelope plots of firing rates for the control group
Figure 4-3 Envelope plots of firing rates for the schizophrenia group
Figure 4-4 Firing rate and excitation inhibition ratio of the control group and the

schizophrenia group
Figure 4-5 Simulated functional connectivity (FC) matrices for the control group and the schizophrenia group
Figure 4-6 Changes of functional connectivity strength with brain regions under group average
Figure 4-7 Functional connectivity strength across brain lobes
Figure 4-8 illustration of the changes in functional connectivity strength across brain networks
Figure 4-9 Schematic diagrams of receptor expression utilized in the study61
Figure 4-10 Results of integrating genetic data into the model
Figure 4-11 Results of Shapiro-Wilk normality tests68
Figure 4-12 Mann-Whitney test
Figure 4-13 Modified result in the prefrontal lobe and the principal component analysis result

List of Abbreviations

SC Structural Connectivity

FC Functional Connectivity

GBC Global Brain Connectivity

MRI Magnetic Resonance Imaging

BOLD Blood Oxygen Level-Dependent Signal

dMRI diffusion Magnetic Resonance Imaging

fMRI functional Magnetic Resonance Imaging

DMN Default Mode Network

ATN Attention Network

AUN Auditory Network

VIS Visual Network

SMN Somatomotor Network

SUN Subcortical Network

TMS Transcranial Magnetic Stimulation

rTMS repetitive Transcranial Magnetic Stimulation

AHBA Allen Human Brain Atlas

OFC Orbitofrontal Cortex

PFC Prefrontal Cortex

DLPFC Dorsolateral Prefrontal Cortex

Introduction

Schizophrenia is a mentally intricate disorder with a multifaceted etiology involving interactions among various genetic, environmental, and biological factors. Despite notable progress in research, the pathogenesis of schizophrenia remains exceptionally intricate and elusive. The absence of standardized therapeutic approaches poses significant challenges for both patients and healthcare professionals, highlighting the urgent need for deeper investigation and exploration to identify more effective treatment modalities.

The brain, comprising billions of neurons forming intricate synaptic networks, stands as one of the most complex structures governing cognitive processes and behaviors. Advancements in computational methods have enabled researchers to explore the dynamic properties of the brain's resting-state networks, unveiling its operational mechanisms through modeling approaches¹. Neural imaging techniques have revealed the patterns of structural connectivity (SC) and the collaborative effects of functional connectivity (FC) in the brain. It has been demonstrated that damage to SC significantly influences FC², with studies indicating that the structure-function relationship is maximized at critical points of dynamic functional or state transitions, optimizing the model's reproduction of brain FC. The integration of large-scale brain simulations with brain imaging techniques facilitates the establishment of refined whole-brain computational models, providing a solid model foundation and theoretical support for investigating the pathogenesis of schizophrenia and developing effective intervention measures³. However, there is currently limited research integrating genetic data with large-scale brain models, which to some extent restricts a comprehensive understanding of the mechanisms of schizophrenia.

In recent years, with the continuous development of technologies such as magnetic resonance imaging, large-scale brain models, and transcriptome data, there is hope that the combination of these technologies can reveal abnormal connectivity patterns within the brains of schizophrenia patients, offering new perspectives for research and intervention. To address this research gap, this study aims to develop a novel approach by integrating magnetic resonance imaging and genetic data into large-scale brain models to delve into the mechanisms and regulatory loci of schizophrenia. Leveraging knowledge from computational neuroscience, we will investigate the characteristics of schizophrenia patients' brains at rest from the perspective of large-scale brain simulations and compare them with healthy control groups.

By combining neuroimaging and genomics research methods, we hope to gain a more comprehensive understanding of the neurobiological basis of schizophrenia, providing more effective choices for the diagnosis and treatment of this disorder to improve patients' quality of life. Additionally, this study will contribute to a deeper exploration of human brain function and related disorders, offering important insights for future schizophrenia research. In summary, this study aims to fill the current gaps in schizophrenia research, providing new perspectives and methods for unraveling the mechanisms of schizophrenia and developing personalized treatment plans, ultimately aiming to enhance the quality of life for patients.

CHAPTER 1: BACKGROUND INFORMATION

1. 1. Complex threads of Schizophrenia

Schizophrenia is a common mental disorder characterized by widespread abnormalities in reality perception and thought processes⁴. Typically, the incidence of schizophrenia is higher among adolescents and young adults, affecting approximately 1% of the global population, with similar prevalence rates in males and females⁵. Symptoms in individuals with schizophrenia can be categorized into positive, negative, and disorganized symptoms⁶. Positive symptoms involve heightened mental activity such as hallucinations, delusions, and thought disorders; negative symptoms include reduced mental activity like emotional blunting, social withdrawal, and slowed thinking; disorganized symptoms typically manifest as speech disturbances, including incoherent or "off-track" speech. Furthermore, schizophrenia also exhibits cognitive impairments such as declining memory and lack of concentration⁷. Schizophrenia poses significant risks to individuals, families, and even public safety. Presently, the pathophysiology of schizophrenia remains under exploration, and there is no standardized medication or physical therapy regimen⁸. If left unaddressed, it will lead to immeasurable serious consequences for individuals, families, and society.

1.1.1. Neuroimaging of Schizophrenia

1. 1. 1. 1. Magnetic resonance imaging

With the advancement of Magnetic Resonance Imaging (MRI) technology, researchers have further developed large-scale brain simulation techniques by acquiring data on structural connectivity (SC) and functional connectivity (FC) of the brain through diffusion Magnetic Resonance Imaging (dMRI) and functional Magnetic Resonance Imaging (fMRI), respectively. dMRI involves scanning the diffusion of water molecules in different directions within the brain to obtain diffusion coefficients in various directions, thereby inferring information about the direction and length of neuronal axons. Utilizing this technique, researchers can acquire information about the connectivity of neural fiber bundles within the brain, including the direction, density, and size of these fiber bundles, and subsequently compute the brain's SC^{9,10}. fMRI, on the other hand, is based on the blood oxygen level-dependent (BOLD) signal¹¹ and

involves the interaction between oxygen in the blood and hemoglobin. The intensity of this interaction is influenced by the local level of neural activity. An increase in local neural activity results in an increased oxygen demand, leading to enhanced blood flow and increased oxygen content in the blood, thereby causing an enhancement in the BOLD signal. Consequently, changes in the BOLD signal across different brain regions can reveal alterations in brain region activities¹². Additionally, fMRI can be categorized into resting-state fMRI and task-based fMRI. Resting-state fMRI measures brain activity when the subject is not performing specific tasks, revealing the functional connectivity between different brain regions¹³. Task-based fMRI measures brain activity while the subject performs specific tasks, disclosing brain activity patterns and functional regions during different tasks¹⁴. By constructing large-scale whole-brain computational models based on acquired SC and FC data from experiments, researchers can better explore the interactions and neural mechanisms between different brain regions. This lays a solid foundation for the further advancement of large-scale brain simulation techniques to higher levels.

1. 1. 2. Current status of Schizophrenia research

In the field of biotechnology, numerous studies have emphasized the multifactorial nature of schizophrenia, including genetic, environmental, neurochemical, neuroimaging, and neural network factors.

1. 1. 2. 1. Neurobiological mechanisms of schizophrenia

In recent years, with the rapid advancement of fMRI technologies, there has been increasing attention towards the abnormal connections within the functional networks of schizophrenia¹⁵. The disruption in functional connections may be a pathological mechanism underlying cognitive impairments in schizophrenic patients. Early research has found widely distributed disruptions in functional connections in schizophrenic patients, presenting abnormalities in connectivity in the medial frontal lobe, frontoparietal junction, occipital-temporal junction, and dorsolateral prefrontal cortex^{16,17,18,19}. Indeed among patients with schizophrenia, the most affected functional network is the attention network, followed by the visual network and the default network²⁰. Studies have also reported disruptions in the connectivity between regions within the cortical-cerebellar-thalamic-cortical circuit and the Default Mode Network (DMN) in schizophrenic

patients^{21,22}. These abnormalities manifest most prominently in clinically relevant brain regions, where anomalies in the medial prefrontal cortex, posterior cingulate cortex, and other DMN areas might lead to deficits in self-control and introspection^{23,24}, whereas abnormalities in the dorsolateral prefrontal cortex may result in decreased information processing capabilities²⁵.

Frontal association with schizophrenia often exhibits a close connection, a fact substantiated by numerous studies. Indeed, studies have highlighted region-specific volumetric deficits in the orbitofrontal cortex (OFC) among individuals with schizophrenia^{26,27}. They emphasize the link between OFC volume deficit and schizophrenia along with thought disorders, and underscores morphological alterations in the orbitofrontal cortex within this population, emphasizing the pivotal role of specific brain regions like the OFC in understanding the neurobiological underpinnings of schizophrenia.

Additionally, research by Waltz and Gold²⁸ suggests that ventral aspect dysfunction of the prefrontal cortex (PFC) is a prevalent phenomenon in the pathophysiology of schizophrenia. This impairment potentially leads to deficits in reinforcement learning exhibited by affected individuals, where the dopaminergic system might play a crucial role, necessitating further research for a comprehensive understanding.

Schizophrenia patients also exhibit reduced gray matter volume in specific temporal lobe regions compared to healthy controls and first-episode affective psychosis individuals²⁹. This includes notable reductions in the left middle temporal gyrus, bilateral inferior temporal gyri, left superior temporal gyrus, and bilateral fusiform gyri. Moreover, the severity of hallucinations correlates significantly with decreased volumes in the left hemisphere's superior and middle temporal gyri³⁰.

In the context of therapeutic interventions, currently available antipsychotic medications predominantly target the blockade of specific receptor subtypes within these neurotransmitter families³¹. By doing so, these medications aim to modulate neurotransmitter signaling, particularly in dopamine pathways, and thereby provide a relative reduction in the occurrence and severity of psychotic episodes in individuals with schizophrenia.

1. 1. 2. 2. Advancements in the regulation of schizophrenia

The treatment of schizophrenia is diverse, including pharmacotherapy, psychotherapy, and

transcranial magnetic stimulation (TMS), among others. Among these modalities, pharmacotherapy is the primary approach, mainly utilizing antipsychotic medications to alleviate patients' symptoms. Currently, available antipsychotic drugs primarily target specific subtypes of neurotransmitter receptors to modulate neurotransmitter signaling³². Typical antipsychotic drugs such as chlorpromazine and haloperidol primarily act by blocking dopamine D2 receptors, thereby reducing their impact on the central nervous system³³. Atypical drugs such as olanzapine and risperidone, on the other hand, modulate the activity of dopamine and serotonin receptors, alleviating patients' symptoms³⁴. Dopamine regulation is also crucial for the function of the prefrontal cortex. Studies have shown that dopamine D2 receptors enhance cellular excitability through a stimulatory G-protein pathway³⁵. Although pharmacotherapy yields significant effects, it often comes with side effects such as obesity and anxiety.

Schizophrenia patients exhibit significant impairments in cognitive functions such as attention, memory, and executive functions³⁶. TMS, as a non-invasive therapeutic method, has attracted attention and interest due to its unique advantages. Research indicates that high-frequency stimulation can improve patients' selective attention deficits and attentional diffusion symptoms³⁷, although not all patients show significant improvements³⁸.

Animal experiments have shown that repetitive Transcranial Magnetic Stimulation (rTMS) stimulation can enhance hippocampal synaptic plasticity and improve spatial cognitive function³⁹. In the treatment of schizophrenia, rTMS has shown promising results, not only improving cognitive impairments but also demonstrating efficacy in alleviating both negative and positive symptoms⁴⁰.

The efficacy of rTMS depends on the stimulation frequency, with low-frequency stimulation helping to reduce auditory hallucinations, while high-frequency stimulation improves negative symptoms and cognitive function. Considering that tissue disruption manifests as brain connectivity disorders in schizophrenia, rs6295 G-carriers exhibit lower HTR1A expression in specific brain regions⁴¹, which may be associated with the relief of symptoms using TMS stimulation of the DLPFC region commonly used in hospitals⁴². However, the therapeutic effects of rTMS are influenced by various factors, including the site of stimulation, frequency range, stimulation intensity, and duration. It should be noted that rTMS may induce adverse reactions such as seizures, thus requiring careful treatment planning.

In summary, the treatment of schizophrenia includes various modalities such as pharmacotherapy, physical therapy, and psychotherapy, among others. Novel treatment methods such as optogenetics and rTMS also show potential therapeutic effects but require further research and clinical validation.

1. 2. Large-scale brain simulation's applications in brain disorders

1. 2. 1. Overview of large-scale brain simulation

To construct scalable brain models, there are two main technical approaches: bottom-up and top-down. The bottom-up approach relies on a large number of interconnected nodes, such as the Hodgkin-Huxley (HH) model⁴³ or the Leaky & Integrate Fire (LIF) model⁴⁴, with the former describing the generation of neuronal action potentials and the latter being a simplified model suitable for simulating large-scale neural networks⁴⁵. In contrast, the top-down approach fits foundational models to neural data and incorporates brain representation properties, although its complexity and "black box" nature may hinder widespread adoption⁴⁶.

In the evolution of neural network models, methods such as ResNet have emerged to address issues like gradient vanishing and overfitting. However, these methods lack biological support, prompting a reexamination of classical neural models based on biological features. It is necessary to construct networks based on classical neural models that preserve biological features, as these traditional models are grounded in experimentation and theory, anchored in biological reality, and therefore possess significant advantages.

In modeling networks with the scale of brain, challenges include not only demanding computational performance and communication efficiency but also fitting real physiological data. Despite the existence of optimization methods⁴⁷, simulating corresponding lengths of real physiological neural activity within the same physical time frame remains elusive. Furthermore, data quality is equally crucial for model construction⁴⁸, requiring assurance to avoid contradictory conclusions in simulated experiments⁴⁹.

The conservatism of brain structure and function provides some guidance for brain modeling research. Large-scale brain simulation aims to establish biologically based models that strive to simulate neuronal structure and function as realistically as possible. These models rely on prior

knowledge obtained from neuroscience research and biological experiments, enabling them to simulate processes closely resembling those within real neural systems.

As research on brain network models progresses, the focus has shifted from the macaque cortex⁵⁰ to the human cortex⁵¹. Scholars have successfully predicted resting-state functional connectivity using nonlinear neural models and structural connections derived from diffusion tensor imaging, revealing significant changes in functional connectivity due to lesions at the junction of the midline and temporal lobe with the parietal lobe⁵². Moreover, researchers have simulated resting-state functional connectivity using a Kuramoto model based on human brain structural connections, revealing the relationship between local oscillatory activity within brain regions and functional connections between different brain regions⁵³. Deco et al. utilized a globally attracting interconnected excitatory pyramidal neuron population and inhibitory GABAergic neuron population network to simulate brain regions and studied the characteristics of brain activity in the resting state. Their research revealed the criticality of brain working states, lying between chaos and order, with multiple competitive states¹².

However, studies on structural connections based on diffusion tensor imaging or diffusion spectrum imaging in the macaque or human brain have revealed a lack of interhemispheric connections in structural connections, leading to low consistency between simulated and experimental functional connections. To address this issue, scholars have proposed a "structure-function" iterative optimization strategy⁵⁴. By using a dynamic mean-field model to construct functional networks of macaques and humans and adjusting and weighting structural connections using empirical functional connections, this method significantly improved the correlation between simulated and experimental functional connections by fine-tuning a small number of anatomical connections.

The Wilson-Cowan model is a commonly used mathematical model for describing the activity of neuronal populations⁵⁵. Some studies have used the Wilson-Cowan model to construct human cortical network models, revealing the criticality of brain working states and the characteristics of the alpha band⁵⁶. Meanwhile, some studies have established hierarchical network models based on the Wilson-Cowan equation to better understand interactions between neurons and signal transmission in different frequency regions⁵⁷.

In conclusion, constructing scalable brain models is a complex and challenging task that requires comprehensive consideration of biological theory, computational methods, and experimental data to better understand and simulate the structure and function of the brain.

1. 2. 2. Brain disease research based on large-scale brain models

The study of psychiatric disorders faces significant challenges, including the difficulty of integrating and analyzing large datasets, as well as physiological and therapeutic challenges. Computational psychiatry, as an emerging approach, provides means to enhance the analysis of large complex datasets and plays an important role in psychiatric disorder research⁵⁸. The development of this field has facilitated progress in psychiatric disorder research and provided opportunities for interdisciplinary collaboration. For example, computational psychiatry involves physical information of neural circuit models applied to predicting treatment outcomes, studying conceptual forms of reward learning and reinforcement learning, and investigating neurobiology and cognitive dysfunction.

Developing computational models that describe the dynamics of subcortical regions can assist us in understanding brain mechanisms at the whole-brain level. For instance, a study utilizing data from 22 patients with left temporal lobe epilepsy and 39 healthy controls constructed a whole-brain computational model, revealing situations where some patients were more prone to transition into epileptic states⁵⁹. Additionally, the combination of neuroscience and computational models also plays a crucial role in researching diseases such as Parkinson's disease. For example, Kringelbach et al. revealed the impact of deep brain stimulation on functional brain networks in Parkinson's disease patients by analyzing pre- and post-operative data⁶⁰.

In drug development, Deco et al.'s study utilized a whole-brain neural imaging model to explain LSD's nonlinear functional effects on the brain, paving the way for new treatments for neurological and psychiatric disorders³. Similarly, Perl et al. revealed potential mechanisms of neurodegenerative diseases through model-based studies of empirically structured connectivity coupled with local dynamics research and proposed corresponding interventions⁶¹.

Functional disorders of the nervous system are a significant feature of schizophrenia; research on neural connectivity, pharmacology, and computational modeling of the etiology of schizophrenia has been of critical importance. Through the lens of computational neuroscience, research

spanning various levels, from receptors and individual cells to intricate neural circuits, can be seamlessly interconnected, culminating in a comprehensive understanding of neural system behavior⁶². For instance, functional connectivity metrics can bridge the gap between various levels, allowing us to systematically explain schizophrenia symptoms through functional neuroimaging and pharmacology. Computational neuroscience can also help explain observed complex behaviors and functional disorders and the underlying neural mechanisms by simulating neural circuits and systems.

In similar studies, researchers found that schizophrenia may be associated with defects in the glutamate neurotransmitter. This study indicates that abnormal inhibitory neural activity in schizophrenia patients affects the excitatory and inhibitory balance in the brain cortex⁶³. Model-based research has proposed some drug options for treating schizophrenia, such as NMDA receptor antagonists (e.g., ketamine) and metabolic glutamate receptor antagonists (e.g., MK-801).

Researchers have also investigated connectivity disruptions at the functional level in schizophrenia patients and proposed neuroscience-based computational models⁶⁴. The model predicts changes in network connectivity in schizophrenia patients by analyzing neuroimaging data, finding that changes in network connectivity in schizophrenia patients are consistent with model predictions, while bipolar affective disorder patients do not show such changes. This indicates that changes in network connectivity in schizophrenia patients may be caused by normal neural circuit characteristics, leading to disruptions at specific functional levels.

The application of multimodal data has become a trend in neuroscience research. Structural data of the brain provide patterns of neuronal connections, while functional connectivity data reveal interaction patterns between different brain regions. By combining these data, a multi-level, multi-scale network model can be established to comprehensively and deeply understand how the brain works. When delving into the mysteries of the brain, combining multiple modalities of data, such as brain structure, functional connectivity, and EEG data, one can establish multi-scale network models. However, despite significant progress in this research approach, particularly in combining diseases and genomics, there is little research in practical applications.

1. 2. 3. Exploration of the genetics and transcriptomics of Schizophrenia

1. 2. 3. 1. Application of AHBA microarray expression data

Genomic data refers to the recording and analysis of genomic information of humans or other biological organisms. These data provide detailed information on the composition, structure, and sequence of genes in organisms, offering essential genetic information and biological characteristics for biological research. Although in the past, integrating and analyzing such genomic data systematically and reliably into disease or model studies often faced challenges due to technological limitations, with the continuous innovation of gene sequencing technology, acquiring and analyzing genomic data has become increasingly integrated with other methods. Researchers can now use high-throughput sequencing technologies such as whole-genome sequencing and genome-wide association studies to obtain large-scale genomic data and conduct in-depth analysis and interpretation.

The Allen Institute for Brain Science has collected and integrated a vast amount of genomic datasets covering the location and intensity of central nervous system gene expression in both healthy and diseased individuals, spanning different developmental stages and including multiple species. The Allen Brain Atlas (www.brain-map.org), a freely accessible multimodal resource website, provides gene expression data, connectome data, and neuroanatomical information. This atlas includes gene expression data based on whole-genome arrays, in situ hybridization (ISH) studies of specific brain regions, and detailed records of neuronal structure and connections for these resources support research involving histology, microarrays, RNA sequencing, reference atlases, mapping, and magnetic resonance imaging. Additionally, they offer comprehensive data on the adult, developing mouse, human, and non-human primate brains, accompanied by powerful search and visualization tools.

In the SMART-seq database included in the Allen Brain Institute, transcriptomic data on receptor expression of various cell types in the human cortex can be accessed. Studies based on these data have revealed significant differences in transcriptional regulation between different anatomical locations and demonstrated highly conserved and stable molecular characteristics among different regions and their cell types⁶⁶. Further research indicates that gene expression and co-expression relationships in different brain regions reflect the distribution of cell types⁶⁷. Moreover, studies have attempted to explore the relationship between transcriptional differences and laminar features, cellular composition, and developmental processes⁶⁸. Thus, the Allen Brain

Atlas has become an essential open data resource driving neuroscience research.

1. 2. 3. 2. Advancements in Genetic Research on Schizophrenia

The structure and function of the human brain are highly conserved, indicating the presence of a conservative molecular program to regulate its development, cellular structure, and function⁶⁹. This finding provides predictability and regularity for scientific research. Studies have shown a close correlation between gene expression and functional circuits, as well as a mutual association between genes and the topological structure of connectomes⁷⁰, highlighting the importance and effectiveness of genes in regulating brain functional connections. However, the genetic inheritance of phenotypes is not immutable, and specific genetic variations may affect subcortical structures in various regions of the human brain⁷¹.

These properties of genes imply that a deeper understanding of normal and pathological brain function can be achieved through the study of genes, providing important clues for further exploration in neuroscience. Therefore, gene expression and transcriptomics contribute to accelerating research on both normal and pathological states of the brain, facilitating comprehensive exploration of the central nervous system⁷².

Schizophrenia often exhibits familial aggregation in genetics; estimates of the heritability of schizophrenia range from 70% to 80%, indicating that 70% to 80% of the risk variation for individuals developing schizophrenia is associated with genetic factors⁷³. The greatest risk factor for developing schizophrenia is having a first-degree relative with the disorder⁷⁴, and over 40% of schizophrenic patients' monozygotic twins are also affected⁷⁵. Candidate gene studies of schizophrenia have often failed to find consistent associations, while genome-wide association studies have identified genetic loci that explain only a small fraction of the disease variance.

Many genes are known to be involved in schizophrenia, but the effect of each gene is small, and the transmission and expression mechanisms are unclear^{76,77}. Approximately 5% of schizophrenia cases are attributed to rare copy number variations (CNVs)⁷⁸, with some anomalies increasing the risk of developing schizophrenia by up to 20 times. These CNVs are often comorbid with autism and intellectual disabilities⁷⁹.

Numerous whole-genome studies have identified multiple genes associated with the pathogenesis

of schizophrenia, such as dopamine receptor D2 (DRD2), serotonin transporter (5-HTT), and glutamate receptor (GRIN1), which play critical roles in neurotransmitter regulation^{80,81,82}. Additionally, some genes related to neurodevelopment and inflammatory responses, such as DISC1, are also considered to be associated with schizophrenia⁸³.

When discussing the pathogenesis of schizophrenia, researchers often establish links between dopamine receptor expression genes in the dopamine family⁸⁴ and serotonin receptor expression genes in the serotonin family⁸⁵, with each model playing a role in the neurobiology of schizophrenia. Aberrant dopamine signaling is considered to be associated with schizophrenia. The most common model is the dopamine hypothesis of schizophrenia, attributing schizophrenia to the brain's misinterpretation of dopamine neuron misfiring⁸⁶. There is also evidence that, compared to controls, levels of 5-HT1A receptor protein are decreased in the prefrontal cortex of female depressed suicide victims⁸⁷. This observation suggests that the prefrontal cortex also plays a crucial role in influencing central nervous system function.

Research by Scarr, Udawela, and Dean revealed significant changes in gene expression in the prefrontal cortex area of schizophrenia patients⁸⁸. This observation suggests that the prefrontal cortex also plays a crucial role in influencing central nervous system function. Changes in gene expression in this region may be related to cortical functional changes, leading to the manifestation of symptoms associated with schizophrenia. This highlights the possible interaction between neurotransmitter pathways, developmental mechanisms, and inflammatory pathways in the pathophysiology of schizophrenia.

Bridging theoretical models of schizophrenia to its genetic underpinning is quite complex and requires further in-depth investigation. Currently, researchers are gradually exploring this field, hoping to eventually construct and refine the overall theoretical framework by accumulating local theoretical knowledge. When discussing the pathogenesis of schizophrenia, we must consider the complex interactions between neurotransmitters, gene expression, brain region connectivity, and other aspects to fully understand the pathogenesis of this complex disease.

The application of multimodal data in neuroscience research has become a trend. Combining structural data and functional connectivity data can establish multi-level, multi-scale network models. Despite facing numerous challenges, combining large-scale brain simulation models

with diseases and genomics has tremendous potential and value in revealing the workings of the brain in disease states, bringing new insights and possibilities to medical research and clinical practice.

CHAPTER 2: RATIONALE & HYPOTHESIS

Modern neuroscience relies heavily on models as crucial instruments for investigation. These models, rich in parameterized features, display high-dimensional characteristics that help elucidate the underlying neural processes. Based on this, we formulate the following hypotheses:

Objective & Hypothesis #1

We plan to employ various algorithms and techniques, including single-patient modeling, Riemann distance computation, Bayesian optimization, and structural and functional connectivity analysis, among others, to conduct an in-depth implementation and optimization of our Wilson-Cowan model to describe brain activity. The utilization of these methods aims to more accurately describe the complex properties of neural networks, thereby enhancing our understanding of their behaviors and functionalities at the system level. Furthermore, these methodologies will enable us to better integrate and interpret intricate structural and functional connectivity patterns within the network architecture through more effective parameter tuning methods and a more rational approach to evaluating model performance. Through meticulous analysis and optimization of these highly parameterized models, we postulate that a deeper comprehension of the core operational principles of neural networks can be attained.

Objective & Hypothesis #2

By merging genomic data with our models in Objective #1 using resources such as the Allen Brain Atlas, we aim to explore the relationship between schizophrenia-related genes and neural networks using mapping methods. This step aims to discover and understand the impact of receptor expression (including the serotonin and dopamine family receptors) on neural system functionality and plasticity, providing new avenues and methods for future neurological disease research. We further hypothesize that the amalgamation of genomic data with these models will unveil profound insights. This deep data integration approach has the potential to reveal connections between genes and the functionalities of neural systems. We believe this comprehensive method will not only bolster our understanding of neural systems but also pave

the way for novel targets and therapeutic strategies in treating neurological disorders.

Objective & Hypothesis #3

Although the specific pathophysiology of schizophrenia remains unclear, its treatment often involves interventions targeting specific brain regions, such as the use of high-frequency repetitive transcranial magnetic stimulation (rTMS) on the patients' left dorsolateral prefrontal cortex (DLPFC). Our approach involves perturbing models to identify potentially affected brain regions and related network changes. This methodology aims to enhance our ability to simulate and predict potential alterations within the neural system affected by the disease. We believe that this step will deepen our understanding of the correlation between model parameters and the actual neural network, contributing to more accurate predictions and interpretations in neural systems research.

CHAPTER 3: MATERIAL & METHODS

3. 1. Data source and analysis

3. 1. 1. The source and statistical analysis of magnetic resonance imaging data

The data used in this study for SC and FC of schizophrenic patients and healthy controls were obtained from the Zenodo platform's publicly available dataset⁸⁹. This dataset comprises 27 healthy participants and 27 schizophrenia patients (https://zenodo.org/record/3758534). All data were acquired using a 32-channel head coil in a 3-Tesla MRI scanner. Schizophrenic patients were recruited from the general psychiatric services at the University Hospital of Lausanne and met the DSM-IV criteria for schizophrenia and schizoaffective disorders. Healthy control participants were recruited through advertisements and assessed using genetic research diagnostic interviews. Participants with severe mood disorders, psychosis, or substance use disorders, and those having first-degree relatives with psychiatric illnesses were excluded. Supplementary information about the participants is presented in Table 3-1.

Table 3-1 Subject Information

	Healthy Controls	Schizophrenia Patients
Number	27	27
Age (years)	35 ± 6.8	41 ± 9.6
Medication	0	421 ⊥ 200
Dosage (mg)	0	431 ± 288

The signal acquisition sequences consisted of the following: (1) Structural MRI: Magnetization Prepared Rapid Gradient Echo (MPRAGE) sequence with a slice resolution of 1mm, slice thickness of 1.2 mm, and a voxel size of $240 \times 257 \times 160$. TR, TE, and TI were 2300, 2.98, and 900 milliseconds, respectively; (2) Diffusion MRI: Diffusion Spectrum Imaging sequence with 128 diffusion-weighted images at b0 as reference, maximum b-value of 8000 s/mm2, acquisition time of 13 minutes and 27 seconds, voxel size of 96*96*34, resolution of 2.2*2.2*3.0 mm, TR of 6100 ms, and TE of 144 ms; (3) fMRI: Acquisition of an 8-minute resting-state fMRI (voxel size 3.3*3.3*3.3mm, TR = 1920ms, TE = 30ms, 32 slices, flip angle 85°). During fMRI

acquisition, participants were instructed to remain awake and refrain from performing any tasks.

The structural and diffusion MRI data were utilized for estimating weighted and undirected SC matrices within the connectivity mapping toolbox. Initially, the structural data underwent segmentation into white matter, gray matter, and cerebrospinal fluid, followed by linear registration to the b0 volume of the DSI dataset. Subsequently, a Lausanne multiscale atlas was employed for segmenting gray matter into 66 cortical regions and 17 subcortical regions, totaling 83 brain areas. Moreover, these 83 brain regions were further parcellated into 129, 234, 463, and 1015 regions. Deterministic streamlined tractography estimated 32 diffusion directions per voxel, reconstructing SC matrices from the DSI data. A normalized connectivity density was employed to quantify structural connections between brain regions, defined as follows:

$$W_{ij} = \frac{2}{S_i S_j} \sum_{f \in E_f} \frac{1}{l(f)}$$
 (3-1)

where W_{ij} represents the connection between brain regions i and j, S_i denotes the surface areas of regions i, $f \in E_f$ signifies a streamline f belonging to the set of streamlines E, and f represents the length of a given streamline f.

The FC matrix is computed based on the fMRI BOLD time series. Initially, four time points were removed, resulting in a total of T = 276 time points for assessment. Rigid-body registration was applied to each time slice for motion correction. Subsequently, signal linear detrending, physiological nuisance correction through regression of white matter, cerebrospinal fluid, and six motion signals, and further correction for motion artifacts were performed. Finally, spatial smoothing and bandpass filtering of signals were executed using a Hamming window with an FIR filter within the range of 0.01-0.1 Hz. Linear registration between the mean fMRI and MPRAGE images was conducted to obtain ROI time series. The FC matrix was derived by computing Pearson correlations among time series of each brain area. All these procedures were executed within the subjects' imaging native space using the Connectome Mapper toolbox, Python, and Matlab scripts.

To construct the functional connectivity (FC) matrix for each subject, the method of computing Pearson correlation coefficients between different brain regions' BOLD signals is utilized. Specifically, assuming the BOLD signal of brain region i is represented as A and the BOLD

signal of brain region j is represented as B, the value of functional connectivity FC_{ij} can be calculated as:

$$FC_{ij} = \frac{\sum_{t=1}^{n} (A_t - \overline{A})(B_t - \overline{B})}{\sqrt{\frac{1}{T} \sum_{t=1}^{T} (A_t - \overline{A})^2} \sqrt{\frac{1}{T} \sum_{t=1}^{T} (B_t - \overline{B})^2}}$$
(3-2)

The Pearson correlation coefficient in the functional connectivity matrix takes real values ranging from 0 to 1 and does not follow a normal distribution. To improve the efficiency of analyzing the functional connectivity matrix, this study employs the Fisher-Z transformation to convert Pearson correlation coefficients. The specific transformation formula is as follows:

$$Z = \frac{1}{2}\log(\frac{1+x}{1-x})$$
 (3-3)

With this formula, one can transform the original Pearson correlation coefficients into Fisher-Z values that follow a normal distribution, thus facilitating better analysis and processing.

3. 1. 2. Genetic data and mapping methodologies

The establishment of heterogeneous models involves the utilization of receptor gene data from the Allen Human Brain Atlas (AHBA) and necessitates the introduction of additional terms in the model. The objective is to compare the macroscopic effects and dynamic changes of different receptors and neurotransmitters in various brain regions, aiming to analyze the underlying pathogenic mechanisms of schizophrenia. The specific methodologies are elaborated in the section "Wilson-Cowan single brain region neural field model", akin to adjusting two parameters governing the firing rates of excitatory and inhibitory neuronal populations based on gene expression levels⁹⁰.

By dissecting the intricate interactions between genetic factors and brain function, avenues for precision medicine approaches can be paved, enabling diagnostics tailored to specific neural circuits and the development of targeted therapeutic interventions for neuro-psychiatric patients.

Despite the availability of openly accessible datasets like AHBA, variations in researchers' methodologies can lead to disparate experimental outcomes using the same data, as the choice of data processing methods can influence study results to some extent. Some key steps include re-

annotating gene expression data probes, data filtering, probe selection, mapping samples to brain region spaces, mitigating the impact of individual differences, and accounting for spatial effects.

Standardizing the steps for genetic data is crucial and adopting standardized and systematic mapping methods becomes paramount. Standardization procedures aid in establishing more reliable benchmarks for human brain genetics, facilitating data exchange and sharing within the field. By employing these methods, consistency, and reproducibility are ensured when dealing with intricate, complex data. Abagen, encompassing procedural workflows for genetic data, is an exemplary toolbox meeting these requirements. It helps reduce various types of errors, enhancing result reliability, and enabling comparability across studies or experiments^{91,92}.

Specifically, to accurately align microarray samples to brain atlases, gene microarray data is mapped to cortical or subcortical spaces in volume space by minimizing the three-dimensional Euclidean distance between microarray samples and template coordinate points. In cases of multiple adjacent regions, determining the closer one involves calculating the centroid of neighboring areas. For areas not directly sampled, any blank areas are assigned the expression value of the nearest tissue sample (defined as the sample with the smallest Euclidean distance to the centroid of the partitioned brain region); an iterative expansion searches neighboring samples, extending the search space (in 1 mm increments) outward by 2 mm to include nearby voxels.

During the exploration of mapping data onto graphs, it is essential to first calculate the Spearman correlation between the expression values of each probe across all donors' brain regions. Computing the average of these correlations and selecting probes with the highest correlations ensures the robustness of probe detection results. Additionally, normalization of the expression values of individual genes in microarray data for each sample and donor is crucial⁹³, achieved by normalizing microarray values using a sigmoid function:

$$x_{y} = \frac{1}{1 + \exp(\frac{-(x_{y} - \langle x \rangle)}{IOR_{x}})}$$
(3-4)

where <x> denotes the median and *IQRx* represents the normalized interquartile range of a given microarray expression value, computed as follows:

$$IQR_{x} = \frac{Q_{3} - Q_{1}}{2 \cdot \sqrt{2} \cdot erf^{-1}(\frac{1}{2})} \approx \frac{Q_{3} - Q_{1}}{1.35}$$
(3-5)

These values are then rescaled to the unit interval using a linear normalization function:

$$x_{norm} = \frac{x_{y} - \min(x)}{\max(x) - \min(x)}$$
(3-6)

Finally, averaging the corresponding values within each region and partitioning them into regions yields the average gene expression values for 83 regions of interest (ROIs). Visualization of the mapping results obtained after using Abagen is illustrated in Figure 3-1.

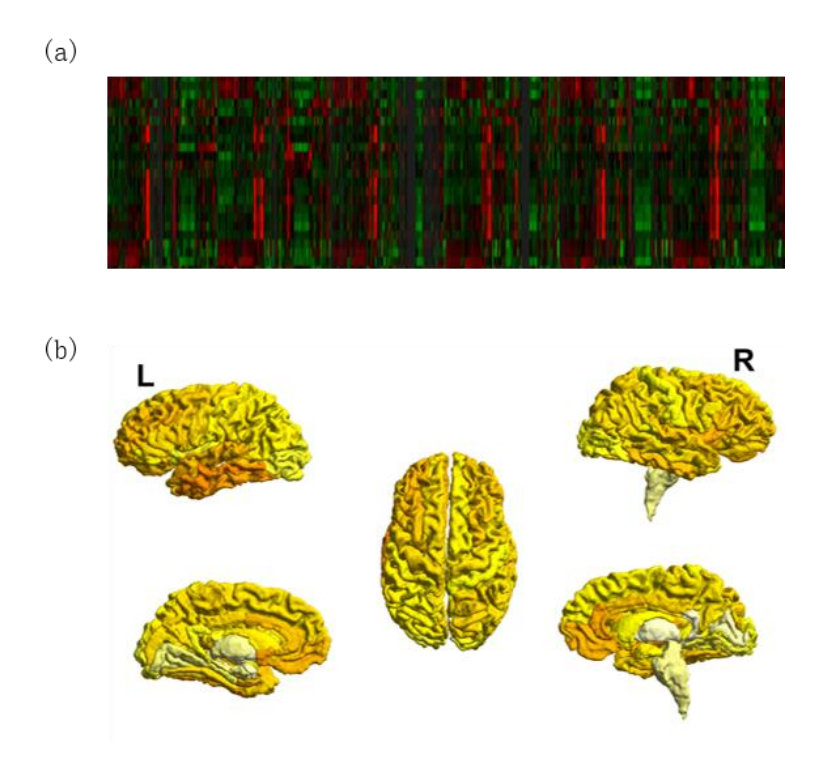


Figure 3-1 Display of Original Microarray Data and Mapping Results. (a) Partial display of original microarray data from the Allen Brain Atlas. (b) Example mapping results, visualizing expression data of the HTR1A receptor mapped to the Lausanne atlas.

3. 2. Develop neural network models of brain activity obtained using MRI imaging

The delineation of brain regions is crucial for brain modeling. Brain modeling often relies on accurate brain region parcellation templates, enabling researchers to represent brain structure and function precisely in computational models⁹⁴. These templates offer detailed descriptions of brain structure, dividing the brain into different regions and defining the spatial locations and connectivity patterns of these regions. In brain modeling, these templates provide a fundamental framework, allowing researchers to accurately simulate and explore the structure and function of the brain. By utilizing brain region parcellation templates, researchers can reproduce the true organization of the brain in computational models, facilitating in-depth investigations into brain activity and function⁹⁵.

Since brain region parcellation templates provide essential guidance and a foundation for brain modeling, studies on brain atlases play a critical role in delineating the complex structure of the human brain. Recent research emphasizes improvements in multi-atlas segmentation techniques, aiming to propose methods that enhance the accuracy and precision of brain region delineation, ultimately allowing for a more comprehensive understanding of neural structure and function^{96,97}. Techniques such as joint label fusion⁹⁸, local weighted voting⁹⁹, and automated anatomical labeling¹⁰⁰ exemplify the continuous efforts of scholars to improve.

Currently, widely used anatomical atlases include the Desikan-Killiany¹⁰¹, AAL¹⁰² (Automated Anatomical Labeling), MNI152¹⁰³ (Montreal Neurological Institute), and Lausanne atlases. By segmenting the brain into regions with specific anatomical and functional attributes, these atlases serve as indispensable tools for analyzing inter-regional differences and understanding the complex organization of the brain.

This study employed data from 27 patients with schizophrenia and 27 healthy controls, using the 83 brain region template from the Lausanne atlas for segmentation. This resulted in a structural connectivity (SC) matrix and functional connectivity (FC) matrix of size 83*83 for subsequent analyses. This whole-brain template comprises cortical and subcortical regions, with the 83 brain region SC and FC matrices used in the study consisting of 66 cortical regions and 17 subcortical regions. Specifically, subcortical regions include the insula, thalamus, caudate nucleus, putamen,

pallidum, ventral tegmental area, hippocampus, amygdala, and brainstem.

Table 3-2 lists the arrangement positions and corresponding English names of each brain region. Figure 3-2 illustrates partial SC and FC matrices of some patients with schizophrenia and normal controls.

Table 3-2 Brain region arrangement and names

Brain region identifiers	Brain region names	Brain region identifiers	Brain region names
1, 43	lateralorbitofrontal	22, 64	pericalcarine
2, 44	parsorbitalis	23, 65	lateraloccipital
3, 45	frontalpole	24, 66	lingual
4, 46	medialorbitofrontal	25, 67	fusiform
5, 47	parstriangularis	26.68	parahippocampal
6, 48	parsopercularis	27, 69	entorhinal
7, 49	rostralmiddlefrontal	28, 70	temporalpole
8, 50	superiorfrontal	29, 71	inferiortemporal
9, 51	caudalmiddlefrontal	30, 72	middletemporal
10, 52	precentral gyrus	31, 73	bankssts
11, 53	paracentral gyrus	32, 74	superior temporal
12, 54	rostralanteriorcingulate	33, 75	transversetemporal
13, 55	caudalanteriorcingulate	34, 76	insula
14, 56	posterior cingulate	35, 77	thalamus proper
15, 57	isthmuscingulate	36, 78	caudate
16, 58	postcentral gyrus	37, 79	putamen
17, 59	supramarginal	38, 80	pallidum
18, 60	superior parietal	39, 81	accumbensarea
19, 61	inferior parietal	40, 82	hippocampus
20, 62	precuneus	41, 83	amygdala
21, 63	cuneus	42	brainstem

A critical component of this modeling study is the Wilson-Cowan model and the blood oxygen level-dependent (BOLD) model, where the Wilson-Cowan model provides simulation of neural

field activity, while fMRI relies on the BOLD signal, translating neural activity into BOLD signals. This enables matching simulated data with experimental data, facilitating the evaluation of simulation results. The Wilson-Cowan model is a simplified model of neuronal population dynamics that uses a mean-field approach¹⁰⁴, neglecting many details between neurons such as chemical synapses and morphological features. It is a mathematical model used to describe the activity of neuronal populations, based on interactions between neurons to simulate the activity of neuronal populations, primarily used to study the dynamic properties of neuronal population activity. The model's construction is based on the following assumptions:

- (1) Neuronal populations can be divided into several interacting subpopulations, with interactions between neurons within each subpopulation.
- (2) The activity state of each neuronal population can be represented by variables, such as the action potential frequency of neurons.
- (3) The interactions between neurons can be represented by functions describing the mutual influence of neuronal activity states.

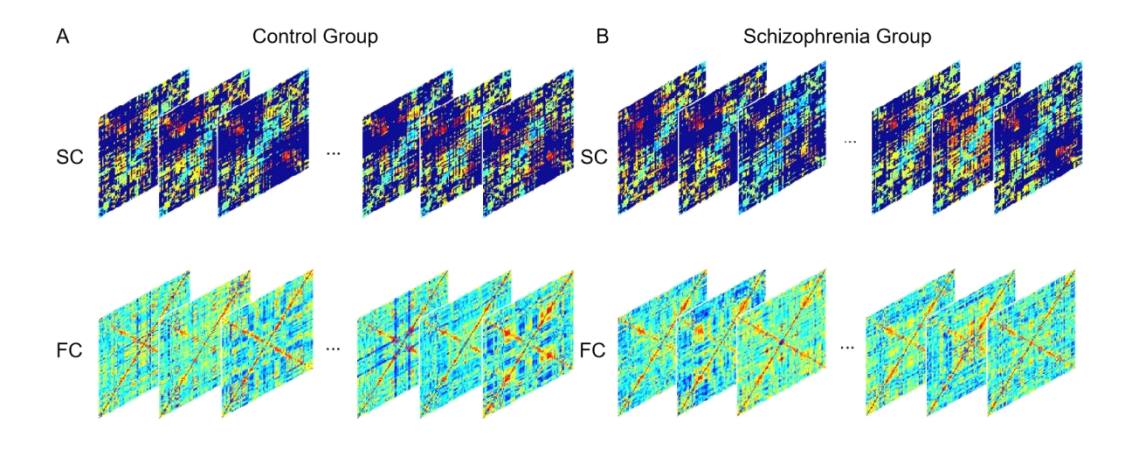


Figure 3-2 The schizophrenia group and the control group experienced SC and FC; a subset of the raw data have been presented. A. SC and FC of the control group. B. SC and FC of the schizophrenia group.

In this study, the whole-brain model treats each brain region as a set of Wilson-Cowan dynamic equations, comprising excitatory and inhibitory neurons. Each pair of differential equations

forms a unit cell, describing the temporal evolution of two mutually coupled inhibitory and excitatory neuronal populations using mean-field methods⁵⁵. The model employs nonlinear functions to represent interactions between neuronal populations, assuming that the neural circuit model in each brain region is composed of local networks formed by excitatory and inhibitory neuronal populations coupled by synaptic connections. The interactions between neuronal populations are described by connection weights estimated based on anatomical connectivity data⁵⁷. The numerical simulation method is commonly used to solve these equations, employing Euler's method or the Runge-Kutta method to approximate the differential equations.

The simulation of the whole brain is constructed using multiple coupled Wilson-Cowan models, with each model including the neural circuit architecture of a single brain region. These models consist of locally interconnected excitatory and inhibitory neuronal populations within each brain region, as illustrated in Figure 3-3.

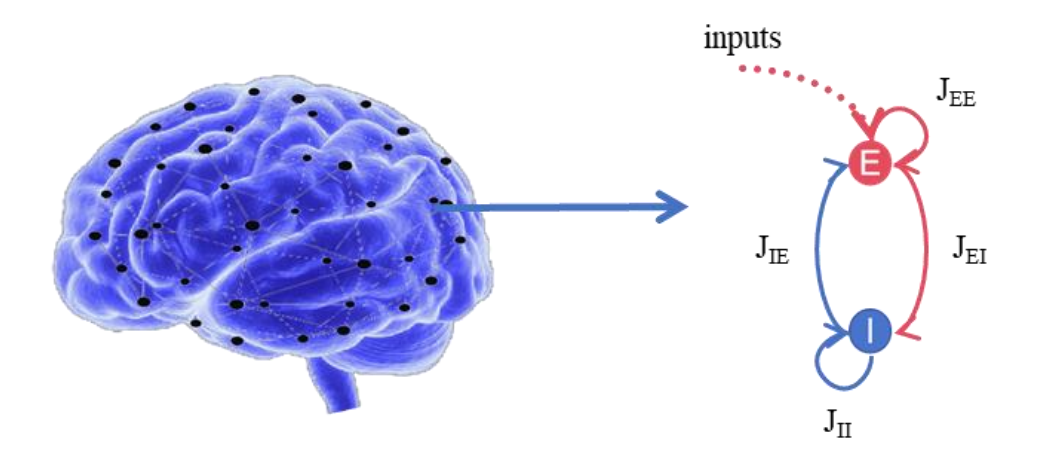


Figure 3-3 Conceptual diagram of the model. Here, JEE represents the synaptic strength between excitatory neurons, JEI signifies the strength of connections from inhibitory to excitatory neurons, JIE indicates connections from excitatory to inhibitory neurons, and JII represents the synaptic strength between inhibitory neurons.

The neural circuit model of each brain region consists of local networks formed by excitatory and inhibitory neuronal populations coupled via synaptic connections. External inputs come from excitatory populations of other brain regions.

3. 2. 1. Wilson-Cowan single brain region neural field model

This study establishes a large-scale brain model consisting of 66 cortical regions and 17 subcortical regions, providing a precise and simplified representation of real pulse networks at the mathematical level. The neuronal types within the network are diverse, encompassing neurons with excitatory and inhibitory synaptic receptors. In the model, these neurons are organized into inhibitory and excitatory populations in an orderly manner to simulate the complex interactions and dynamic balance in the brain. Notably, the coupling of individual regions in the model is initially achieved through an empirical structural connectivity (SC) matrix, ensuring a high degree of realism and practicality in both structure and function. The establishment of this brain model provides a powerful tool for delving into the workings of the brain⁵⁶, as depicted in Figure 3-3. Assuming each brain region as a local network of excitatory and inhibitory populations and utilizing the Wilson-Cowan equations to characterize their dynamic behavior⁹⁰, the global brain dynamics of the interconnected local networks in this study can be succinctly and consistently described by the following set of coupled differential equations:

$$\begin{cases}
\tau_{E}^{i} \frac{dr_{E}^{i}}{dt} = -r_{E}^{i} + \Phi(J_{EE}r_{E}^{i} + J_{EI}r_{I}^{i} + I_{b} + I_{g}) + \sqrt{\tau_{E}^{i}} \xi_{E}^{i}(t) \\
\tau_{I}^{i} \frac{dr_{I}^{i}}{dt} = -r_{I}^{i} + \Phi(J_{IE}r_{E}^{i} + J_{II}r_{I}^{i}) + \sqrt{\tau_{I}^{i}} \xi_{I}^{i}(t)
\end{cases}$$
(3-7)

$$\Phi(x) = \frac{x}{1 - e^{-x}} \tag{3-8}$$

where 'i' serves as the identifier of brain regions, ' $r_{E,I}^i$ ' stands for the firing rates of excitatory and inhibitory neuronal populations, ' $\tau_{E,I}^i$ ' represent the time constants for these populations, the term ' $\xi_{E,I}^i(t)$ ' signifies the intensity of Gaussian white noise, with zero mean and standard deviation, specific to both excitatory and inhibitory neuronal populations, and the function ' $\Phi(x)$ ' is the transfer function, converting electrical current into firing rates.

Within the microcircuit, synaptic inputs are denoted by $J_{EE}r_E^i$, $J_{EI}r_I^i$, $J_{IE}r_E^i$, $J_{II}r_I^i$, where J_{EE} signifies the strength of excitatory-excitatory synaptic connections, J_{EI} represents inhibitory-excitatory synaptic connections, and J_{II} signifies inhibitory-inhibitory synaptic connections. The term I_b symbolizes background

current, while ${}^{\prime}I_{E,I}^{ext}{}^{\prime}$ denotes external currents for both excitatory and inhibitory neuronal populations.

To formulate equations describing the dynamics of the entire brain, this study introduces a coupled current I_g^i constrained by the brain's structural connectivity (SC)⁵⁶ into the excitatory neuronal groups of microcircuit models. This coupled current is designed to receive the coupled currents from other brain regions' excitatory neuronal groups. Building upon this framework, we introduce a global coupling factor G for weighting, as described in the following equation:

$$I_{g}^{i} = G \sum_{j=1}^{n} SC_{ij} r_{E}^{j}$$
 (3-9)

By applying a global coupling factor G for weighted processing, this study effectively regulates the dynamic stability of the system.

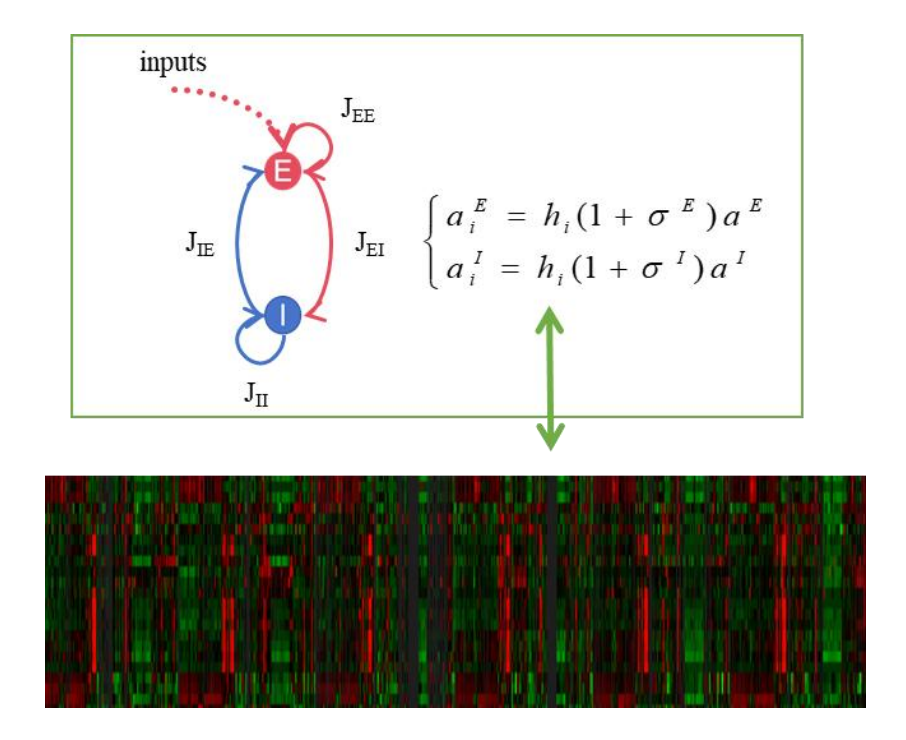


Figure 3-4 illustration of Incorporating Transcriptomic Data into the Model.

Furthermore, the constraint of transcriptomic data in the model is manifested as the adjustment of neural population gains, which are achieved through parameterized transfer functions $\Phi(x)$. This function determines how neural populations convert received currents into firing rates. Transcriptomic data provide information about gene expression within neural populations, which

can be used to adjust the parameters of $\Phi(x)$, thereby influencing the response characteristics and interaction strength of neural populations. This model adjustment based on transcriptomic data of gene expression levels within neural populations enables a more accurate simulation of the intrinsic behavior of neural populations, as illustrated in Figure 3-4.

The introduction of gain parameters a^p for excitatory and inhibitory neuronal population $p \in \{E,I\}$ in the model allows for scaling proportionally to the regional gene expression levels, as specifically introduced through the following expressions:

$$\Phi(x) = \frac{a^p x}{1 - e^{-a^p x}}$$
 (3-10)

$$\begin{cases} a_i^E = h_i (1 + \delta^E) a^E \\ a_i^I = h_i (1 + \delta^I) a^I \end{cases}$$
(3-11)

where subscript 'i' represents brain regions, and ' h_i ' represents the expression level of receptors in brain region 'i', provided by transcriptomic data, while ' $\delta^{E'}$ and ' δ'' are used to modulate the amplitude of excitatory and inhibitory population currents, respectively. In Equation (3-10), when a^p equals 1, the transfer function in this case is identical to the original transfer function in the Wilson-Cowan equation.

Following model simulations, average firing rate of each brain region was obtained, as depicted in Figure 3-5 (excitatory firing rates) and Figure 3-6 (inhibitory firing rates). The results indicate that certain brain regions such as the superior frontal gyrus, angular gyrus, and thalamus exhibit higher average excitatory firing rates compared to others, while regions like the precentral gyrus and the superior frontal gyrus display relatively lower average excitatory firing rates. Concerning inhibitory firing rates, regions like the orbitofrontal cortex and thalamus show relatively higher average inhibitory firing rates, whereas the superior frontal gyrus also presents higher average inhibitory firing rates.

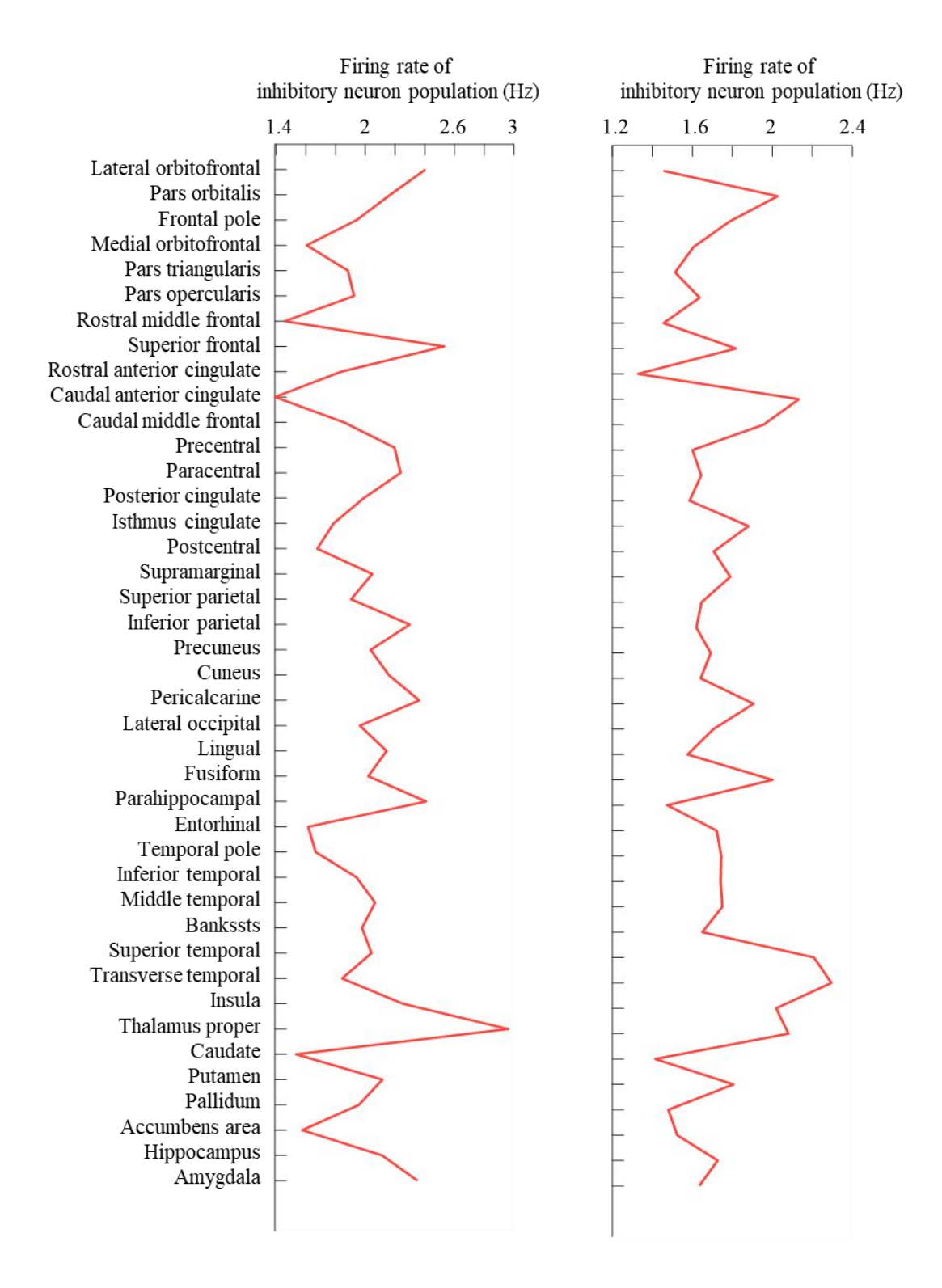


Figure 3-5 illustration of the average excitatory firing rates across various brain regions obtained through model simulations. Due to space constraints, only results for four subjects are displayed.

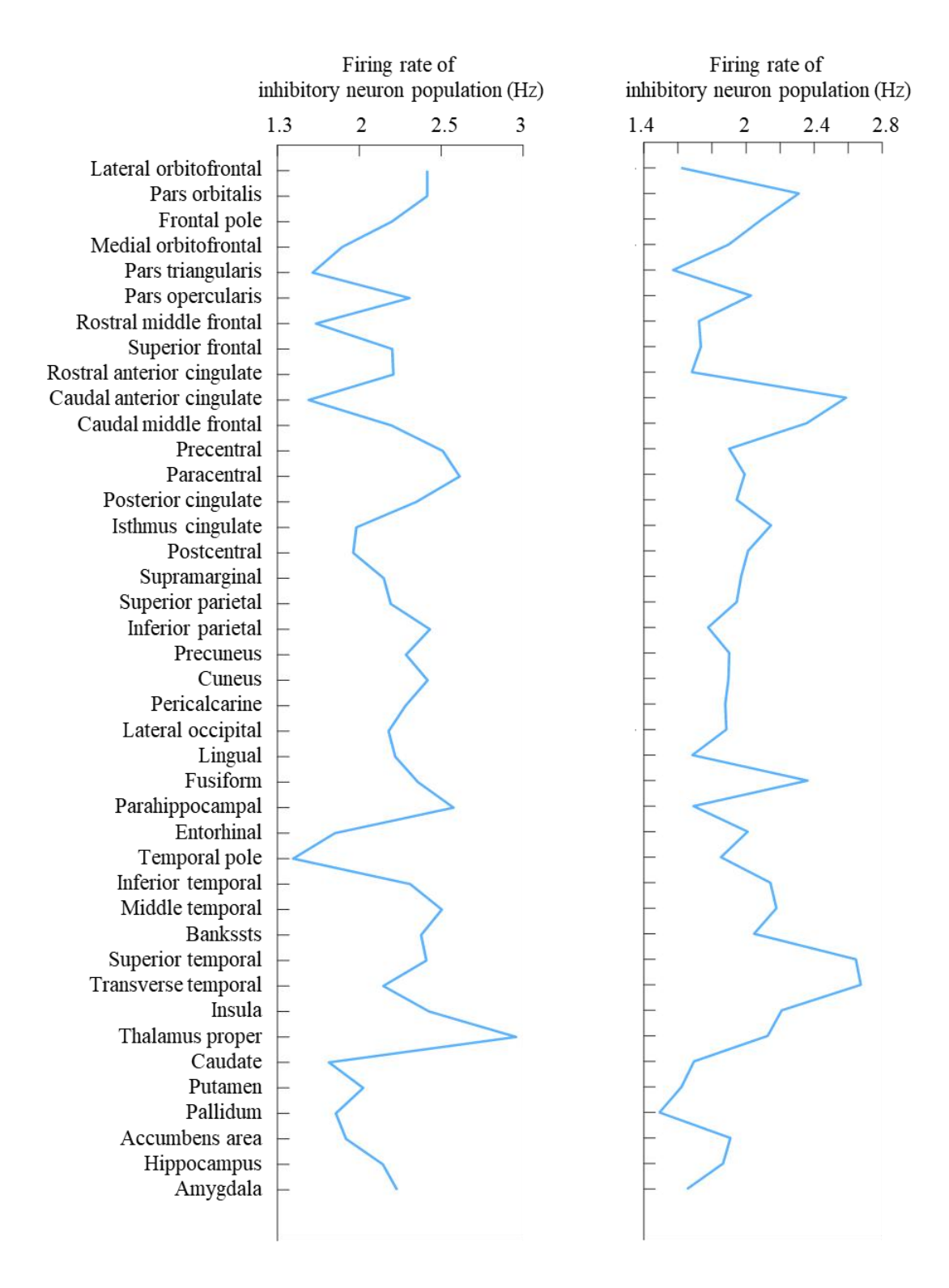


Figure 3-6 illustration of the average inhibitory firing rates across various brain regions obtained through model simulations. Due to space constraints, results for only four subjects are presented.

Given that schizophrenia may involve multiple brain regions^{21,28,60}, it is essential to consider the functions and interactions of multiple brain regions comprehensively. Specific brain regions may play crucial roles in the onset of schizophrenia, potentially responsible for the processing of important functions such as emotion, cognition, and social interaction^{20,22}. When the activity in these regions becomes abnormal, it may lead to various symptoms in individuals with schizophrenia. Therefore, these simulation results provide clues for further investigating the pathogenesis of schizophrenia.

3. 2. 2. Blood oxygen level dependence model

When the brain is activated, neuronal activity consumes oxygen and glucose, leading to an increase in local blood flow, an increase in oxygenated hemoglobin, and a decrease in deoxygenated hemoglobin, thereby increasing the local cortical signal intensity¹⁰⁵. This physiological process can be simulated using the Balloon-Windkessel hemodynamic model^{11,12} (also known as the Balloon Model), a model used to describe changes in blood flow and oxygen saturation during brain activation. This model considers the venous system in the brain as a balloon, which expands when blood flow into the brain increases during activation, leading to increased pressure until reaching a new steady state. The model can explain the dynamic processes of changes in blood flow and oxygen saturation during brain activation. The mathematical representation of the dynamic equations corresponding to this model are as follows:

$$\begin{cases} \frac{ds}{dt} = r - ks - \gamma(f - 1) \\ \frac{df}{dt} = s \\ \tau \frac{dv}{dt} = f - v^{\frac{1}{\alpha}} \\ \tau \frac{dq}{dt} = f \frac{E(f)}{E_0} - v^{\frac{1}{\alpha}} \frac{q}{v} \\ E(f) = 1 - (1 - E_0)^{\frac{1}{f}} \end{cases}$$

$$(3-12)$$

where s stands for vascular dilation signal, r represents neural activity signal, k indicates signal decay rate, γ signifies the blood-flow-dependent elimination rate, f denotes cerebral blood inflow, v represents blood volume, q represents baseline deoxyhemoglobin content, $E_0 = 0.34$

denotes the resting oxygen extraction fraction, τ indicates the blood oxygenation dynamics time constant, and a = 0.32 represents the *Grubb*'s constant. The blood oxygen signal can be expressed through the Balloon-Windkessel model given by:

$$y = \frac{100}{E_0} V_0 [k_1 (1 - q) + k_2 (1 - \frac{q}{v}) + k_3 (1 - v)]$$
 (3-13)

where $V_0 = 0.02$ represents the resting-state blood volume ratio, while k1, k2, and k3 denote signal decay rates, given respectively by 2.38, 2, and 0.48, and 'y' represents the blood oxygen signal.

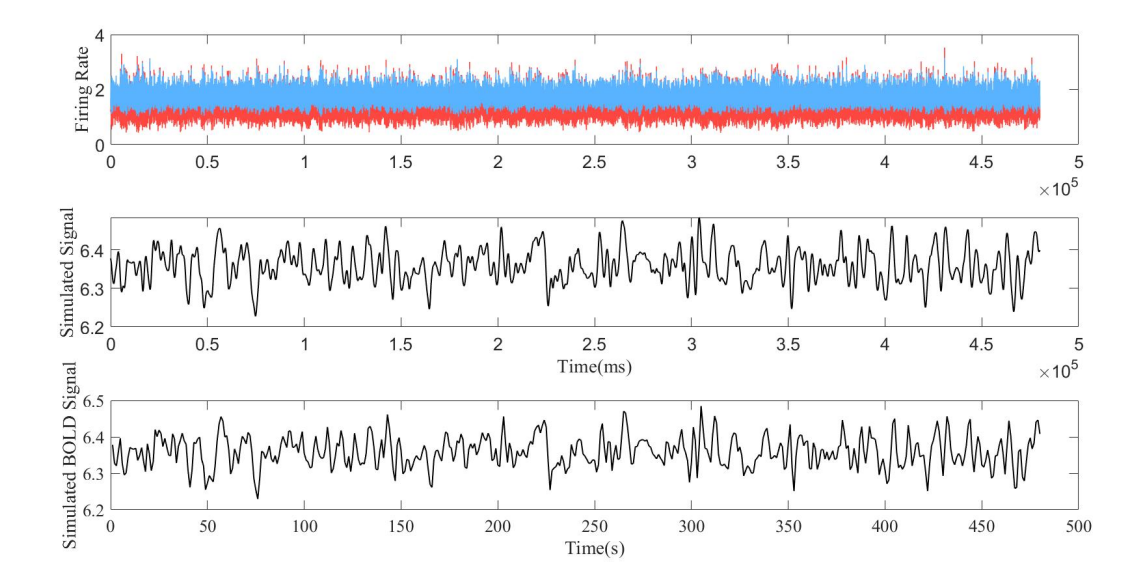


Figure 3-7 The process of BOLD signal simulation for control group subjects in the model. (a) Firing rates of excitatory and inhibitory neuronal population for 480s; (b) The simulated signal; (c) The simulated BOLD signal after downsampling for 480s.

To obtain simulated BOLD signals closer to experimental data, this study used a whole-brain computational model to generate simulated electrical signals with a sampling frequency of 1000 Hz and a duration of 500 seconds. To reduce errors, the first 20 seconds of signal data were discarded. Subsequently, the Balloon-Windkessel hemodynamic model was employed to transform the simulated neural activity signals. Based on the simulated firing rate signals, simulated BOLD signals were generated, followed by downsampling to match the temporal resolution of experimentally acquired BOLD signals. The simulated signals obtained through

these processes are shown in Figure 3-7 and Figure 3-8.

After obtaining the BOLD signals of each brain region simulated by the model, the Pearson correlation coefficients between the BOLD signals of each brain region and all other brain regions were calculated. Through this step, a simulated functional connectivity (FC) matrix with dimensions of 83*83 was obtained. When constructing this matrix, the diagonal elements were set to 0 to avoid calculating the correlation between any brain region and itself. To ensure the stability and reliability of the results, the above process was repeated 7 times, each time generating a simulated FC matrix. Finally, the average of these 7 matrices was calculated to obtain an averaged simulated FC matrix, which more accurately reveals the functional connectivity patterns between brain regions.

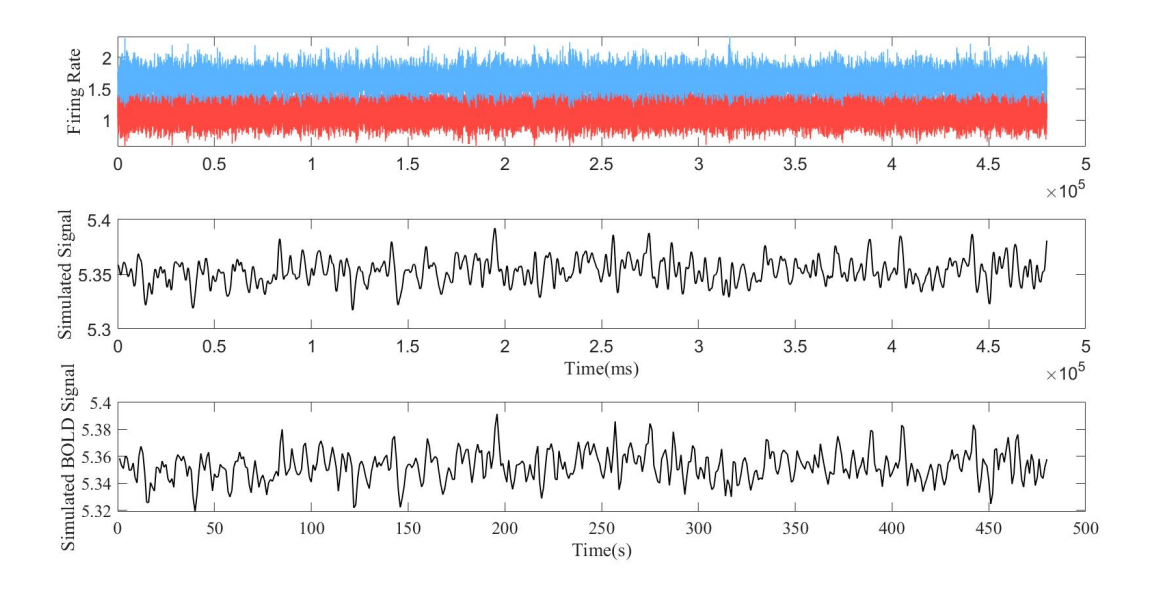


Figure 3-8 The process of BOLD signal simulation for schizophrenia group patients in the model. (a) The firing rates of the excitatory and inhibitory neuronal population for 480s; (b) The simulated signal; and (c) The simulated BOLD signal after downsampling for 480s.

3. 3. Model optimization methods

3. 3. 1. Optimization strategy for whole brain model

Utilizing the aforementioned model construction approach, we systematically varied the global coupling factor G within the range of 0 to 0.8 with increments of 0.025. The aim was to select the G value corresponding to the maximum correlation, thus obtaining simulated average functional connectivity (FC) as a preliminary FC simulation. The search process yielded initial optimal simulation results, as depicted in Figure 3-9.

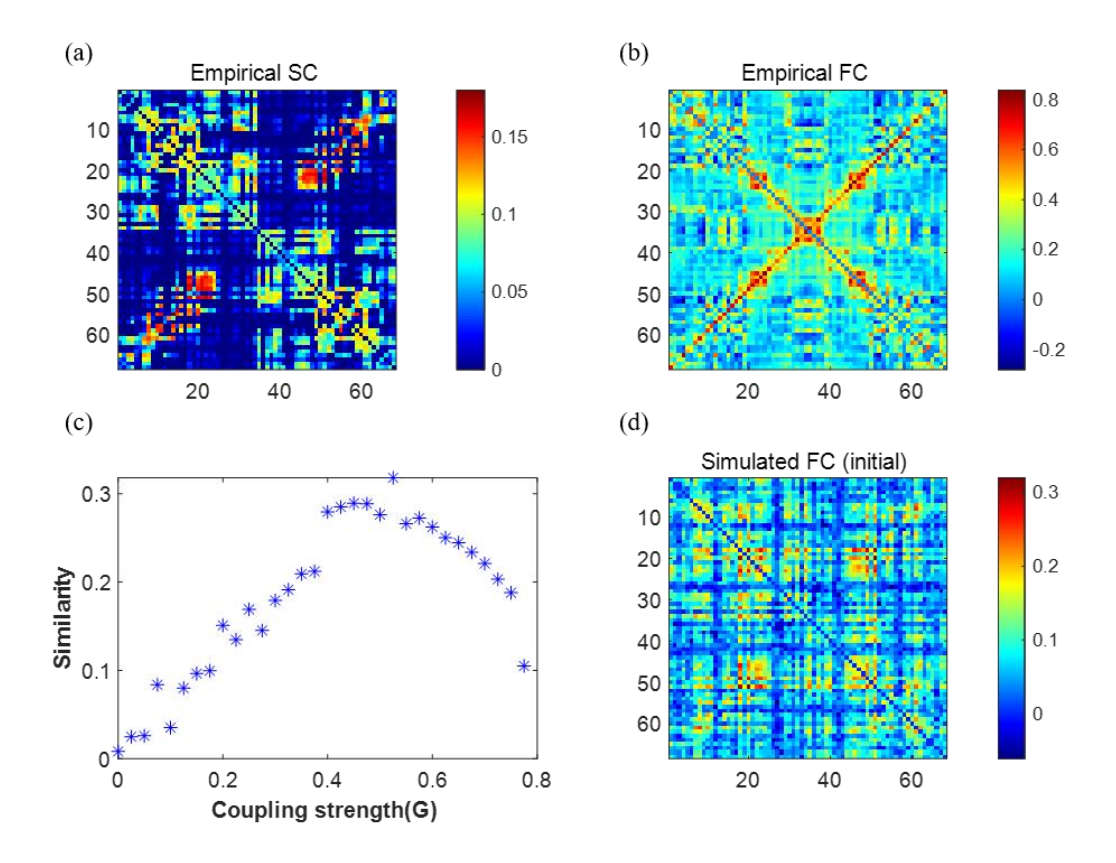


Figure 3-9 Traversing the coupling factor *G* to simulate the optimal functional connectivity. (a) Empirical structural connectivity matrix; (b) Empirical functional connectivity matrix; (c) Variation of the influence of coupling factor *G* on correlation during the traversal process; (d) Preliminary simulated functional connectivity matrix based on the aforementioned analysis.

However, the simulated FC matrix generated solely from the initial structural connectivity (SC) matrix exhibited relatively low similarity to the experimental FC matrix, manifesting some missing connections and thus failing to fully replicate the genuine dynamics of the whole brain. Consequently, new algorithms need to be proposed for optimization.

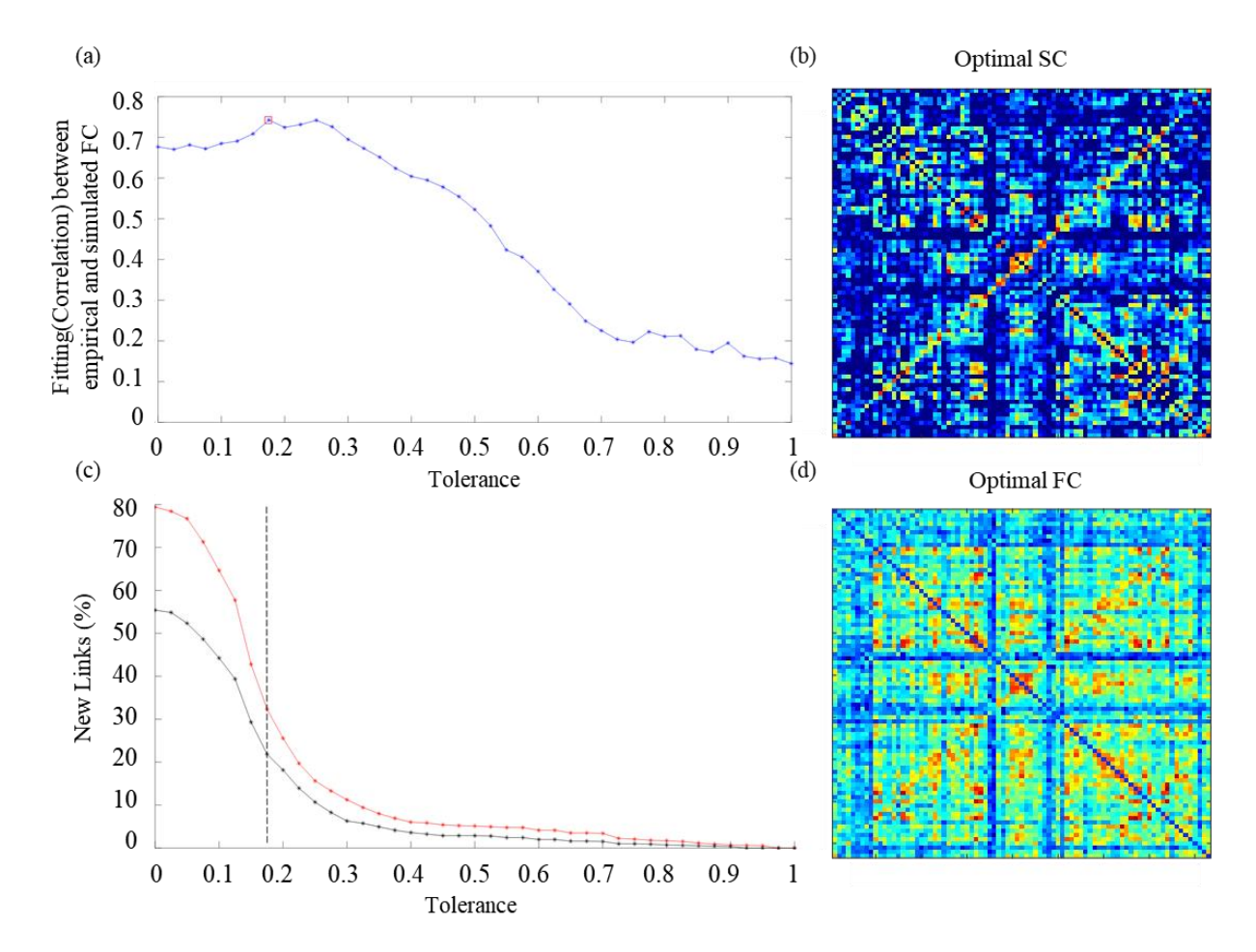


Figure 3-10 The iterative optimization process. (a) The change in correlation between empirical FC and simulated FC as the threshold decreases. (b) The addition of new connections within and between hemispheres as the threshold decreases from 1 to 0. (c) The optimal SC matrix (threshold at 0.175). (d) The optimal FC matrix (threshold at 0.175).

In this study, the iterative self-consistency enhancement process based on empirical FC-SC is implemented through the following steps:

First, empirical SC matrix SCe is used to simulate neural and synaptic activities in each region

using the Wilson-Cowan model and generate BOLD signals through the balloon model. During this process, the global coupling parameter G is adjusted to operate the system at the edge of spontaneous instability bifurcation. Pearson correlation coefficients of BOLD signals between different brain regions are computed to obtain a simulated FC_s matrix. The obtained FC_s are then fitted with empirical FC data FC_e, and the differences between the connections are compared.

Next, based on FC data, iterative enhancement of the SC matrix is performed. The algorithm sets the threshold level T to 1 initially, and for connections with differences exceeding T, SC_{ij} is modified according to the inversion rules proposed by Deco et al⁵⁴. In the next iteration, the new SC matrix is used to constrain the whole-brain model. Subsequently, the error level is gradually reduced (e.g., by decreasing T from 1 to 0.025 in increments of 0.025), and the fitting between simulated FC_s and empirical FC_e is reassessed. This process continues until the error level reaches the predefined minimum. In summary, this algorithm is integrated with the Wilson-Cowan model to enhance the fitting between simulated FC_s and empirical FC_e by adjusting SC weights. The iterative process and related illustrations are shown in Figure 3-10.

Through optimization analysis, it is observed that when the threshold is adjusted to 0.175, the fitting between simulated functional connections (FC) and empirical FC reaches its highest level, approximately 0.74 (Pearson correlation coefficient). Furthermore, as the threshold gradually decreases from 1 to 0, the addition of new connections within and between hemispheres shows varying degrees of growth. Specifically, interhemispheric connections increase by 32.37%, while intrahemispheric connections increase by 21.85%. These changes indicate that by moderately increasing effective connections, this study can more accurately replicate the overall brain dynamic processes. Based on the above analysis, this study concludes that the optimal performance of the corresponding structural connectivity (SC) matrix and functional connectivity (FC) matrix is achieved when the threshold is set at 0.175.

3. 3. 2. Parameter optimization process based on Bayesian optimization

Optimization is a process of locating points aimed at minimizing a real-valued function (i.e., the objective function). Traditional optimization methods, such as grid search, have certain limitations in practical applications. One notable drawback is their high computational cost. Grid search systematically explores all possible combinations of parameters, resulting in exponential

growth in time complexity as the number of parameters increases. Especially in cases with numerous model parameters, this method may become impractical. Additionally, these methods face challenges when dealing with continuous parameters, as they require discretizing the parameter space, potentially overlooking optimal values within the parameter space. Moreover, these traditional methods lack flexibility during the search process, making it difficult to dynamically adjust the search space based on temporary results. Therefore, despite their simplicity and ease of use, these techniques encounter significant limitations when dealing with complex and extensive parameter spaces.

Among various optimization methods, Bayesian optimization stands out prominently. This optimization demonstrates outstanding performance in searching the parameter space by optimizing sample points to reduce computational costs while swiftly identifying the optimal parameter combination. This method significantly enhances the fitting performance of mathematical models, particularly in fields such as human brain research involving high-dimensional space attributes¹⁰⁶.

Its advantages mainly manifest in several aspects: Bayesian optimization accelerates the search for the optimal solution by employing efficient strategies to select sample points through predictive modeling. Compared to random search or fixed-step methods, it avoids inefficient search paths, significantly improving search efficiency. Moreover, Bayesian optimization significantly reduces computational resources and time consumption compared to traditional methods. Its intelligent sampling strategy enables obtaining optimal results with fewer iterations, thereby reducing computational costs. Additionally, Bayesian optimization can automatically adjust sampling strategies based on previous observation results, dynamically adjusting the position of the next sample point. This feature allows the method to maintain a high possibility of accommodating optimal solutions even in addressing complex non-convex optimization problems. It is worth mentioning that it does not rely on gradient information, thus possessing unique advantages in optimizing complex models where computing gradients or function costs are expensive. Additionally, owing to its probabilistic model characteristics, it excels in identifying global optimal solutions rather than being limited to local optimal solutions, which is crucial for solving certain practical problems.

As for the method itself, Bayesian optimization is a probabilistic model-based optimization

method, assuming that the prior distribution of the target function follows a Gaussian process. It utilizes surrogate models such as Gaussian processes for approximation and continuously evaluates the objective function to select the next point most likely to lead to optimization. During the iteration process, Bayesian optimization continuously employs a "sampling function" strategy to search for the optimal solution globally. Based on the latest sampling results, the Bayesian theorem is applied to derive the posterior distribution of the function. At each selected parameter point, the algorithm probabilistically evaluates based on the current surrogate model. After each sampling round, the surrogate probability model is updated. This process continues until convergence is achieved.

Based on the above analysis, the process of Bayesian optimization can be outlined as follows:

- 1. For each sampling point t = 1, 2, ..., perform the following steps:
- 2. Optimize the surrogate model Gaussian process GP to find the optimal solution x_{t_0}

$$x_t = \arg\max_{x} u(x \mid D_{1:t-1})$$
 (3-14)

3. Define the objective function for the sample as:

$$y_t = f(x_t) + \varepsilon_t \tag{3-15}$$

4. Add the new sample (x_t, y_t) to the sample set $D_{I:t}$, and then update GP:

$$D_{1:t} = \{D_{1:t-1}, (x_t; y_t)\}$$
 (3-16)

5. Repeat the above steps until the termination condition is met.

Here, x represents the parameter vector, corresponding to model parameters in this paper; y represents the observation value corresponding to x, corresponding to the similarity between the model output matrix and the empirical matrix; u represents the sampling function; D represents the set of observation data; f is the target function to be estimated, which in this study can be regarded as the relationship function between the model parameter vector and the fitting result; to avoid falling into local optima, a bias ε_t is usually added at (3-15).

There are two important components in the process: the posterior distribution of the target and

the sampling function. Focusing first on the posterior distribution, when accumulating observation values $D_{I:t} = \{x_{I:t}, y_{I:t}\}$, the prior distribution P(f) is combined with the likelihood function $P(D_{I:t}|f)$ to maximize the posterior probability given the observation values:

$$\underset{f}{\operatorname{arg max}} P(f \mid D_{1:t}) = \underset{f}{\operatorname{arg max}} \frac{P(D_{1:t} \mid f)P(f)}{P(D_{1:t})}$$
(3-17)

Because $P(D_{I:t})$ in the f space is constant given the sample $D_{I:t}$, it can be simplified as:

$$\arg \max_{f} P(f \mid D_{1:t}) = \arg \max_{f} P(D_{1:t} \mid f) P(f)$$
 (3-18)

This simplifies to:

$$P(f | D_{t,t}) \propto P(D_{t,t} | f)P(f)$$
 (3-19)

The posterior distribution captures updated information about the unknown target function and can also replace the target function f at this step with the acquisition function (surrogate function). The core idea is to use the Gaussian process model to characterize the target function and gradually improve model accuracy by evaluating this function f 107.

The Gaussian process (GP) is an extension of the multivariate Gaussian distribution to infinite-dimensional random processes. Its characteristics lie in maintaining the attributes of Gaussian distribution for any finite combination in dimensions. Similar to how the Gaussian distribution is a distribution of random variables fully determined by its mean and covariance, the distribution characteristics of Gaussian processes on functions are determined by its mean function m and kernel function k:

$$f(x) \sim GP(m(x), k(x, x'))$$
 (3-20)

Intuitively, GP is analogous to the target function, except that it does not return a scalar f(x) for any x, but rather the mean and variance of the normal distribution corresponding to the x value. Among the many kernel functions, one typical example is the exponential square function with an ARD (automatic relevance determination) vector¹⁰⁸:

$$k(x_i, x_j) = \exp(-\frac{1}{2}(x_i - x_j)^T diag(\theta)^{-2}(x - x'))$$
 (3-21)

Where $diag(\theta)$ is a diagonal matrix with θ on the diagonal, generally resulting in a function close to 1 when x values are close, and close to 0 when x values are separated. Assuming that $\{x_{1:t}\}$ has been sampled from the prior, and the values of the function are sampled at these indices to generate the sample pair set $\{x_{1:t}, f_{i:t}\}$ (where $f_{1:t} = f(x_{1:t})$). Function values are drawn according to the multivariate normal distribution N(m(x), K), where the kernel matrix is:

$$K = \begin{bmatrix} k(x_1, x_1) & \dots & k(x_1, x_t) \\ \vdots & \ddots & \vdots \\ k(x_t, x_1) & \dots & k(x_t, x_t) \end{bmatrix}$$
(3-22)

For example, after t sampling iterations, accumulated observation samples $D_{I:t} = \{x_{I:t}, y_{I:t}\}$. Because any point f_{t+I} and previous observation data in the Gaussian process follow a joint Gaussian distribution,

$$\begin{bmatrix} f_{1:t} \\ f_{t+1} \end{bmatrix} \sim N \begin{pmatrix} m(x_{1:t}) \\ m(x_{t+1}) \end{pmatrix}, \begin{bmatrix} K & k \\ k^T & k(x_{t+1}, x_{t+1}) \end{bmatrix}$$

$$(3-23)$$

Where,

$$k = [k(x_{t+1}, x_1) \quad k(x_{t+1}, x_2) \quad \dots \quad k(x_{t+1}, x_t)]$$
 (3-24)

Given the prior mean function as the zero function here, i.e., m(x) = 0, the expression for predicting the distribution of the sample point after using existing observation data is derived using the Sherman-Morrison-Woodbury formula¹⁰⁹:

$$P(f_{t+1} \mid D_{1:t}, x_{t+1}) = N(\mu_t(x_{t+1}), \sigma_t^2(x_{t+1}))$$
(3-25)

Where the mean and variance functions are:

$$\begin{cases} \mu_t(x_{t+1}) = k^T K^{-1} f_{1:t} \\ \sigma_t^2(x_{t+1}) = k(x_{t+1}, x_{t+1}) - k^T K^{-1} k \end{cases}$$
(3-26)

The acquisition function plays a crucial role in the Bayesian optimization algorithm, guiding the algorithm to select the next evaluation point, thus achieving a balance between modeling low-value areas of the objective function and exploring areas of insufficient modeling. Through continuously iterating and refining estimates, Bayesian optimization eventually converges to the

optimal parameter values.

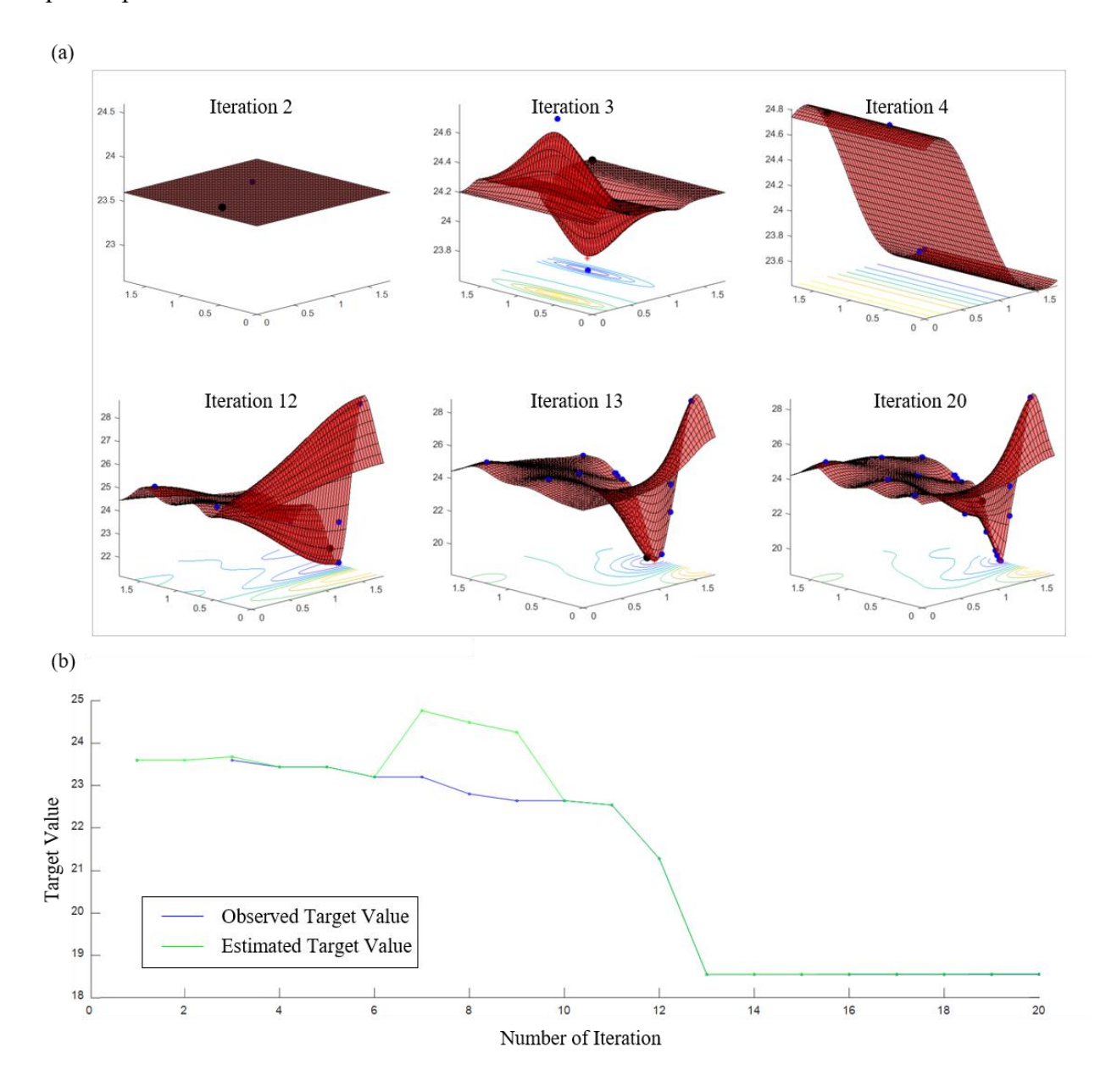


Figure 3-11 The iterative process of the Bayesian optimization algorithm in the twodimensional parameter space of the Wilson-Cowan model. (a) Represents six typical iterations (Iteration 2, Iteration 3, Iteration 4, Iteration 12, Iteration 13, Iteration 20); (b) The variation of the estimated proxy value and the sampled observation value with the number of iterations.

Figure 3-11 illustrates the iterative process of the algorithm in practical use, employing Bayesian optimization in the two-dimensional parameter space of the Wilson-Cowan model. After only twenty iterations of searching the parameter space, the results gradually converge.

In the initial state, the surrogate model significantly differs from the true function; after the 3rd and 4th iterations, the surrogate model improves but still deviates from the truth; by the 12th iteration, the surrogate model finds a local optimum; after the 13th iteration, it quickly converges to that point; the algorithm converges to the global optimum in the 20th iteration.

It is noteworthy that Bayesian optimization is not a panacea; its performance depends largely on the nature of the objective function and the complexity of the search space. However, with appropriate prior settings and flexible sampling function selection, Bayesian optimization demonstrates powerful global optimization capabilities in many practical problems.

3. 3. 3. Riemann distance

In the intersection of neuroscience and genetics, a pivotal issue is how genes influence brain function. With advancements in scientific technology, researchers are increasingly recognizing the highly complex mechanisms through which genes affect brain function^{110,111}. These mechanisms may exhibit non-linear and non-Euclidean characteristics, a viewpoint gradually gaining recognition in the scientific community.

Firstly, the influence of genes on the brain is not a simple one-to-one relationship. Humans possess tens of thousands of genes, each of which may play different roles in various circumstances. Even different alleles of the same gene may lead to markedly different outcomes. This complexity renders the influence of genes on brain function non-linear.

Secondly, the brain itself is a highly complex network structure, comprised of billions of neurons and synapses interconnected. These connections form intricate networks, and genes play crucial roles in influencing the number of neurons, the structure and function of synapses, and even the connectivity of neural networks. This influence is largely non-Euclidean, as it involves highly complex network structures and dynamic processes, rather than simple linear relationships. To better understand the impact of genes on brain function, more advanced statistical and computational methods need to be developed to analyze and interpret the vast amount of genetic

and neuroscience data.

To accurately quantify the similarity of brain functional connectivity matrices, selecting appropriate comparison methods becomes crucial¹¹². This method not only directly affects the model construction process but also determines, to some extent, the effectiveness and generalization ability of the model. Traditional methods for comparing matrix similarities often lead to overfitting during the optimization process of large parameter spaces, thereby limiting the model's performance on other datasets.

In the exploration of the human brain, scientists have discovered the unique advantages of using Riemannian distance as the loss function to measure the similarity of mathematical model fits. Compared to traditional Euclidean distance, Riemannian distance performs better when dealing with non-linear parameter spaces, capturing the complex features of actual brain dynamics and model simulation results more accurately¹¹³.

Riemannian distance considers the curvature and non-Euclidean geometric structure of parameter spaces, reflecting the differences between data more accurately. This characteristic makes Riemannian distance more biologically relevant in the study of brain functional connectivity matrices, aiding in a deeper understanding of the complexity of the human brain. Adopting advanced comparison methods like Riemannian distance allows for a more accurate measurement of model fit similarity.

Furthermore, Riemannian distance possesses several advantages. Firstly, in terms of convergence speed, models using Riemannian distance as the loss function typically converge faster. This is because Riemannian distance metrics consider the geometric structure on positive definite matrix manifolds, allowing the model to search more effectively along the manifold during optimization, thereby finding the optimal solution more quickly. In contrast, traditional distances do not consider the manifold structure, which may cause the model to deviate from the optimal solution during optimization, thereby increasing convergence time.

Secondly, in terms of accuracy, models using Riemannian distance as the loss function usually achieve higher accuracy. This is because Riemannian distance metrics more accurately reflect the distance relationship between points on positive definite matrix manifolds, allowing the model to better learn the inherent patterns of the data during training. Meanwhile, Euclidean

distance, due to ignoring the manifold structure, may cause the model to learn surface features of the data during training, thereby reducing the model's accuracy.

Lastly, in terms of robustness to outliers, models using Riemannian distance as the loss function typically exhibit stronger robustness. This is because Riemannian distance metrics are more sensitive to shape changes in matrix manifold space, enabling the model to better identify and handle outliers. Meanwhile, Euclidean distance does not possess this characteristic, which may lead to poorer robustness when the model encounters outlier data.

Essentially, the Riemannian distance is a metric used to measure the geodesic distance between two points on a Riemannian manifold¹¹⁴. The formula for computing geodesic distance is as follows:

$$d_R(P_1, P_2) = \|\log(P_1^{-1}, P_2)\|_F$$
(3-27)

where P_1 and P_2 are two points in the Riemannian space. This formula reveals the fundamental principle of using the metric tensor to calculate the geodesic distance between two points on a Riemannian manifold.

Because FC typically falls within the realm of covariance matrices, when manipulating these matrices, operations leverage their inherent properties as Symmetric Positive Definite (SPD) matrices, which are part of the unique structure of Riemannian manifold¹¹⁴. Specifically, for $P \in S(n)$ (where S(n) is defined as the set of all $n \times n$ symmetric matrices) and any vector $u \in \mathbb{R}^n$, $u^T P u > 0$. This endows it with the property of explicit formulaic operations on Riemannian manifolds. Riemannian geometry provides a rich framework for operating on these matrices, facilitating algorithm implementation.

Assuming the space of positive definite matrices P(n) is a differentiable Riemannian manifold, the tangent space is associated with each point on the manifold, representing the space of minimal variations at that point. On the manifold of Symmetric Positive Definite (SPD) matrices, the tangent space lies within the space of SPD matrices at the corresponding point. Each point on the tangent space has an inner product $<.>_P$, corresponding to the angle and magnitude between two vectors on the tangent space. This inner product, associated with each point on the tangent space, allows for smooth variation between different points. It is used to define the natural metric

on the manifold of positive definite matrices, i.e., a distance metric defined at each point on the manifold reflecting its local geometric properties. In this case, the natural metric is defined by the local inner product formula:

$$\langle S_1, S_2 \rangle_P = Tr(S_1 P^{-1} S_2 P^{-1})$$
 (3-28)

This metric smoothly varies with changes in points on the manifold.

Furthermore, assuming the space of positive definite matrices P(n) is a differentiable Riemannian manifold, the tangent space T_p lies within the corresponding space S(n) at the given point. The introduction of Riemannian geodesic distance is represented by paths: $\Gamma(t):[0,1] \rightarrow P(n)$, with length:

$$L(\Gamma(t)) = \int_0^1 ||\dot{\Gamma}(t)||_{\Gamma(t)} dt$$
 (3-29)

Finally, by introducing the natural metric, the geodesic distance can be expressed as:

$$d_{R}(P_{1}, P_{2}) = \|\log(P_{1}^{-1}, P_{2})\|_{F} = \left[\sum_{i=1}^{n} \log^{2} \lambda_{i}\right]^{\frac{1}{2}}$$
(3-30)

where λ_i , i=1...n are the generalized eigenvalues of the matrix $P_{i}^{-1}P_{2}$. The logarithmic operation for SPD matrices is obtained through the eigenvalue decomposition of P:

$$\log(P) = Udiag(\log(\sigma_1),...,\log(\sigma_n))U^T$$
(3-31)

Then, the Frobenius norm of the matrix is given by the following expression:

$$||A||_F^2 = Tr(AA^T) = \sum |A_{ij}|^2$$
 (3-32)

This Riemannian distance metric provides a theoretical basis for measuring the distance relationship between points on the manifold of positive definite matrices.

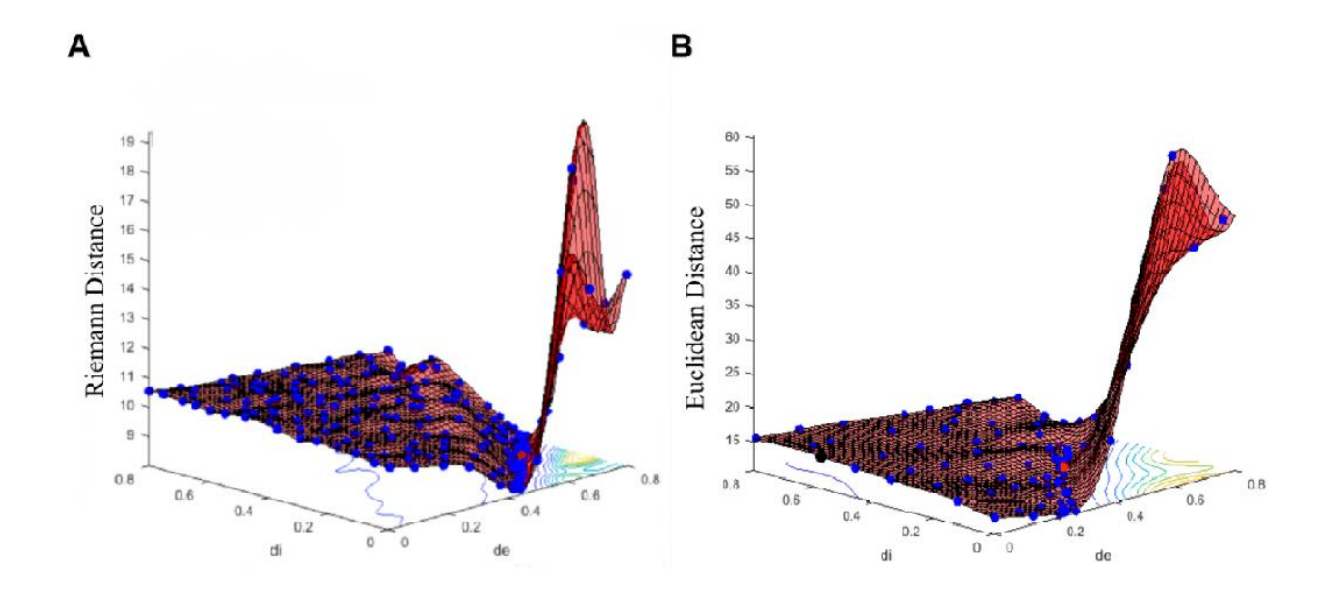


Figure 3-12 Parameter topology space using different distance metrics during model parameter search. (a) Riemannian distance. (b) Euclidean distance.

Comparison of the results of model fitting using Riemannian distance and Euclidean distance as loss functions (as shown in Figure 3-12) reveals differences between them in the parameter topology space.

CHAPTER 4: RESULTS

4. 1. Single patient modeling

Personalized modeling, also known as single-subject modeling, is one of the core methods in current research. Its importance lies in its unique information mining advantages and indispensable data completeness. One of its key advantages is the ability to avoid the common problem of key information loss in ensemble or group models. Customizing models for each individual can overcome the limitations of ignoring individual differences in population analysis, thus capturing complex subtle differences and specificities that may be overlooked¹¹⁵. This precision can more accurately reflect the unique biological, physiological, or behavioral processes of the research subjects.

With the development of computing technology, especially the widespread application of parallel computing technology, the feasibility of modeling individual patients becomes increasingly important. Parallel computing enables researchers to utilize vast computing resources to handle computations that require complex simulations and analyses, thereby driving the implementation of personalized modeling¹¹⁶. This computational capability greatly reduces the time required for processing large-scale datasets and complex algorithms, accelerating the development and refinement of personalized models¹¹⁷. Therefore, by leveraging parallel computing capabilities, single-subject modeling has become an indispensable tool in contemporary scientific research, deeply exploring personalized characteristics within populations and promoting customized interventions across research fields.

When multiple simulations are required for each subject, the complexity of the task significantly increases, and the demand for computational resources also grows exponentially. To address this challenge, this study fully utilized computing resources, with cluster nodes serving as the primary computing processors. By combining the advantages of cluster multi-core multithreading and high storage performance, it provided powerful computing and data processing storage capabilities for simulating and processing large-scale neural network models, significantly reducing the time required for the simulation process. This approach not only improves research efficiency but also provides strong support for in-depth exploration of the application of personalized modeling in scientific research.

In the current study, a thorough exploration of the parameter space of two sets of experimental model parameters (G, τ_E , τ_I , J_{EE} , J_{EI} , J_{IE} , J_{II}) was conducted using Bayesian optimization methods, and the experimental results are presented in Figure 4-1.

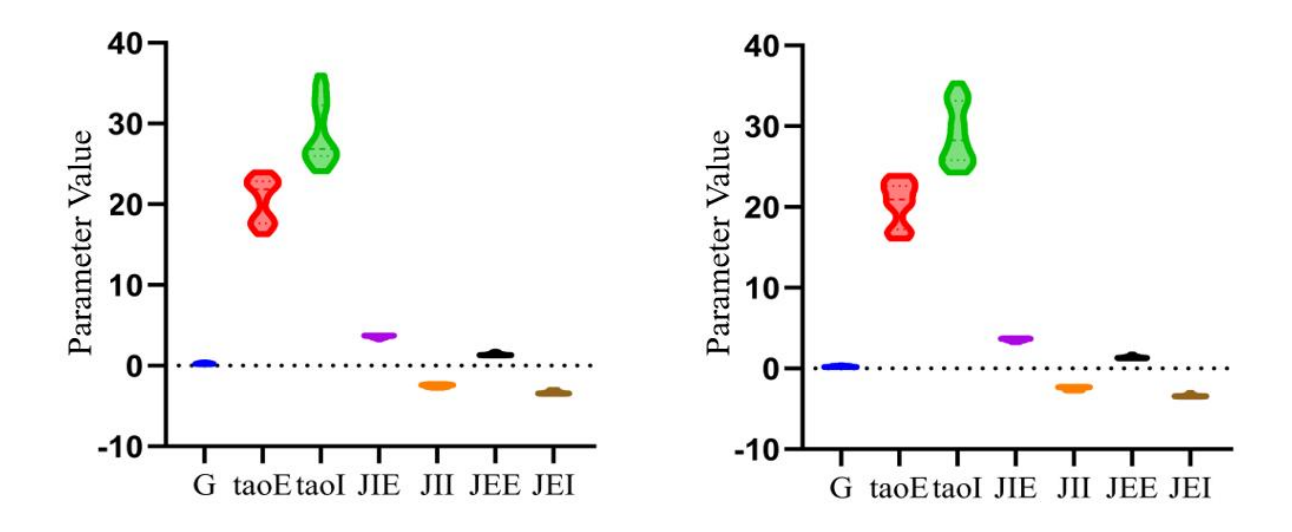


Figure 4-1 The results of the model parameter search using the Bayesian optimization method are as follows: (a) Model parameters for the control group. (b) Model parameters for the schizophrenia group.

Independent samples t-tests were conducted on each parameter in the two groups to assess whether there were significant differences between the two groups. The results of the calculations are as follows: Independent samples t-test for G: p = 0.15326; Independent samples t-test for $\tau_E: p = 0.1605$; Independent samples t-test for $\tau_I: p = 0.6502$; Independent samples t-test for $J_{IE}: p = 0.6066$; Independent samples t-test for $J_{II}: p = 0.40132$; Independent samples t-test for $J_{EE}: p = 0.6455$; Independent samples t-test for $J_{EI}: p = 0.54600$.

From these results, it can be observed that there were no significant differences in the distribution of model variables between the schizophrenia group and the control group. Although there were some differences between the parameters of the two groups, these differences did not reach statistical significance. Therefore, the specific sources of differences between the two groups cannot be determined at present, and further research and experiments are needed to explore the underlying reasons.

In the previous section, it was elaborated on how to construct a whole-brain model covering 66 cortical regions and 17 subcortical regions using the Wilson-Cowan equation, accurately depicting the dynamic behavior of each brain region. Subsequently, personalized modeling was conducted for each subject, and the firing rates of excitatory and inhibitory neuron populations in each brain region were calculated through the model. Detailed results are shown in Figure 4-2 and Figure 4-3.

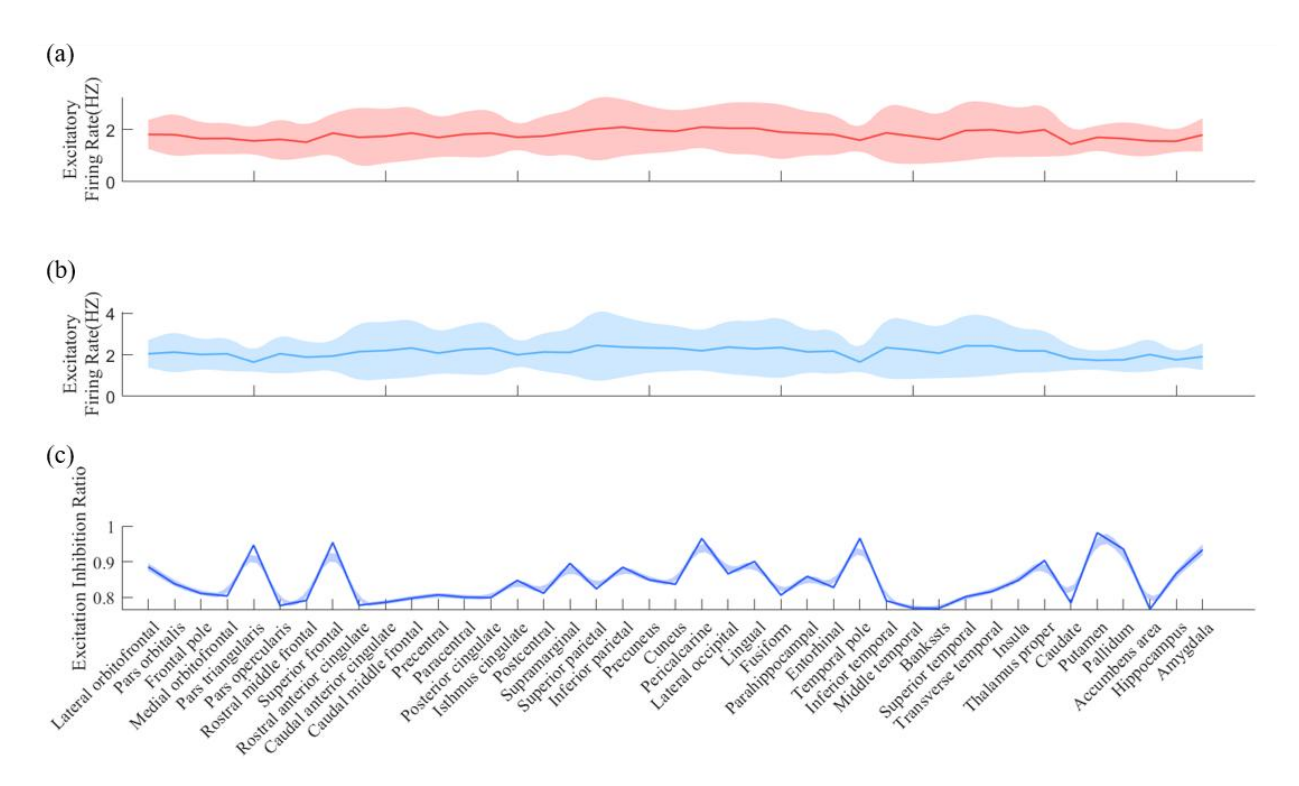


Figure 4-2 Envelope plots of firing rates for the control group: (a) Envelope plot of excitatory neuron firing rates in different brain regions for 27 subjects in the control group; (b) Envelope plot of inhibitory neuron firing rates in different brain regions for 27 subjects in the control group; (c) Envelope plot of the ratio between excitatory and inhibitory firing rates in different brain regions for 27 subjects in the control group

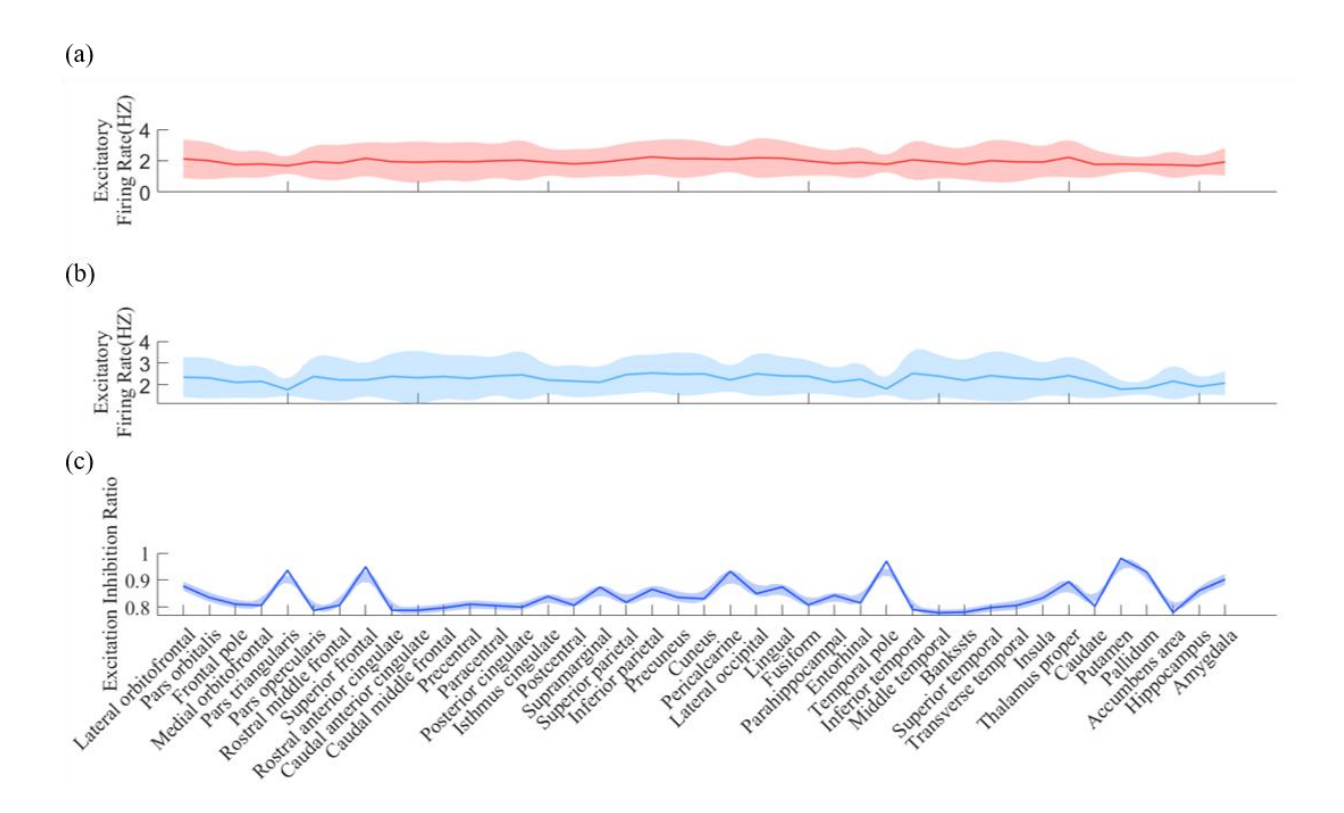


Figure 4-3 Envelope plots of firing rates for the schizophrenia group: (a) Envelope plot of excitatory neuron firing rates in different brain regions for 27 subjects in the schizophrenia group; (b) Envelope plot of inhibitory neuron firing rates in different brain regions for 27 subjects in the schizophrenia group; (c) Envelope plot of the ratio between excitatory and inhibitory firing rates in different brain regions for 27 subjects in the schizophrenia group

After completing the group averages of firing rates and excitatory-inhibitory ratios, a statistical analysis was conducted to determine whether there were significant differences between them. The specific results are shown in Figure 4-4.

Through independent sample t-tests, it was found that the p-value for excitatory firing rates was 0.5714, for inhibitory firing rates was 0.5643, and for the excitatory-inhibitory ratio was 0.0783. Under the significance threshold of 0.05, the null hypothesis could not be rejected, indicating that there were no significant differences in firing rate data between the two groups at the network level. However, from the perspective of the excitatory-inhibitory ratio, there was a near-significant difference between the two groups.

Based on this, firing rate signals from various brain regions simulated by the Wilson-Cowan equation were used to model the BOLD signal using the Balloon-Windkessel hemodynamic model. This model, based on hemodynamic principles, can simulate the hemodynamic response of the brain during neural activity. Through this model, changes in BOLD signals in various brain regions during neural activity can be obtained.

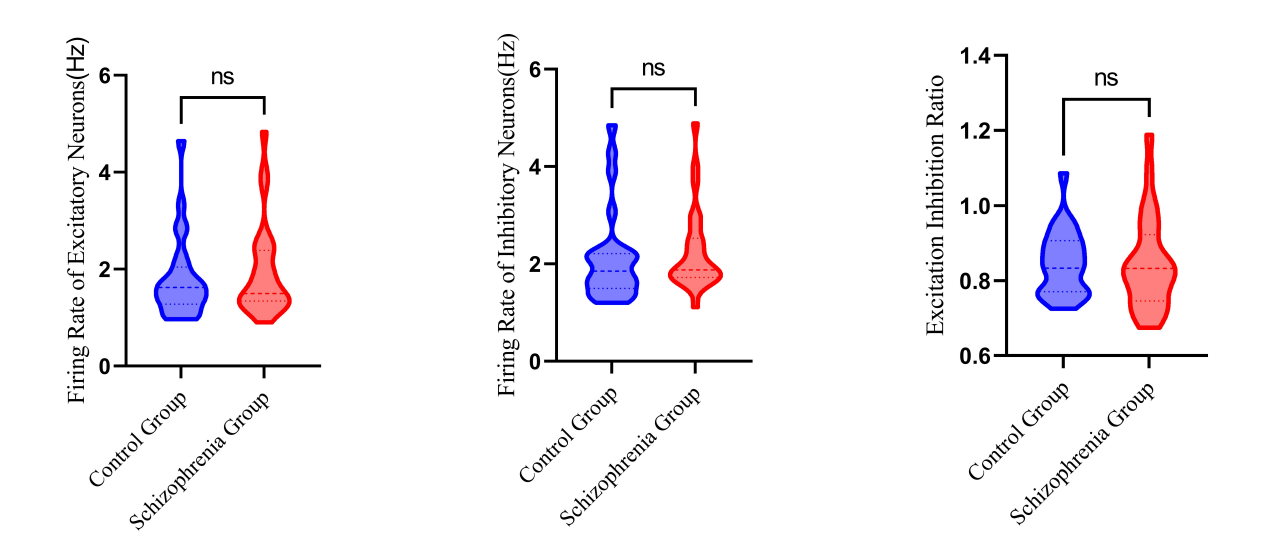


Figure 4-4 The firing rate and excitation inhibition ratio of the control group and the schizophrenia group were compared

To quantify the functional connectivity between different brain regions, the Pearson correlation coefficients of BOLD signals between each pair of brain regions were calculated. In this study, a separate simulated functional connectivity (FC) matrix of size 83×83 was constructed for each participant, where each element represented the functional connectivity strength between two brain regions. To increase the stability and reliability of the results, the above process was repeated multiple times in this study, and multiple simulated FC matrices were averaged to provide a more stable estimation of functional connectivity. Ultimately, each participant obtained an averaged FC matrix, the results of which are shown in Figure 4-5.

By observing Figure 4-5, it can be observed that the functional connectivity between different brain regions exhibits a complex network structure. Some brain regions show positive correlations, indicating that they tend to synchronize their activity during neural processes, while

other brain regions may exhibit negative correlations, suggesting the presence of inhibition or complementary relationships in their functions. Further analysis of these functional connectivity patterns is needed to understand how the brain processes information and coordinates activities between different brain regions.

When exploring the complex neural networks of the biological brain, the concept of connection strength is particularly important as it provides essential references for weighted connections between network nodes. In this study, these nodes represent neural populations in the brain, and the connection strength reflects the efficiency and intensity of information exchange between them, such as neuronal synchronization and signal transmission efficiency.

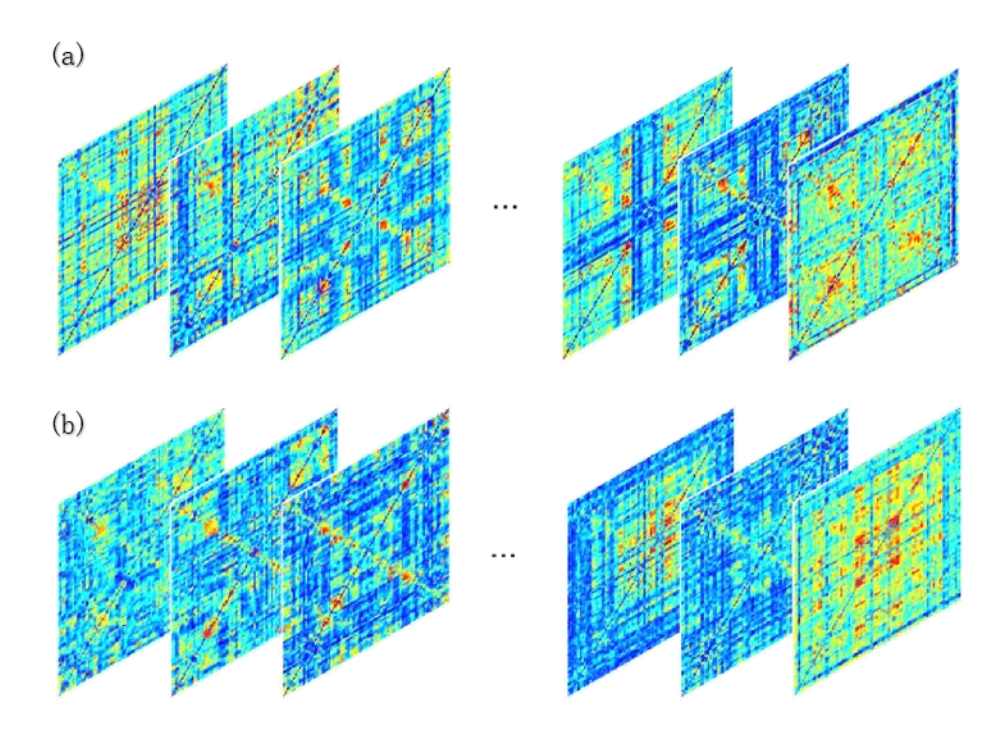


Figure 4-5 The simulated functional connectivity (FC) matrices for the control group and the schizophrenia group. Due to space limitations, only partial data results are displayed. Each lateral matrix represents the simulated FC matrix for a specific participant. (a) Simulated FC for the control group. (b) Simulated FC for the schizophrenia group.

4. 2. Computing and Analyzing Global Brain Connectivity

To assess the strength of connections between brain regions in the brain network, this study computed the sum of the connectivity strengths of all edges directly connected to a brain region, known as Global Brain Connectivity (GBC), and performed statistical analysis on the connectivity at the level of brain lobes. The formula for calculating GBC is as follows:

$$GBC_{i} = \frac{1}{N} \sum_{i=1}^{N} w_{ij}$$
 (4-1)

where N represents the total number of network nodes, which is the total number of brain regions, and w_{ij} represents the connection weight between node i and node j.

Table 4-1 Division of brain lobes

Brain Lobe	Brain Region Name	Number of Brai
		n Regions
Prefrontal Lobe	Lateralorbitofrontal, Parsorbitalis, Frontalpole,	
	Medialorbitofrontal, Parstriangularis, Parsopercularis,	22
	Rostralmiddlefrontal, Superiorfrontal,	
	Caudalmiddlefrontal, Rostralanteriorcingulate,	
	Caudalanteriorcingulate	
Frontal Lobe	Precentral, Paracentral	4
Parietal Lobe	Posterior cingulate, Isthmuscingulate, Postcentral,	12
	Supramarginal, Superiorparietal, Inferiorparietal	
Occipital Lobe	Precuneus, Cuneus, Pericalcarine, Lateraloccipital, Lingual	10
Temporal Lobe	Fusiform, Parahippocampal, Entorhinal, Temporalpole,	18
	Inferiortemporal, Middletemporal, Bankssts,	
	Superiortemporal, Transversetemporal	
Subcortical	Insula, Thalamusproper, Caudate, Putamen, Pallidum,	17
	Accumbensarea, Hippocampus, Amygdala, Brainstem	

To further analyze the differences in FC between the control group and patients with schizophrenia, based on prior anatomical information, the brain regions in the atlas were

classified according to the categories listed in Table 4-1. The brain was divided into six main lobes: prefrontal lobe (PFL), frontal lobe (FL), parietal lobe (PL), temporal lobe (TL), occipital lobe (OL), and subcortical regions (SUB)

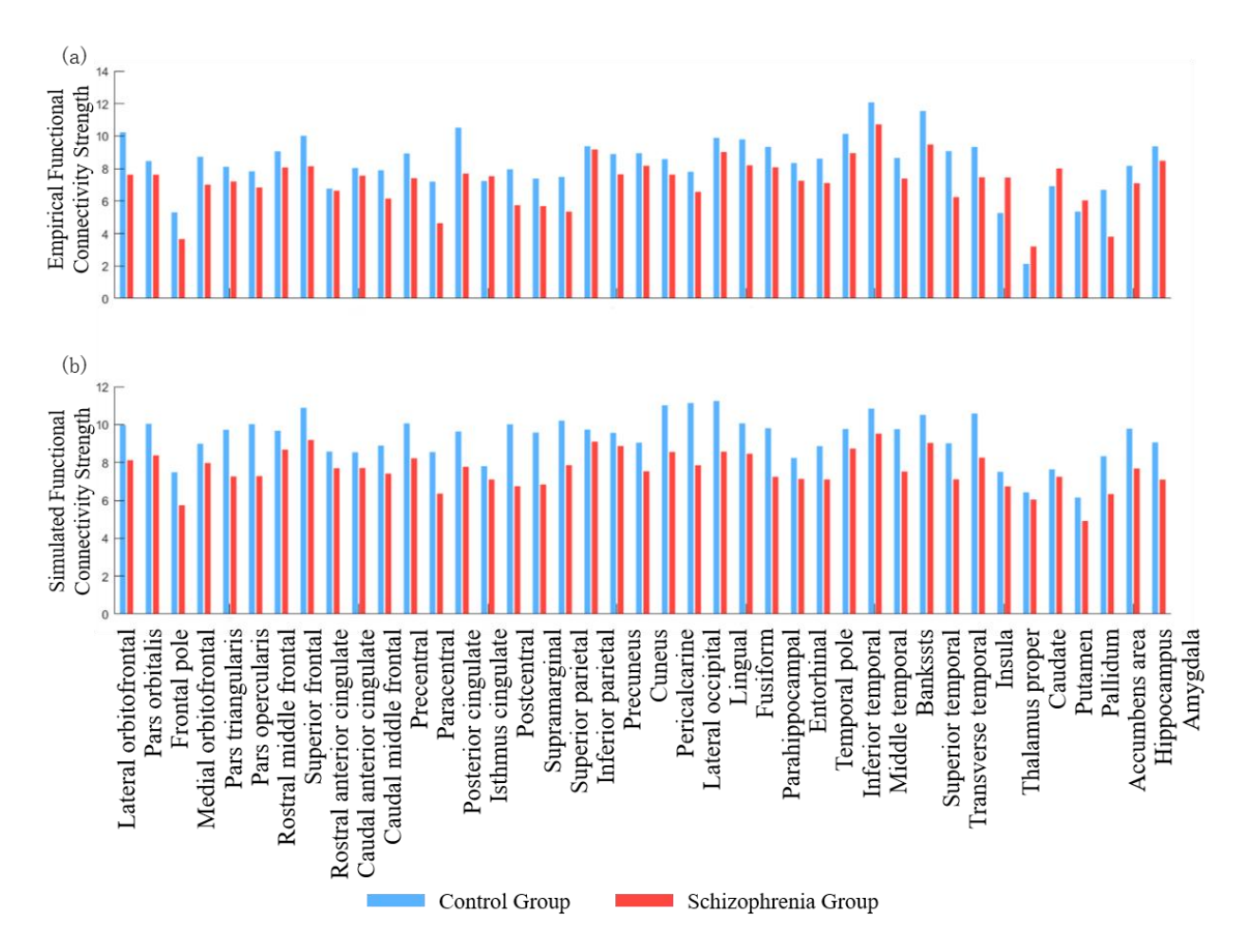


Figure 4-6 The changes of functional connectivity strength with brain regions under group average. (a) Comparison of empirical functional connectivity (FC) strengths between the control group and the schizophrenia group; (b) Comparison of model-simulated FC strengths between the control group and the schizophrenia group.

Subsequently, we can use Equation (4-1) to calculate the connectivity strength of each brain region, and further compare the differences in connectivity strength between the control group and schizophrenia patients at both brain region and lobe levels. These differences may reveal abnormal changes in the brain network structure of schizophrenia patients, as shown in the computational results in Figure 4-6 and Figure 4-7.

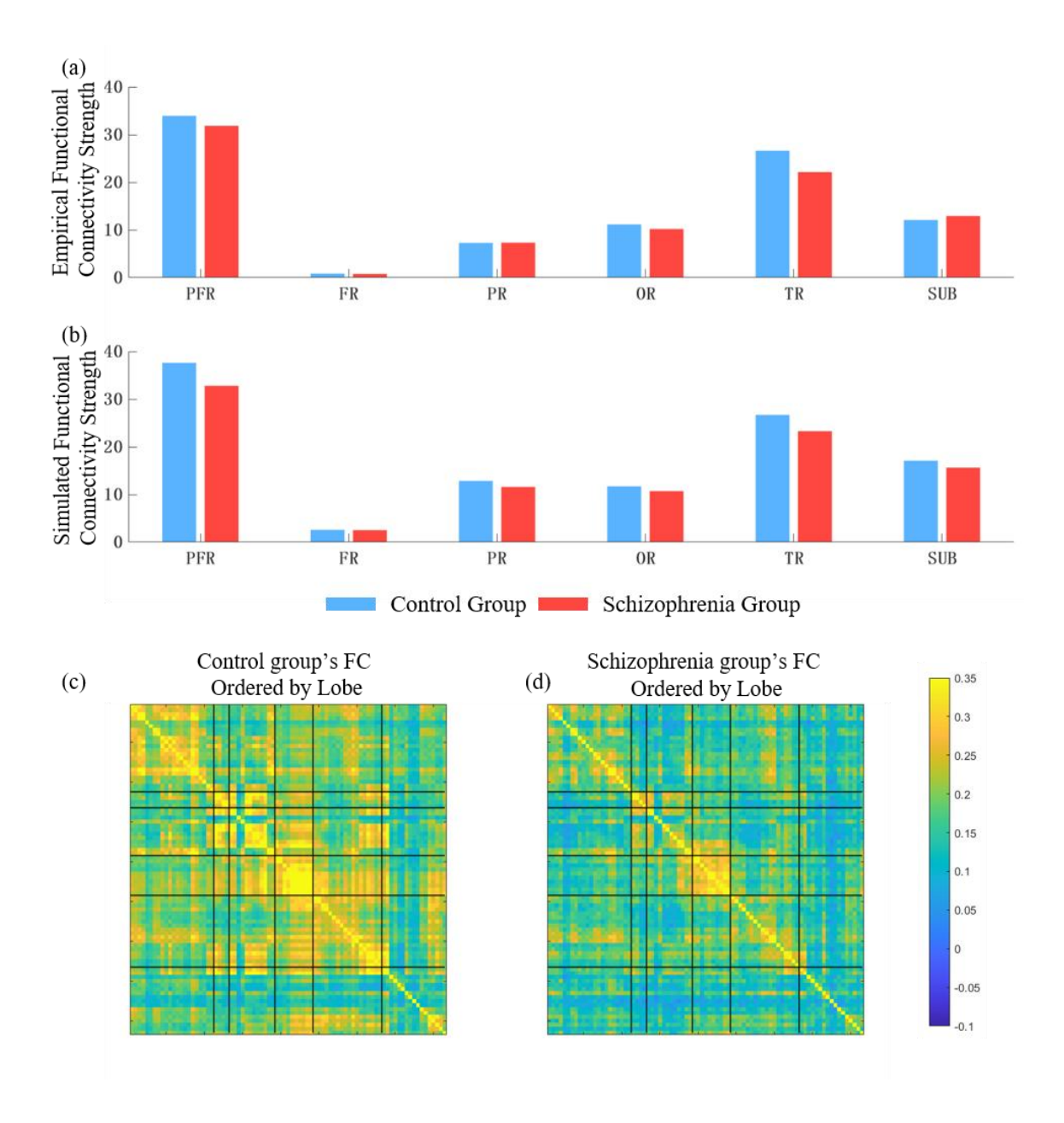


Figure 4-7 Functional connectivity strength across brain lobes (a) Empirical functional connectivity data at the lobe level; (b) Model-simulated functional connectivity at the lobe level; (c) Model-simulated mean FC of the control group arranged by lobe order; (d) Model-simulated mean FC of the schizophrenia group arranged by lobe order. Blue represents the control group, and red represents the schizophrenia group.

Comparing the FC differences in these lobes between the control group and schizophrenia patients, it can be observed that schizophrenia patients exhibit decreased functional connectivity strength in multiple brain regions and lobes, especially in the frontal and temporal lobes. This

finding is consistent with previous research results, further supporting the hypothesis of abnormal brain connectivity in schizophrenia patients.

Specifically, schizophrenia patients show weakened FC in areas such as the lateral orbitofrontal cortex, frontal pole, and superior frontal gyrus in the frontal lobe. The frontal lobe is responsible for cognitive control, decision-making, and emotion regulation, among other higher-order functions. Therefore, the reduction in FC in the frontal lobe may lead to functional impairments in these cognitive and emotional domains in patients.

Furthermore, decreased FC is also observed in areas such as the temporal pole and superior temporal gyrus in the temporal lobe. The temporal lobe is closely associated with functions such as auditory processing, language comprehension, and memory. Hence, the decrease in FC in the temporal lobe may affect the patients' auditory and language processing abilities, as well as memory function.

The brain, as an extremely complex biological structure, contains billions of neurons and synapses that are interconnected and interact with each other, forming an incredibly intricate functional system. To better understand the workings of the brain, it is necessary to analyze and discuss it from a network perspective. From the perspective of functional subnetworks, the brain can be divided into six subnetworks: the Default Mode Network (DMN), Attention Network (ATN), Auditory Network (AUN), Visual Network (VIS), Somatomotor Network (SMN), and Subcortical Network (SUN). These networks perform different cognitive and functional tasks, collectively constituting the intricate functional system of the brain. It is worth mentioning that the Default Mode Network (DMN) is the most active one in the brain during rest. When at rest, the DMN spontaneously activates and is responsible for processing thoughts related to self-reflection, imagination, and memory. Research suggests that schizophrenia patients often exhibit abnormalities in the DMN network. The division of subnetworks is detailed in Table 4-2.

Table 4-2 Brain functional sub-network partitions

Subnetwork	Brain Regions	Number of Regi ons
	Superior	
Default Mode Netwo rk (DMN)	frontal, Rostralanteriorcingulate, Caudalanteriorcingu	
	late, Posterior	18
	cingulate, Isthmuscingulate, Inferiorparietal, Precune	
	us, Entorhinal, Middletemporal	
	Lateralorbitofrontal, Parsorbitalis, Frontalpole, Media	
Attention Network	lorbitofrontal, Parstriangularis, Parsopercularis, Rostr	18
(ATN)	almiddlefrontal, Caudalmiddlefrontal, Superiorparieta	
	1	
Auditory Network	Supramarginal, Temporalpole, Bankssts, Superiortem	12
(AUN)	poral, Transversetemporal, Insula	
Visual Network	Cuneus, Pericalcarine, Lateraloccipital, Lingual, Fusifor	10
(VIS)	m	
Sensorimotor Netwo		
rk	Precentral, Paracentral, Postcentral	6
(SMN)		
Cub carties 1 Nature :-1-	Parahippocampal, Inferior temporal, Thalamusproper,	
Subcortical Network (SUN)	Caudate, Putamen, Pallidum, Accumbensarea,	19
	Hippocampus, Amygdala, Brainstem	

Based on Table 4-2 and Equation (4-1), this study further analyzed the Global Brain Connectivity (GBC) at the network level to compare the differences in connectivity strength between the control group and schizophrenia patients. The results are shown in Figure 4-8.

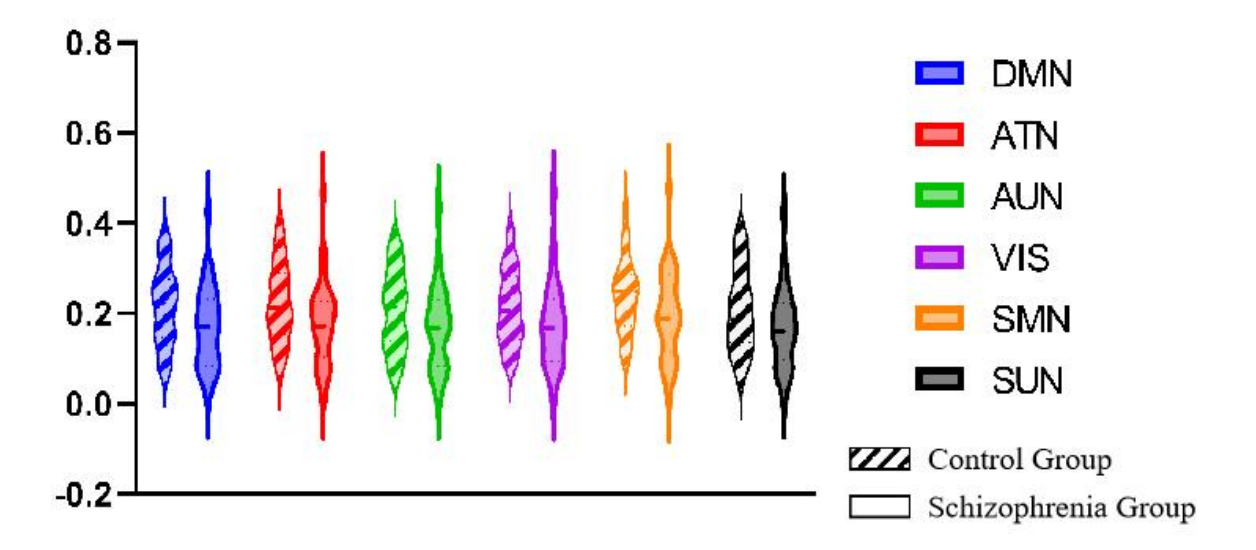


Figure 4-8 illustrates the changes in functional connectivity strength across brain networks. Dashed boxes represent the control group, while solid-colored boxes represent the schizophrenia group.

Independent sample t-tests were conducted on the GBC data for each network to assess whether significant differences existed between the two groups. The calculations yielded the following results: for the DMN network, p = 0.7450; for the ATN network, p = 0.6368; for the AUN network, p = 0.8204; for the VIS network, p = 0.4904; for the SMN network, p = 0.3244; and for the SUN network, p = 0.8371. Accepting the null hypothesis at a significance threshold of 0.05, it was concluded that there were no significant differences in GBC data between the two groups at the network level.

Possibly due to the stability and consistency of GBC data within networks, the differences between the two groups' GBC data were not significant across all networks. This may suggest that such data exhibit similar distribution patterns and characteristics in both groups, indicating the need for further exploration of the potential pathogenesis of schizophrenia using more methods.

4. 3. Model construction from a genetic perspective

While some p-values of certain parameters approached significance levels (as shown in Figure 4-1 and Figure 4-8), the existing data are still insufficient to confirm the statistical significance of

these differences. Particularly, during the parameter search process of the Wilson-Cowan model using Bayesian optimization methods, no significant differences in model parameters between the control group (CTRL) and the schizophrenia group (SCHZ) were observed. Similarly, no significant differences were found in subsequent functional GBC analysis. Therefore, introducing new elements into the model is crucial.

4. 3. 1. Integration results of transcriptome data models

The influence of genes on brain structure and function is gradually becoming apparent and increasingly significant. Integrating genomic data with neural system models has demonstrated enormous research potential. This depth of data integration aids in uncovering the close relationship between genes and neural system function. Not only does this method provide an opportunity to delve deeper into the characteristics of the neural system, but it may also offer new methodologies and treatment targets for neurological disorders. By combining genomic data obtained from resources such as the Allen Brain Atlas with models, this study aims to explore the relationship between schizophrenia-related genes and neural networks.

The brain contains various neurotransmitters, each with its unique topological characteristics, capable of mediating diverse neural activity patterns. Neurotransmitters released by the Ascending Arousal System (AAS) project extensively to various brain areas, exerting profound effects on local and global neural activity. Connectionist models are based on specific assumptions regarding the effects of neurotransmitters, such as regulating the input-output relationships of neurons and the overall synaptic strength of specific connections¹¹⁸.

The widespread distribution of neurotransmitters in the brain and their diffusion characteristics significantly influence the stability and plasticity of neural activity. To better understand brain function and neural regulatory mechanisms, it is crucial to investigate the topological characteristics of neurotransmitters and their modes of propagation. Such research may also reveal the crucial role of neurotransmitters in brain disorders and neurological conditions, providing important insights for the development of new therapies. Previous studies have attempted to introduce the expression of serotonin and dopamine receptors into large-scale brain simulation models to further explore their roles^{3,90}.

Serotonin and dopamine receptors are two important neurotransmitters in the nervous system,

playing broad biological roles and often being associated with schizophrenia¹¹⁹. Serotonergic neurons are mainly distributed in regions such as the midline nucleus, cortex, and amygdala, participating in the regulation of emotions, sleep, appetite, and various physiological functions¹²⁰. Dopaminergic neurons are mainly distributed in the mesencephalic dopaminergic system, closely related to functions such as reward, motivation, and cognition¹²¹. The expression levels, distribution, and functional characteristics of these neurotransmitters in the nervous system significantly impact neuronal excitability, synaptic plasticity, and the overall function of neural networks.

Receptors, on the other hand, are structural proteins embedded in the cell surface capable of recognizing and binding specific signaling molecules, thereby initiating a series of intracellular signal transduction processes. In the nervous system, receptors play a crucial role, as they can receive signaling molecules such as neurotransmitters, thereby regulating the excitability of neurons, synaptic plasticity, and the information transmission of the entire neural network, with their expression levels often influenced by genetic regulation.

In this study, various methods such as neuroimaging, model construction, and transcriptomics will be employed to investigate the expression, distribution, and functional characteristics of serotonin and dopamine receptor families in depth, as well as their roles in neural system function and plasticity among two groups of individuals. Additionally, this study will focus on the abnormal expression of these receptors in neurological disorders and their relationship with the occurrence and development of diseases, aiming to provide new perspectives and methodologies for the study of neurological disorders.

The expression data of dopamine and serotonin receptor families have been incorporated into the model using the parameter " h_i ", where " h_i " represents the expression level of receptors in brain region "i". In this process, the search results of the parameters of the original W-C model obtained through Bayesian optimization were first fixed, and then a search and fitting of the gene-related parameters introduced into the model were conducted. These parameters are represented as δ^E and δ^I . The visualization results of dopamine and serotonin receptor expression data mapped onto the Lausanne anatomical atlas are shown in Figure 4-9. The schematic diagram of HTR1A receptor expression can be found in Figure 3-1. Differences in the expression levels of different receptors in different brain regions can be observed. These differences reflect

the uniqueness and complexity of different brain regions in processing information, regulating emotions, and performing other cognitive functions.

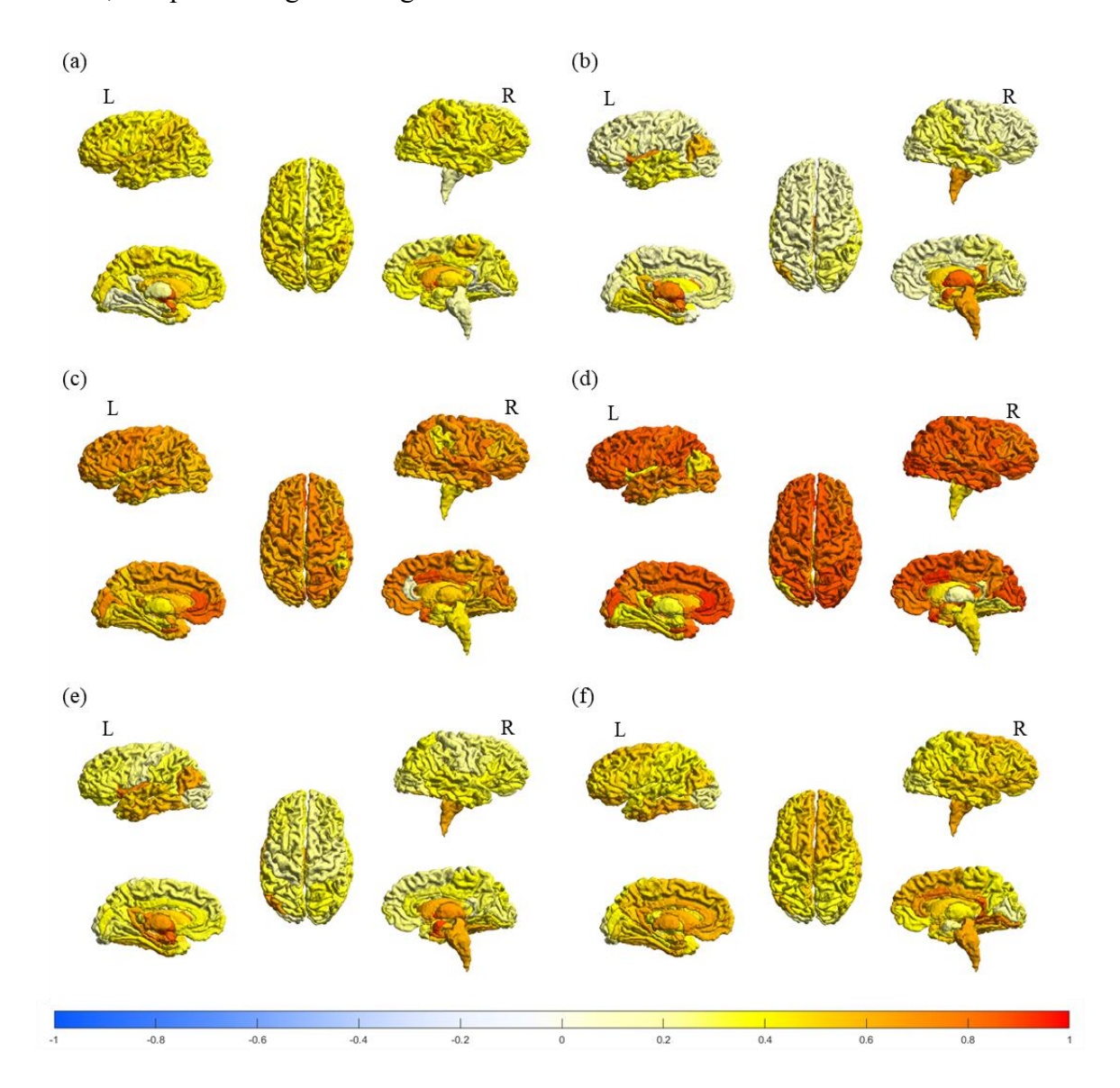


Figure 4-9 The schematic diagrams of receptor expression utilized in this study. (a) DRD1 receptor expression. (b) DRD2 receptor expression (c) DRD4 receptor expression. (d) HTR2A receptor expression. (e) HTR2C receptor expression. (f) HTR7 receptor expression

After the aforementioned transcriptomic data are incorporated into the process of model simulation, to evaluate the fit of the model, a fitness index is typically generated for each participant. However, handling and analyzing these data is a complex task that requires the use

of statistical models and computational methods. When evaluating the fit of multiple models, a unified indicator is needed for comparison and measurement. AIC (Akaike Information Criterion) is a comprehensive indicator of model fit and complexity, which penalizes complex models to avoid overfitting. In general, AIC can be expressed as:

$$AIC = \frac{(2K - 2L)}{n} \tag{4-2}$$

In this context, K represents the number of parameters in the fitted model, L denotes the logarithm of likelihood, and n is the number of observations.

However, when the sample size is small, AIC may underestimate the model's complexity, leading to the selection of overly complex models. In such cases, the AICc (Akaike Information Criterion with correction) is introduced into the research. AICc, a modification of AIC, is employed to address the issue of small sample sizes¹²². Consequently, in scenarios with small sample sizes, researchers tend to favor using AICc to assess model fit. The formula for calculating AICc is as follows¹²³:

AICc =
$$n \ln(\frac{SSE}{n}) + 2K + \frac{2K(K+1)}{n-K-1}$$
 (4-3)

Here, SSE represents the sum of squared errors between actual observed data and model-predicted values, K is the number of model parameters, and n is the sample size. As the sample size n increases, AICc gradually converges to AIC, thus making the difference between AIC and AICc negligible in cases with large sample sizes. This property allows for the application of AICc across various sample sizes¹²⁴. By incorporating the AICc criterion, the goodness-of-fit indicators for each subject are amalgamated, forming a unified evaluation standard, which facilitates model comparison and selection in this study.

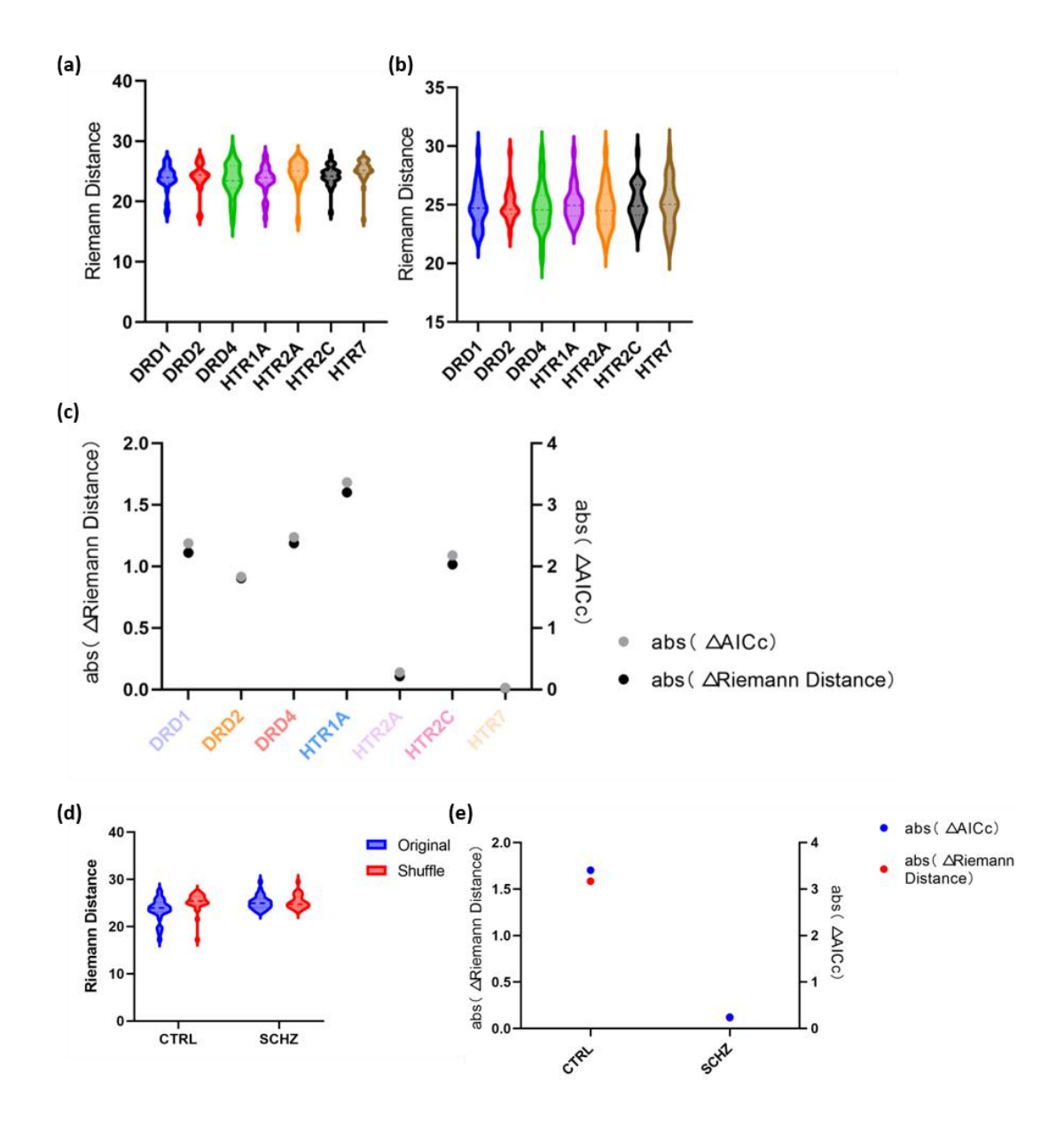


Figure 4-10 The results of integrating genetic data into the model. *DRDx* represents receptors of the dopamine family, while *HTRx* represents receptors of the serotonin family. (a) The distribution of Riemann distances among subjects in the control group (where smaller distances imply greater similarity); (b) The distribution of Riemann distances among subjects with schizophrenia; (c) The mean Riemann distances and absolute AICc values when adjusting the expression levels of various receptors; (d) The distribution of Riemann distances calculated using original and shuffled HTR1A receptor expressions in the model; (e) The mean Riemann distances and absolute AICc values when adjusting the expression levels of shuffled HTR1A receptors.

Figure 4-10 highlights pertinent findings. Notably, when adjusting the gain of HTR1A receptor expression levels, both the absolute differences in Riemann distances (left vertical axis) and AICc values (right vertical axis) peak (as depicted in Figure 4-10 (c)), indicating differences in 5-HT1A receptors between the two subject groups. Further validation was conducted by employing randomly shuffled HTR1A expression for model computation, revealing a lower goodness of fit in the shuffled results compared to the original expression. Moreover, larger absolute differences in Riemann distances (left vertical axis) and AICc values (right vertical axis) were observed in the control group, thereby affirming the rationality of incorporating transcriptome data into the model.

As a crucial member of the serotonin family, 5-HT1A receptors play key roles in neuronal activity, synaptic transmission, and neural plasticity. Therefore, the findings of this study may offer new insights into individual differences and the mechanisms of neuropsychiatric disorders, holding potential scientific and practical significance.

4. 4. Model modification

To explore the impact of receptor expression on brain function, a more nuanced analysis of the intricate associations between these receptors and the functional networks of the brain is required, alongside an investigation into how they influence the functional integration of brain networks. This analytical process will offer a more comprehensive perspective on the role of receptors in neuropsychiatric disorders and their potential correlations.

As previously mentioned, genome-wide studies have identified several genes closely related to the pathogenesis of depression and schizophrenia, including genes such as DRD2 and 5-HTT^{80,81}. Studies have indicated decreased levels of 5-HT1A receptor protein in the prefrontal cortex of female depression suicide victims⁸⁷, while significant changes in gene expression in the prefrontal pole area have been observed in schizophrenia patients⁸⁸. These changes may be related to cortical functional abnormalities, thereby triggering associated symptoms.

Of particular note is the significant cognitive impairment in schizophrenia patients, especially in attentional aspects. Despite repetitive transcranial magnetic stimulation (rTMS) being attempted as a non-invasive treatment method for schizophrenia, research findings regarding the impact of

rTMS on patient attention are inconsistent^{37,38}. Therefore, devising personalized treatment plans for patients is crucial.

Currently, available antipsychotic drugs primarily alleviate or relieve patient symptoms by modulating specific neurotransmitter receptor subtypes. When exploring the relationship between receptor expression and schizophrenia, attention should be paid not only to subtle differences in receptor gene expression but also to a comprehensive analysis within the broader context of brain network statistical properties. This holistic analysis not only aids in understanding the role of receptor expression in the nervous system but also provides a unique perspective for research, revealing the interplay between receptor expression variability and the overall structure and function of brain networks.

Further exploration of the role of brain network characteristics in the development of schizophrenia is crucial for devising more effective treatment strategies. Although the specific pathophysiology of schizophrenia is not yet fully understood, its treatment typically involves interventions targeting specific brain regions, such as using high-frequency repetitive transcranial magnetic stimulation (rTMS) to intervene in the left dorsolateral prefrontal cortex (DLPFC) of patients.

To gain a deeper understanding of this intervention process, this paper employs simulation experimental methods, identifying potentially affected brain regions and associated network changes through perturbation models. This approach aims to enhance the ability to simulate and predict potential changes within the neural system affected by the disease. Through this step, a deeper understanding of the correlation between model parameters and actual neural networks will be gained, thus promoting more accurate predictions and explanations of the nervous system and providing important references for future research and treatment.

4. 4. 1. Network properties of schizophrenic patients and healthy controls

In the field of neuroscience, the exploration of network properties holds significant importance. The brain represents a highly intricate network system, housing a vast array of neurons and synaptic connections. These connections constitute functionally interrelated neural networks, and the topological structure of these networks is crucial for understanding information transmission. Grasping the network attributes of the brain can assist us in gaining a deeper understanding of

how information is conveyed and processed within the nervous system.

Graph theory analysis is built upon the foundation of topology mathematics, abstracting brain regions into nodes and connections between brain regions into edges. Therefore, it allows for the representation of the topological characteristics of brain networks using graph theory metrics, including global efficiency, local efficiency, characteristic path length, clustering coefficient, and others. The human brain is often likened to a vast, intricate network with efficient small-world attributes that enable the efficient generation and integration of information. Numerous prior neuroimaging investigations have consistently shown evidence of "dysfunctional connectivity" between different brain regions in individuals with schizophrenia. The results revealed that the brain's functional networks exhibited efficient small-world characteristics among healthy individuals, but these attributes were disrupted in individuals with schizophrenia. Particularly noteworthy was the significant alteration of small-world topological attributes in numerous brain regions within the prefrontal, parietal, and temporal lobes of schizophrenia patients¹²⁵. These findings align with the hypothesis of impaired brain integration in this disorder. The calculation of the majority of network coefficients can be achieved using the Brain Connectivity Toolbox (BCT) package¹²⁶. This offers a unique perspective for understanding brain networks. Currently, these graph theory metrics have been widely applied to various studies of brain disorders, such as Parkinson's disease, depression, autism, schizophrenia, and other mental disorders¹²⁷.

The specific descriptions and calculation formulas for four network metrics: global efficiency, local efficiency, characteristic path length, and clustering coefficient, are provided as follows:

(1) Global efficiency

Global efficiency measures a network's capability for parallel information processing and is defined as the average of the reciprocal of the shortest paths between any two nodes. Typically, the shortest path length is used in conjunction with global efficiency to assess a network's overall transmission capacity; shorter paths correspond to higher global efficiency, while longer paths indicate lower global efficiency, signifying a decrease in information transmission and interaction capabilities among nodes. The calculation formula for global efficiency is as follows:

$$E_{global} = \frac{1}{N(N-1)} \sum_{i,j=1}^{N} \frac{1}{d_{i,j}}$$
 (4-4)

(2) Local efficiency

Local efficiency measures the capability of propagating information through the directly connected neighbors of a node. In contrast to global efficiency, local efficiency reflects the integration level of the immediate neighboring nodes for a given node. Typically, local efficiency is used in conjunction with the clustering coefficient to measure the efficiency of information transmission within a network. It also partially reflects the network's resilience to random attacks, indicating whether the removal of a node affects the communication efficiency among its adjacent nodes. The calculation formula for local efficiency is as follows:

$$E_{local} = \frac{1}{N} \sum_{i=1}^{N} E_{local_i} = \frac{1}{N} \sum_{i=1}^{N} \frac{\sum_{j,h \in N, j \neq i} a_{i,j} a_{i,h} [d_{j,h}(N_i)]^{-1}}{k_i (k_i - 1)}$$
(4-5)

(3) Characteristic path length

The characteristic path length measures the overall routing efficiency and the network's capability for parallel information processing. In contrast to global efficiency, an increase in the characteristic path length reflects a decrease in the efficiency of information transmission and interaction between nodes. The characteristic path length of a network is the average of the shortest paths between any two nodes in the network. Here, the shortest path refers to the path with the fewest edges between two nodes, and the number of edges this path passes through represents the length of the shortest path between these two nodes. The calculation formula for the characteristic path length is as follows:

$$L = \frac{1}{N(N-1)} \sum_{i,j=1}^{N} d_{i,j}$$
(4-6)

(4) Clustering coefficient

The clustering coefficient of a node in a graph is defined as the ratio between the actual number of edges among the node's directly connected neighboring nodes and the maximum possible number of edges among these neighboring nodes. The clustering coefficient of a node describes the density of connections between a node and its neighboring nodes, while the average clustering coefficient of all nodes represents the clustering coefficient of the entire network. Generally, the clustering coefficient of the entire network is used to assess the efficiency of local

information processing. A higher value indicates stronger local communication capability. The calculation formula for the clustering coefficient is as follows:

$$C = \frac{1}{N} \sum_{i=1}^{N} \frac{\sum_{j,k \in N} (w_{i,j} w_{i,h} w_{j,h})^{\frac{1}{3}}}{k_i (k_i - 1)}$$
(4-7)

To compare the distribution of network coefficient data between the two groups, we initially assessed whether the network coefficient data in both groups adhered to a normal distribution. Given the relatively small sample size, we employed the Shapiro-Wilk test. The results are illustrated in Figure 4-11.

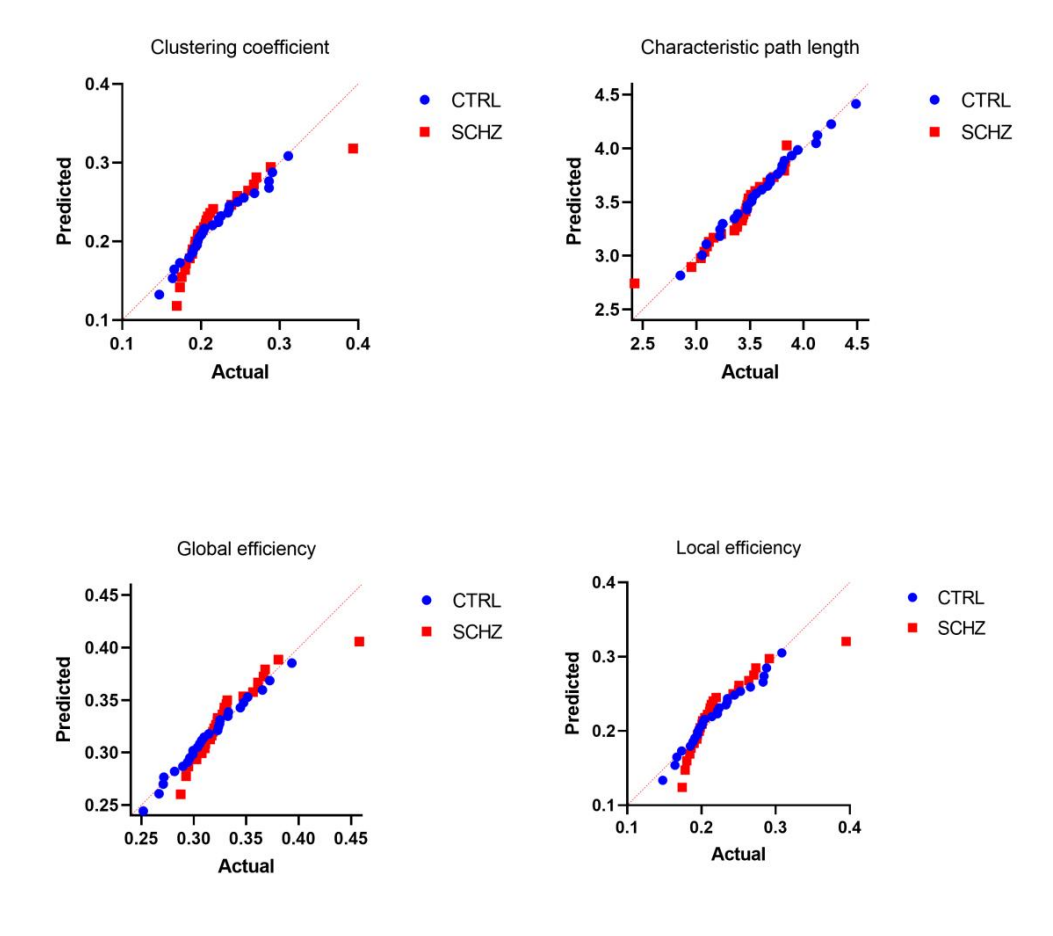


Figure 4-11 Results of Shapiro-Wilk normality tests. (a) Normality test for clustering coefficient; (b) Normality test for characteristic path length; (c) Normality test for global efficiency; (d) Normality test for local efficiency

We performed the Shapiro-Wilk test on the network coefficient data from both groups to assess their adherence to a normal distribution. A significance level of 0.05 was set, assuming the null hypothesis that the data follows a normal distribution. In the case of the control group, the resulting p-values were as follows: p=0.439 (ns) for clustering coefficient, p=0.996 (ns) for characteristic path length, p=0.954 (ns) for global efficiency, and p=0.476 (ns) for global efficiency. Hence, considering this threshold, we substantiate the hypothesis of a normal distribution for all network coefficient data within the control group.

In the case of the schizophrenia group, the resulting p-values were: p < 0.0001 (****) for clustering coefficient, p = 0.0409 (*) for characteristic path length, p < 0.001(***) for global efficiency, and p < 0.0001 (***) for global efficiency. Considering this threshold, we reject the hypothesis of a normal distribution for all network coefficient data within the schizophrenia group.

Through Shapiro-Wilk tests, it was found that the network coefficient data of the control group conforms to a normal distribution, while the network coefficient data of the schizophrenia group does not follow a normal distribution, exhibiting significant within-group differences, possibly related to functional network abnormalities caused by schizophrenia. Due to some data not conforming to a normal distribution, the non-parametric Mann-Whitney test was chosen to compare the two data sets. The test results are shown in Figure 4-12.

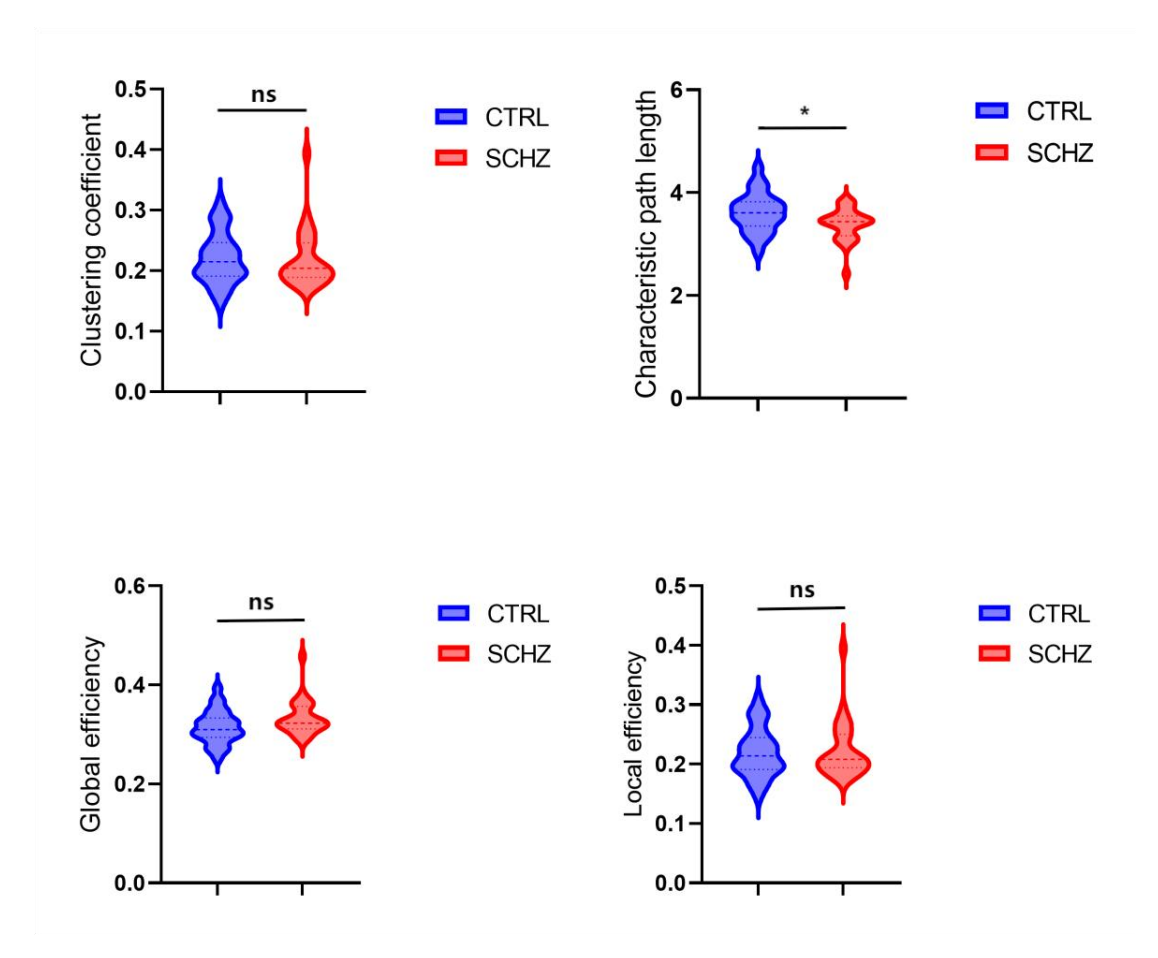


Figure 4-12 Mann-Whitney test. (a) Distribution test of clustering coefficient between groups; (b) Distribution test of characteristic path length between groups; (c) Distribution test of global efficiency between groups; (d) Distribution test of local efficiency between groups.

Given that none of the network coefficient data within the schizophrenia group follows a normal distribution, the Mann-Whitney test was conducted to compare the distributions of network coefficient data between both groups. A significance level of 0.05 was utilized to test the null hypothesis, which examines the existence of significant differences between the distributions of the two groups. The resulting p-values were computed as 0.6067 (ns) for the clustering coefficient, 0.027 (*) for characteristic path length, 0.078 (ns) for global efficiency, and 0.918 (ns) for global efficiency. These outcomes suggest the absence of significant differences in the distributions of network coefficient data between the groups except for characteristic path length.

4. 5. Identification of Potentially Impaired Brain Regions

Previous research has revealed the largest differences in integrated receptor expression of HTR1A receptors between the control group and the schizophrenia group. To further investigate the impact of gene expression changes in the frontal lobe and DLPFC region on overall brain functional changes, this study modified the HTR1A receptor expression data based on control group data to make it more similar to the data of the schizophrenia group. Specifically, the DLPFC is located in the frontal lobe, and based on literature references, its location in Brodmann areas 9 and 46 were determined 128,129. Based on this, the corresponding location of the DLPFC in the brain atlas (Lausanne Anatomy Atlas) used in this study was determined.

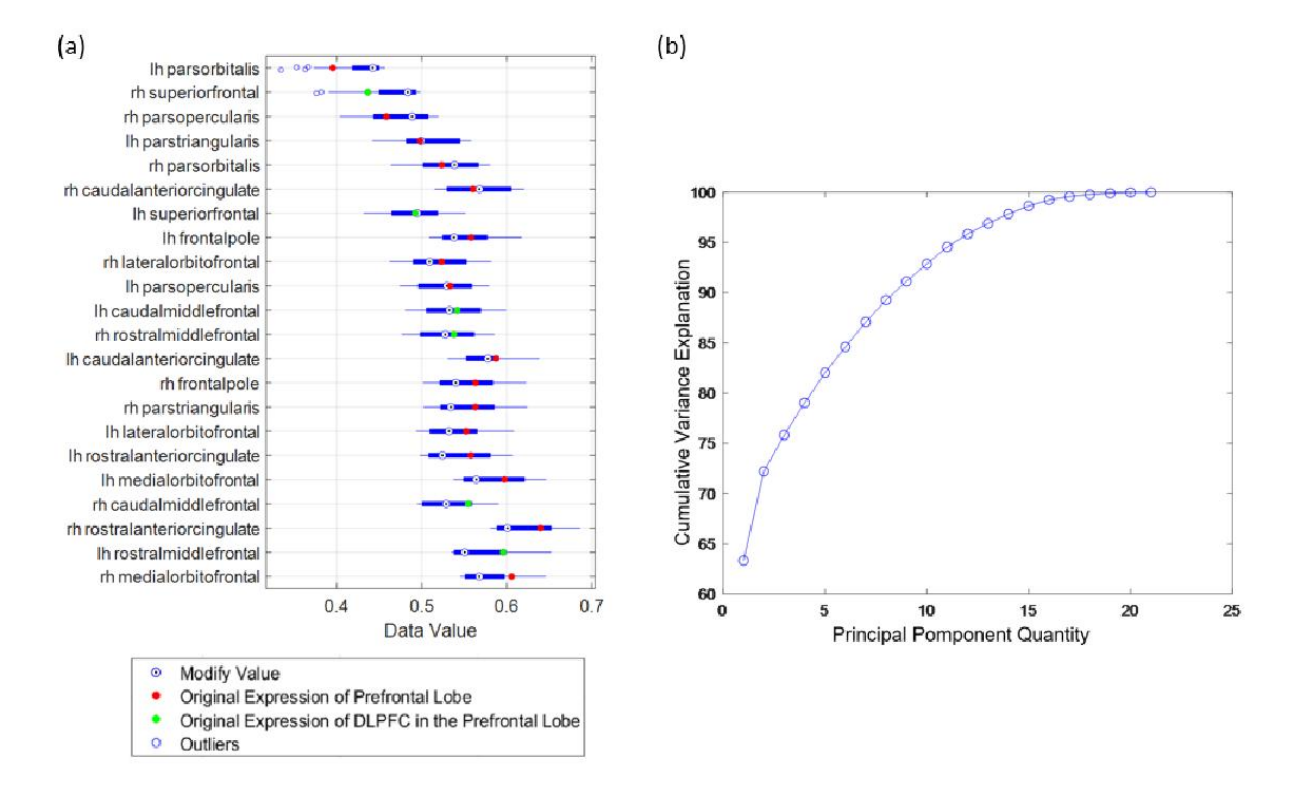


Figure 4-13 Modified result in the prefrontal lobe and the principal component analysis result. (a) The results of the frontal lobe modification, where the blue bars represent the distribution values of gene expression after modification for each subject, with the DLPFC region highlighted in green. (b) The results of the Principal Component Analysis, with the number of principal components and the cumulative variance explained ratio depicted

During the simulation process, the Kolmogorov-Smirnov statistical test method¹³⁰ was utilized to compare the simulated FC with empirical FC network properties, assessing the consistency of the coefficient distribution of generated data with real data, thereby imposing certain constraints on the generation process. The modified results are shown in Figure 4-13.

Figure 4-13 reveals the results of the frontal lobe modification, showing a decrease in the average expression level of HTR1A compared to the original expression in most cortical areas of the frontal lobe. Since the frontal lobe plays a crucial role in cognitive and emotional processing, changes in HTR1A expression levels may have implications for these functions.

Although the direct presentation of these results provides preliminary insights, further processing with mathematical methods is necessary to obtain a deeper and more intuitive understanding. Principal Component Analysis (PCA), as an analysis tool widely used in neuroscience, holds significant value. The work of researchers such as Karamizadeh¹³¹ and Gauch Jr¹³² has demonstrated the advantages of PCA in noise reduction and extraction of key information. In this case, even in the face of complex influences between multiple brain regions, PCA can still help accurately identify the main contributors affecting the results. Therefore, Principal Component Analysis (PCA) is employed for further analysis of the existing results.

Further observation of Figure 4-13(b) shows that the first 5 principal components explain 82.05% of the total variance, while the first 8 principal components explain 89.27% of the total variance. This indicates that these principal components capture most of the variability in the data. The brain regions contributing significantly to the variance include the Lateral Orbitofrontal, Parsopercularis, Parstriangularis, Medial Orbitofrontal, Rostral Middle Frontal, Parsorbitalis, Superior Frontal and Rostral Anterior Cingulate. Many of these regions are associated with schizophrenia, as confirmed by extensive neuroimaging or genomic reports^{26,27,29,30,88}. It is noteworthy that many of these prominent brain regions belong to the Attention Network (ATN) and Default Mode Network (DMN). These results suggest that the attention network and default mode network of schizophrenia patients may be more severely impaired.

CHAPTER 5: SUMMARY & DISCUSSION

The brain is comprised of intricately interconnected neurons and various types of associated cells, forming a precise synaptic network that serves as the core structure governing cognitive processes and behaviors within the nervous system. This paper aims to investigate the differences in brain activity patterns between individuals with schizophrenia and healthy controls. By integrating multidimensional perspectives from neuroimaging, genetics, and computational neuroscience, this study seeks to unveil the pathogenesis of schizophrenia through large-scale brain simulations, offering novel insights and methodologies for a deeper understanding of this complex disorder.

Initially, this paper elaborates on the sources and processing procedures of the dataset, including the acquisition and preprocessing of magnetic resonance imaging (MRI) and genetic data. The integration of neuroimaging and brain simulation technologies enables an in-depth exploration of brain operation mechanisms, revealing the close relationship between structural and functional connections. The paper attempts to simulate the neural behaviors of different populations and individuals using a mesoscale brain model constructed with standard MRI datasets containing details of structural and functional connections, employing field modeling methodology. This mesoscale neural network model, based on the coupled Wilson-Cowan model, assigns each node to a specific brain region, further enhancing the understanding of brain operation under different conditions through traversing high-dimensional parameter spaces.

Subsequently, the Wilson-Cowan model and its extended application in whole-brain modeling are detailed, with the Balloon-Windkessel hemodynamic model employed to transform neural electrical signals into BOLD signals. To enhance model accuracy, this study utilizes an empirical structural connectivity (SC) matrix as a constraint, weighting it via a global coupling term G and compensating for its deficiencies through a "structure-function" iterative optimization strategy. Furthermore, a Bayesian optimization algorithm based on probabilistic modeling is employed in the parameter space to improve model fitting performance. Through these methods, an individualized whole-brain model is successfully constructed. However, a comparative analysis of model parameters between schizophrenia patients and controls does not reveal significant differences. Nevertheless, global brain connectivity analysis indicates reduced functional connectivity strength in schizophrenia patients, particularly in the frontal and temporal regions.

Based on these findings, it is deemed necessary to further integrate research on neurotransmitters, neural networks, and personalized therapeutic approaches to delve deeper into the neurobiological basis of schizophrenia and provide more effective diagnostic and therapeutic strategies for patients. Additionally, to explore the role of receptor expression in schizophrenia, this study integrates receptor gene expression data from the Allen Brain Institute, aiming to uncover potential variations in receptor expression among schizophrenia patients and establish connections between computational models and receptor expression to explore potential biological impact processes. The research results suggest that abnormal brain connectivity in patients may be related to changes in 5-HT1A receptor expression levels.

Furthermore, based on 5-HT1A receptor expression and under the constraint of brain network indicators, the whole-brain computational model of healthy control subjects is modified to identify potential differences between schizophrenia patients and normal individuals. Regarding the modified results, attention is focused on brain regions contributing significantly to variance, concentrated in the attention network (ATN) and default mode network (DMN), including the lateral orbitofrontal cortex, insula, triangular part, inferior frontal gyrus, medial orbitofrontal cortex, inferior frontal gyrus, and anterior cingulate gyrus. An in-depth study of these regions is expected to provide personalized treatment options for schizophrenia patients, such as cognitive training or drug therapy targeting impaired ATN.

The results of this study indicate reduced connectivity levels in the frontal and temporal regions of schizophrenia patients. Furthermore, by establishing connections between computational models and receptor expression, it is discovered that abnormal brain activity in patients may be associated with changes in 5-HT1A receptor expression levels. The modified whole-brain computational model shows that the attention network and default mode network of schizophrenia patients are more severely impaired. In conclusion, by combining research methods from modeling, neuroimaging, and genomics, a more comprehensive understanding of the neurobiological basis of schizophrenia can be achieved. In-depth studies focusing on specific brain regions or neural pathways can more accurately identify issues. Such precision-targeted therapeutic approaches are expected to provide more effective diagnostic and treatment options for patients, realizing more targeted interventions. Research in this field not only holds promise for improving the quality of life for patients but also provides deeper insights into human brain function and disorders.

CHAPTER 6: FUTURE RESEARCH

While this article provides insights into some potential mechanisms of schizophrenia based on large-scale brain models constrained by transcriptomic data, there are still some limitations that need to be addressed:

- (1) Despite the utilization of a whole-brain computational model at the mesoscale and the attempt to simulate individual-level dynamics using existing data and computational resources, the construction of the model still lacks precision compared to the detailed information covered at the neuronal scale. To establish a high-precision model that truly reflects the dynamics at the microscale of the human brain, future research could consider integrating prior information from layered heterogeneous T1w/T2w-weighted images, high-density electroencephalography (EEG), magnetoencephalography (MEG), and other modalities to build a multimodal whole-brain model.
- (2) Although receptor gene expression data were incorporated into the model, the complex interactions among neurotransmitters and receptors were not considered. Subsequent studies could employ more targeted and refined data, as well as more accurately design physiological models based on relevant literature reports.
- (3) While modifications to receptor gene expression in this study were targeted at certain brain regions delineated by templates, they did not further specify more finely divided brain regions and lacked actual experimental data for result validation. Additionally, due to limited sample sizes or datasets, there may be insufficient subjects. Future research should focus on recruiting more schizophrenia patients, grouping them based on disease subtypes using data analysis methods and conducting intervention experiments. Through these experiments, a deeper exploration of the association between brain function and specific symptoms can be conducted, thereby formulating more effective treatment plans for different symptoms.
- (4) Researchers with practical experimental capabilities may consider integrating physical field interventions, involving simulating low-frequency or high-frequency repetitive transcranial magnetic stimulation (rTMS) in computational models to stimulate and influence specific brain regions of patients. This comparative approach will introduce a new perspective of data to explore the activity of the model and relevant system-level neural circuits in practice.

Despite schizophrenia being a complex disorder, with the continuous development and advancement of science and technology, we have reasons to believe that in the future, researchers will be able to gain a deeper understanding of this disease and develop more effective treatment methods. This will bring hope to those affected by this condition and help them live better.

References

- Wang X-J, Hu H, Huang C, et al. Computational neuroscience: a frontier of the 21st century [J]. 2020, 7(9): 1418-22.
- Ghosh A, Rho Y, McIntosh A R, et al. Noise during rest enables the exploration of the brain's dynamic repertoire [J]. PLoS computational biology, 2008, 4(10): e1000196.
- Deco G, Cruzat J, Cabral J, et al. Whole-brain multimodal neuroimaging model using serotonin receptor maps explains non-linear functional effects of LSD [J]. 2018, 28(19): 3065-74. e6.
- 4 Insel T R. Rethinking Schizophrenia [J]. Nature, 2010, 468(7321): 187-93.
- Jaeschke K et al. Global estimates of service coverage for severe mental disorders: findings from the WHO Mental Health Atlas 2017 Glob Ment Health 2021;8:e27.
- 6 Andreasen N C, Flaum M J S b. Schizophrenia: the characteristic symptoms [J]. 1991, 17(1): 27-49.
- Harrison G, Hopper K, Craig T, Laska E, Siegel C, Wanderling J. Recovery from psychotic illness: a 15-and 25-year international follow-up study. Br J Psychiatry 2001;178:506-17.
- 8 Diagnostic and Statistical Manual of Mental Disorders: DSM-5 (5th ed.). Arlington, VA: American Psychiatric Association. 2013. pp. 99–105.
- Wedeen V J, Hagmann P, Tseng W Y I, et al. Mapping complex tissue architecture with diffusion spectrum magnetic resonance imaging [J]. 2005, 54(6): 1377-86.
- Alexander A L, Lobaugh N J J H o b c. Insights into brain connectivity using quantitative MRI measures of white matter [J]. 2007: 221-71.
- Buxton R B, Frank L R J J o c b f, metabolism. A model for the coupling between cerebral blood flow and oxygen metabolism during neural stimulation [J]. 1997, 17(1): 64-72.
- Deco G, Jirsa V K J J o N. Ongoing cortical activity at rest: criticality, multistability, and ghost attractors [J]. 2012, 32(10): 3366-75.
- Lee M H, Smyser C D, Shimony J S J A J o n. Resting-state fMRI: a review of methods and clinical applications [J]. 2013, 34(10): 1866-72.
- Mwansisya T E, Hu A, Li Y, et al. Task and resting-state fMRI studies in first-episode Schizophrenia: A systematic review [J]. 2017, 189: 9-18.
- Karbasforoushan, 15 H.; Woodward, N.D. (2012-11-01)."Resting-State Networks in 2404-Schizophrenia". Current Topics in Medicinal Chemistry. 12 (21): 2414. doi:10.2174/156802612805289863. PMID 23279179.

- 16 Tan H-Y, Sust S, Buckholtz J W, et al. Dysfunctional prefrontal regional specialization and compensation in Schizophrenia [J]. 2006, 163(11): 1969-77.
- Paulus M P, Hozack N E, Zauscher B E, et al. Parietal dysfunction is associated with increased outcomerelated decision-making in Schizophrenia patients [J]. 2002, 51(12): 995-1004.
- Kim J-J, Seok J H, Park H-J, et al. Functional disconnection of the semantic networks in Schizophrenia [J]. 2005, 16(4): 355-9.
- Spence S A, Liddle P F, Stefan M D, et al. Functional anatomy of verbal fluency in people with Schizophrenia and those at genetic risk: focal dysfunction and distributed disconnectivity reappraised [J]. 2000, 176(1): 52-60.
- Guo S, Kendrick K M, Yu R, et al. Key functional circuitry altered in Schizophrenia involves parietal regions associated with sense of self[J]. Human brain mapping, 2014, 35(1): 123-139.
- Honey G D, Pomarol-Clotet E, Corlett P R, et al. Functional dysconnectivity in Schizophrenia associated with attentional modulation of motor function [J]. 2005, 128(11): 2597-611.
- Bluhm R L, Miller J, Lanius R A, et al. Spontaneous low-frequency fluctuations in the BOLD signal in schizophrenic patients: anomalies in the default network [J]. 2007, 33(4): 1004-12.
- Holt D J, Cassidy B S, Andrews-Hanna J R, et al. An anterior-to-posterior shift in midline cortical activity in Schizophrenia during self-reflection [J]. 2011, 69(5): 415-23.
- Whitfield-Gabrieli S, Ford J M J A r o c p. Default mode network activity and connectivity in psychopathology [J]. 2012, 8: 49-76.
- White T P, Joseph V, Francis S T, et al. Aberrant salience network (bilateral insula and anterior cingulate cortex) connectivity during information processing in Schizophrenia [J]. 2010, 123(2-3): 105-15.
- Nakamura M, Nestor P G, Levitt J J, et al. Orbitofrontal volume deficit in Schizophrenia and thought disorder[J]. Brain, 2008, 131(1): 180-195.
- Nakamura M, Nestor P G, McCarley R W, et al. Altered orbitofrontal sulcogyral pattern in Schizophrenia[J]. Brain, 2007, 130(3): 693-707.
- Waltz J A, Gold J M. Probabilistic reversal learning impairments in Schizophrenia: further evidence of orbitofrontal dysfunction[J]. Schizophrenia research, 2007, 93(1-3): 296-303.
- Onitsuka T, Shenton M E, Salisbury D F, et al. Middle and inferior temporal gyrus gray matter volume abnormalities in chronic Schizophrenia: an MRI study[J]. American Journal of Psychiatry, 2004, 161(9): 1603-1611.

- Kuroki N, Shenton M E, Salisbury D F, et al. Middle and inferior temporal gyrus gray matter volume abnormalities in first-episode Schizophrenia: an MRI study[J]. American Journal of Psychiatry, 2006, 163(12): 2103-2110.
- 31 Carlsson A. Antipsychotic drugs, neurotransmitters, and Schizophrenia[J]. American Journal of Psychiatry, 1978, 135(2): 164-173.
- 32 Carlsson A. Antipsychotic drugs, neurotransmitters, and Schizophrenia[J]. American Journal of Psychiatry, 1978, 135(2): 164-173.
- Crossley N A, Constante M, McGuire P, et al. Efficacy of atypical v. typical antipsychotics in the treatment of early psychosis: meta-analysis [J]. 2010, 196(6): 434-9.
- Geddes J, Freemantle N, Harrison P, et al. Atypical antipsychotics in the treatment of Schizophrenia: systematic overview and meta-regression analysis [J]. 2000, 321(7273): 1371-6.
- Robinson S E, Sohal V S J J o N. Dopamine D2 receptors modulate pyramidal neurons in mouse medial prefrontal cortex through a stimulatory G-protein pathway [J]. 2017, 37(42): 10063-73.
- Johnson J A, Strafella A P, Zatorre R J J J o c n. The role of the dorsolateral prefrontal cortex in bimodal divided attention: two transcranial magnetic stimulation studies [J]. 2007, 19(6): 907-20.
- Guse B, Falkai P, Gruber O, et al. The effect of long-term high frequency repetitive transcranial magnetic stimulation on working memory in Schizophrenia and healthy controls—a randomized placebo-controlled, double-blind fMRI study [J]. 2013, 237: 300-7.
- Mittrach M, Thünker J, Winterer G, et al. The tolerability of rTMS treatment in Schizophrenia with respect to cognitive function [J]. 2010, 43(03): 110-7.
- Shang Y, Wang X, Li F, et al. rTMS Ameliorates Prenatal Stress Induced Cognitive Deficits in Male-Offspring Rats Associated With BDNF/TrkB Signaling Pathway [J]. 2019, 33(4): 271-83.
- Zhuo K, Tang Y, Song Z, et al. Repetitive transcranial magnetic stimulation as an adjunctive treatment for negative symptoms and cognitive impairment in patients with Schizophrenia: a randomized, double-blind, sham-controlled trial[J]. Neuropsychiatric disease and treatment, 2019, 15: 1141-1150.
- 41 Yoshikawa A, Li J, Meltzer H Y. A functional HTR1A polymorphism, rs6295, predicts short-term response to lurasidone: Confirmation with meta-analysis of other antipsychotic drugs[J]. The pharmacogenomics journal, 2020, 20(2): 260-270.
- Lorentzen R, Et Al. The efficacy of transcranial magnetic stimulation (TMS) for negative symptoms in Schizophrenia: a systematic review and meta-analysis[J]. Schizophrenia, 2022, 8(1): 35.

- Hodgkin A L, Huxley A F. A quantitative description of membrane current and its application to conduction and excitation in nerve[J]. The Journal of physiology, 1952, 117(4): 500.
- Abbott L F. Lapicque's introduction of the integrate-and-fire model neuron (1907)[J]. Brain research bulletin, 1999, 50(5-6): 303-304.
- 45 Gerstner W, Kistler W M. Spiking neuron models : single neurons, populations, plasticity[M]. Cambridge University Press, 2002.
- Madsen A, Reddy S, Chandar S. Post-hoc interpretability for neural nlp: A survey[J]. ACM Computing Surveys, 2022, 55(8): 1-42.
- 47 Huang Y, Et Al. Gpipe: Efficient training of giant neural networks using pipeline parallelism, 2019.
- 48 Gorgolewski K J, Poldrack R A. A practical guide for improving transparency and reproducibility in neuroimaging research, 2016: e1002506.
- 49 Brodoehl S, Et Al. Surface-based analysis increases the specificity of cortical activation patterns and connectivity results, 2020: 5737.
- Honey C J, Kötter R, Breakspear M, et al. Network structure of cerebral cortex shapes functional connectivity on multiple time scales [J]. 2007, 104(24): 10240-5.
- Honey C J, Sporns O, Cammoun L, et al. Predicting human resting-state functional connectivity from structural connectivity [J]. 2009, 106(6): 2035-40.
- Alstott J, Breakspear M, Hagmann P, et al. Modeling the impact of lesions in the human brain [J]. 2009, 5(6): e1000408.
- Cabral J, Hugues E, Sporns O, et al. Role of local network oscillations in resting-state functional connectivity [J]. 2011, 57(1): 130-9.
- Deco G, McIntosh A R, Shen K, et al. Identification of optimal structural connectivity using functional connectivity and neural modeling [J]. 2014, 34(23): 7910-6.
- Destexhe A, Sejnowski T J. The Wilson Cowan model, 36 years later[J]. Biological Cybernetics, 2009, 101(1): 1-2.
- Zhang G, Cui Y, Zhang Y, et al. Computational exploration of dynamic mechanisms of steady state visual evoked potentials at the whole brain level[J]. NeuroImage, 2021, 237: 118166.
- Mejias J F, Murray J D, Kennedy H, et al. Feedforward and feedback frequency-dependent interactions in a large-scale laminar network of the primate cortex [J]. 2016, 2(11): e1601335.
- 58 Krystal J H, Murray J D, Chekroud A M, et al. Computational Psychiatry and the Challenge of Schizophrenia[J]. Schizophrenia Bulletin, 2017, 43(3): 473-475

- Hutchings F, Han C E, Keller S S, et al. Predicting surgery targets in temporal lobe epilepsy through structural connectome based simulations [J]. 2015, 11(12): e1004642.
- Van Hartevelt T J, Cabral J, Deco G, et al. Neural plasticity in human brain connectivity: the effects of long term deep brain stimulation of the subthalamic nucleus in Parkinson's disease [J]. 2014, 9(1): e86496.
- Perl Y S, Fittipaldi S, Campo C G, et al. Model-based whole-brain perturbational landscape of neurodegenerative diseases [J]. 2023, 12: e83970.
- Anticevic A, Cole M W, Repovs G, et al. Connectivity, Pharmacology, and Computation: Toward a Mechanistic Understanding of Neural System Dysfunction in Schizophrenia[J]. Frontiers in Psychiatry, 2013, 4.
- 63 Krystal J H, Anticevic A, Yang G J, et al. Impaired Tuning of Neural Ensembles and the Pathophysiology of Schizophrenia: A Translational and Computational Neuroscience Perspective[J]. Biological Psychiatry, 2017, 81(10): 874-885.
- Yang G J, Murray J D, Wang X-J, et al. Functional hierarchy underlies preferential connectivity disturbances in Schizophrenia[J]. Proceedings of the National Academy of Sciences, 2015, 113(2).
- Sunkin S M, Ng L, Lau C, et al. Allen Brain Atlas: an integrated spatio-temporal portal for exploring the central nervous system[J]. Nucleic acids research, 2012, 41(D1): D996-D1008.
- Kang H J, Kawasawa Y I, Cheng F, et al. Spatio-temporal transcriptome of the human brain[J]. Nature, 2011, 478(7370): 483-489.
- Hawrylycz M J, Lein E S, Guillozet-Bongaarts A L, et al. An anatomically comprehensive atlas of the adult human brain transcriptome[J]. Nature, 2012, 489(7416): 391-399.
- 68 Miller J A, Ding S L, Sunkin S M, et al. Transcriptional landscape of the prenatal human brain[J]. Nature, 2014, 508(7495): 199-206.
- 69 Hawrylycz M, Miller J A, Menon V, et al. Canonical genetic signatures of the adult human brain[J]. Nature neuroscience, 2015, 18(12): 1832-1844.
- Fornito A, Arnatkevičiūtė A, Fulcher B D. Bridging the gap between connectome and transcriptome[J]. Trends in cognitive sciences, 2019, 23(1): 34-50.
- Hibar D P, Stein J L, Renteria M E, et al. Common genetic variants influence human subcortical brain structures[J]. Nature, 2015, 520(7546): 224-229.
- Shen E H, Overly C C, Jones A R. The Allen Human Brain Atlas: comprehensive gene expression map** of the human brain[J]. Trends in neurosciences, 2012, 35(12): 711-714.

- Combs DR, Mueser KT, Gutierrez MM (2011). "Chapter 8: Schizophrenia: Etiological considerations". In Hersen M, Beidel DC (eds.). Adult psychopathology and diagnosis (6th ed.). John Wiley & Sons.
- O'Donovan M C, Williams N M, Owen M J. Recent advances in the genetics of Schizophrenia[J]. Human molecular genetics, 2003, 12(suppl 2): R125-R133.
- 75 Picchioni M M, Murray R M. Schizophrenia[J]. 2007, 335(7610): 91-95.
- Schork A J, Wang Y, Thompson W K, et al. New statistical approaches exploit the polygenic architecture of Schizophrenia—implications for the underlying neurobiology[J]. 2016, 36: 89-98.
- 77 Coelewij L, Curtis D: Mini-review: Update on the genetics of Schizophrenia, 2018: 239-243.
- Kendler K S. The Schizophrenia Polygenic Risk Score: To What Does It Predispose in Adolescence?[J]. 2016, 73(3): 193-194.
- Lowther C, Costain G, Baribeau D A, et al. Genomic Disorders in Psychiatry—What Does the Clinician Need to Know?[J]. 2017, 19(11): 82.
- 80 González-Castro T B, Hernandez-Diaz Y, Juárez-Rojop I E. The role of C957T, TaqI, and Ser311Cys polymorphisms of the DRD2 gene in Schizophrenia: systematic review and meta-analysis[J]. 2016, 12(1): 1-14.
- Božina N, Jovanović N, Podlesek A. Suicide ideators and attempters with Schizophrenia the role of 5-HTTLPR, rs25531, and 5-HTT VNTR intron 2 variants[J]. 2012, 46(6): 767-773.
- Begni S, Moraschi S, Bignotti S. Association between the G1001C polymorphism in the GRIN1 gene promoter region and Schizophrenia[J]. 2003, 53(7): 617-619.
- Hirohata S, Miyamoto T J. Elevated levels of interleukin 6 in cerebrospinal fluid from patients with systemic lupus erythematosus and central nervous system involvement[J]. 1990, 33(5): 644-649.
- Zhang Y-Q, Lin W-P, Huang L-P, et al. Dopamine D2 receptor regulates cortical synaptic pruning in rodents[J]. Nature communications, 2021, 12(1): 6444.
- 85 Svob Strac D, Pivac N, Mück-Seler D. The serotonergic system and cognitive function[J]. Translational neuroscience, 2016, 7(1): 35-49.
- 66 Grace A A. Dysregulation of the dopamine system in the pathophysiology of Schizophrenia and depression[J]. Nature Reviews Neuroscience, 2016, 17(8): 524-532.
- 87 Le François B, Et Al. Transcriptional regulation at a HTR1A polymorphism associated with mental illness[J]. Neuropharmacology, 2008, 55(6): 977-985.

- Scarr E, Udawela M, Dean B. Changed frontal pole gene expression suggest altered interplay between neurotransmitter, developmental, and inflammatory pathways in Schizophrenia[J]. npj Schizophrenia, 2018, 4(1): 4.
- 89 Vohryzek J, Aleman-Gomez Y, Griffa A, et al. Structural and functional connectomes from 27 schizophrenic patients and 27 matched healthy adults [data set][J]. Zenodo. doi, 2020, 10.
- 90 Burt J B, Preller K H, Demirtas M, et al. Transcriptomics-informed large-scale cortical model captures topography of pharmacological neuroimaging effects of LSD[J]. Elife, 2021, 10: e69320.
- Markello R D, Arnatkeviciute A, Poline J-B, et al. Standardizing workflows in imaging transcriptomics with the abagen toolbox[J]. elife, 2021, 10: e72129.
- Hawrylycz M J. An anatomically comprehensive atlas of the adult human brain transcriptome[J]. Nature, 2012, 489(7416): 391-399.
- ArnatkevicIūtė A, Fulcher B D, Fornito A. A practical guide to linking brain-wide gene expression and neuroimaging data[J]. NeuroImage, 2019, 189: 353-367.
- ArnatkevicIūtė A, Fulcher B D, Fornito A. A practical guide to linking brain-wide gene expression and neuroimaging data[J]. NeuroImage, 2019, 189: 353-367.
- He Y, Chen Z J, Evans A C. Small-world anatomical networks in the human brain revealed by cortical thickness from MRI[J]. Cerebral cortex, 2007, 17(10): 2407-2419.
- Beckmann M, Johansen-Berg H, Rushworth M F. Connectivity-based parcellation of human cingulate cortex and its relation to functional specialization[J]. The Journal of Neuroscience, 2009, 29(4): 1175-1190.
- 97 Nelson S M, Cohen A L, Power J D, et al. A parcellation scheme for human left lateral parietal cortex[J]. Neuron, 2010, 67(1): 156-170.
- Wang H, Suh J W, Das S R. Multi-atlas segmentation with joint label fusion[J]. IEEE Transactions on Pattern Analysis and Machine Intelligence, 2012, 35(3): 611-623.
- 99 Artaechevarria X, Munoz-Barrutia A, Ortiz-de-Solorzano C. Combination strategies in multi-atlas image segmentation: application to brain MR data[J]. IEEE transactions on medical imaging, 2009, 28(8): 1266-1277.
- 100 Fischl B, Salat D H, Busa E, et al. Whole Brain Segmentation: Neurotechnique Automated Labeling of Neuroanatomical Structures in the Human Brain. 33, 341 355[J]. 2002.
- 101 Klein A, Tourville J. 101 labeled brain images and a consistent human cortical labeling protocol[J]. Frontiers in neuroscience, 2012, 6: 171.

- Rolls E T, Huang C C, Lin C P, et al. Automated anatomical labelling atlas 3[J]. Neuroimage, 2020, 206: 116189.
- French L, Paus T. A FreeSurfer view of the cortical transcriptome generated from the Allen Human Brain Atlas[J]. Frontiers in neuroscience, 2015, 9: 323.
- 104 Joglekar M R, Mejias J F, Yang G R, et al. Inter-areal Balanced Amplification Enhances Signal Propagation in a Large-Scale Circuit Model of the Primate Cortex[J]. Neuron, 2018, 98(1): 222-234 e228.
- Buxton R B, Wong E C, Frank L R. Dynamics of blood flow and oxygenation changes during brain activation: the balloon model[J]. Magnetic Resonance in Medicine, 1998, 39(6): 855-864.
- Hadida J, Sotiropoulos S N, Abeysuriya R G, et al. Bayesian optimisation of large-scale biophysical networks[J], 2018, 174: 219-236.
- Brochu E, Cora V M, De Freitas N J a p a. A tutorial on Bayesian optimization of expensive cost functions, with application to active user modeling and hierarchical reinforcement learning[J], 2010.
- 108 Williams C K, Rasmussen C E. Gaussian processes for machine learning[M]. 2. MIT press Cambridge, MA, 2006.
- 109 Press W H. Numerical recipes 3rd edition: The art of scientific computing[M]. Cambridge university press, 2007.
- Davies W, Isles A R, Wilkinson L S J N, et al. Imprinted gene expression in the brain[J]. 2005, 29(3): 421-430.
- 111 Gräff J, Kim D, Dobbin M M, et al. Epigenetic regulation of gene expression in physiological and pathological brain processes[J]. 2011, 91(2): 603-649.
- 112 Ghosh S, Raj A, Nagarajan S S. A joint subspace mapping between structural and functional brain connectomes[J]. NeuroImage, 2023, 272: 119975.
- 113 Yger F, Lotte F, Sugiyama M. Averaging covariance matrices for EEG signal classification based on the CSP: an empirical study[C]. 2015 23rd European signal processing conference (EUSIPCO), 2015: 2721-2725.
- Barachant A, Bonnet S, Congedo M, et al. Multiclass brain computer interface classification by Riemannian geometry[J]. IEEE Transactions on Biomedical Engineering, 2011, 59(4): 920-928.
- Herculano-Houzel S. The human brain in numbers: a linearly scaled-up primate brain[J]. Frontiers in Human Neuroscience, 2009, 3(1): 1.
- 116 Mehonic A, Kenyon A J. Brain-inspired computing needs a master plan[J]. Nature, 2022, 604: 255-260.

- Amunts K, Lippert T. Brain research challenges supercomputing[J]. Science, 2021, 374: 1054-1055.
- 118 Safron A. Making and breaking symmetries in mind and life[J]. Interface Focus, 2023, 13(3): 20230015.
- 119 Carlsson A, Waters N, Holm-Waters S, et al. Interactions between monoamines, glutamate, and GABA in Schizophrenia: new evidence[J]. 2001, 41(1): 237-260.
- 120 Okaty B W, Commons K G, Dymecki S M J N R N. Embracing diversity in the 5-HT neuronal system[J]. 2019, 20(7): 397-424.
- Westbrook A, Frank M J, Cools R J T i C S. A mosaic of cost benefit control over cortico-striatal circuitry[J]. 2021, 25(8): 710-721.
- Burnham K P, Anderson D R J S m, research. Multimodel inference: understanding AIC and BIC in model selection[J]. 2004, 33(2): 261-304.
- Bozdogan H J P. Model selection and Akaike's information criterion (AIC): The general theory and its analytical extensions[J]. 1987, 52(3): 345-370.
- 124 McQuarrie A D, Tsai C-L. Regression and time series model selection[M]. World Scientific, 1998.
- Liu Y, Liang M, Zhou Y, et al. Disrupted small-world networks in Schizophrenia[J]. Brain, 2008, 131(4): 945-961.
- Rubinov M, Sporns O. Complex network measures of brain connectivity: uses and interpretations[J]. Neuroimage, 2010, 52(3): 1059-1069.
- 127 Keyvanfard, F., Nasab, A. R., & Nasiraei-Moghaddam, A. (2023). Brain subnetworks most sensitive to alterations of functional connectivity in Schizophrenia: a data-driven approach. Frontiers in Neuroinformatics, 17, 1175886.
- 128 Cardenas V A. Anatomical and fMRI-network comparison of multiple DLPFC targeting strategies for repetitive transcranial magnetic stimulation treatment of depression[J]. Brain Stimulation, 2022, 15(1): 63-72.
- 129 Cieslik E C. Is there "one" DLPFC in cognitive action control? Evidence for heterogeneity from coactivation-based parcellation[J]. Cerebral cortex, 2013, 23(11): 2677-2689.
- 130 Berger, Vance W., and YanYan Zhou. "Kolmogorov smirnov test: Overview." Wiley statsref: Statistics reference online (2014).
- 131 Karamizadeh S, Abdullah S M, Manaf A A, et al. An overview of principal component analysis[J]. Journal of Signal and Information Processing, 2013, 4(3B): 173.
- 132 Gauch Jr H G. Noise reduction by eigenvector ordinations [J]. Ecology, 1982, 63(6): 1643-1649.